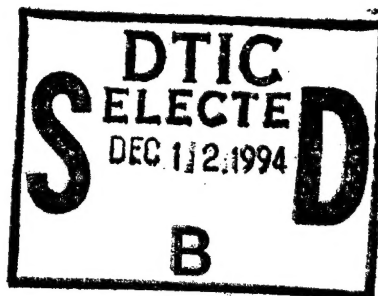


NAVAL POSTGRADUATE SCHOOL

Monterey, California



THESIS

**TIME-FREQUENCY DOMAIN DISTRIBUTION AND ITS
APPLICATION TO RECIPROCATING MACHINERY
ANALYSIS**

by

John E. Harding

September 1994

Thesis Advisor:

Young S. Shin

Approved for public release; distribution is unlimited.

DTIC QUALITY INSPECTED 5

19941202 155

REPORT DOCUMENTATION PAGE			Form Approved OMB No. 0704
Public reporting burden for this collection of information is estimated to average 1 hour per response, including the time for reviewing instruction, searching existing data sources, gathering and maintaining the data needed, and completing and reviewing the collection of information. Send comments regarding this burden estimate or any other aspect of this collection of information, including suggestions for reducing this burden, to Washington headquarters Services, Directorate for Information Operations and Reports, 1215 Jefferson Davis Highway, Suite 1204, Arlington, VA 22202-4302, and to the Office of Management and Budget, Paperwork Reduction Project (0704-0188) Washington DC 20503.			
1. AGENCY USE ONLY	2. REPORT DATE September 1994	3. REPORT TYPE AND DATES COVERED Master's Thesis	
4. TITLE AND SUBTITLE: TIME-FREQUENCY DOMAIN DISTRIBUTION AND ITS APPLICATION TO RECIPROCATING MACHINERY ANALYSIS (u)		5. FUNDING NUMBERS	
6. AUTHOR(S) Harding, John E.		8. PERFORMING ORGANIZATION REPORT NUMBER	
7. PERFORMING ORGANIZATION NAME(S) AND ADDRESS(ES) Naval Postgraduate School Monterey, CA 93943-5000		10. SPONSORING/MONITORING AGENCY REPORT NUMBER	
9. SPONSORING/MONITORING AGENCY NAME(S) AND ADDRESS(ES)			
11. SUPPLEMENTARY NOTES The views expressed in this thesis are those of the author and do not reflect the official policy or position of the Department of Defense or the U.S. Government.			
12a. DISTRIBUTION/AVAILABILITY STATEMENT Approved for public release; distribution is unlimited.		12b. DISTRIBUTION CODE *A	
13. ABSTRACT Accurate assessment of shipboard machinery condition is essential in increasing the operational capability of naval vessels. Current shipboard machinery vibration monitoring and diagnostic procedures use frequency domain spectra to identify possible faults and problem areas. This method has proven to be inadequate for reciprocating machinery analysis. In reciprocating machinery the vibration signal is no longer a stationary, ergodic process, but is time-dependent and in some cases transient. This study proposes the use of Pseudo Wigner-Ville Distribution and introduces Wavelet analysis as two advanced methods for condition monitoring of non-stationary and transient shipboard machinery. These methods employ a time-frequency domain distribution for the detection of fault location and severity level. To demonstrate the benefits of a time-frequency representation, vibration data from two types of reciprocating air compressors will be processed for analysis. To simulate faulty conditions, constructed artificial fault signals will be introduced into the vibration data and analyzed. It is proposed Wavelet Analysis will play a complementary role to the Pseudo Wigner-Ville Distribution technique.			
14. SUBJECT TERMS Pseudo Wigner-Ville Distribution, Wavelet Analysis, Time Domain Analysis, Frequency Spectrum		15. NUMBER OF PAGES 138	
		16. PRICE CODE	
17. SECURITY CLASSIFICATION OF REPORT Unclassified	18. SECURITY CLASSIFICATION OF THIS PAGE Unclassified	19. SECURITY CLASSIFICATION OF ABSTRACT Unclassified	20. LIMITATION OF ABSTRACT UL

Approved for public release; distribution is unlimited.

Time-Frequency Domain Distribution and Its Application to Reciprocating
Machinery Analysis

by

John E. Harding
Lieutenant, United States Coast Guard
B.S., United States Coast Guard Academy, 1987

Submitted in partial fulfillment
of the requirements for the degree of

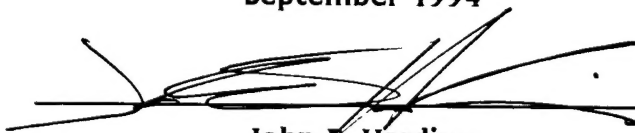
MASTER OF SCIENCE IN MECHANICAL ENGINEERING

from the

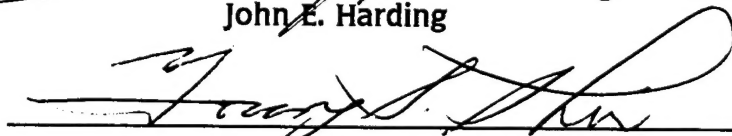
NAVAL POSTGRADUATE SCHOOL


September 1994

Author:


John E. Harding

Approved by:


Young S. Shin, Thesis Advisor


Matthew D. Kelleher, Chairman
Department of Mechanical Engineering

Accession For	
NTIS GRA&I	<input checked="" type="checkbox"/>
DTIC TAB	<input type="checkbox"/>
Unannounced	<input type="checkbox"/>
Justification	
By	
Distribution/	
Availability Codes	
Dist	Avail and/or
A-1	Special

ABSTRACT

Accurate assessment of shipboard machinery condition is essential in increasing the operational capability of naval vessels. Current shipboard machinery vibration monitoring and diagnostic procedures use frequency domain spectra to identify possible faults and problem areas. This method has proven to be inadequate for reciprocating machinery analysis. In reciprocating machinery the vibration signal is no longer a stationary, ergodic process, but is time-dependent and in some cases transient. This study proposes the use of Pseudo Wigner-Ville Distribution and introduces Wavelet Analysis as two advanced methods for condition monitoring of non-stationary and transient shipboard machinery. These methods employ a time-frequency domain distribution for the detection of fault location and severity level. To demonstrate the benefits of a time-frequency representation, vibration data from two types of reciprocating air compressors will be processed for analysis. To simulate faulty conditions, constructed artificial fault signals will be introduced into the vibration data and analyzed. It is proposed that Wavelet Analysis will play a complementary role to the Pseudo Wigner-Ville Distribution technique.

TABLE OF CONTENTS

I.	INTRODUCTION	1
A.	GENERAL BACKGROUND	1
	1. Rational For Maintenance and Monitoring Programs	1
	2. Current Maintenance and Repair Practices	3
	3. Predictive Maintenance	5
B.	DEVELOPMENT OF VIBRATION ANALYSIS TECHNIQUES FOR RECIPROCATING MACHINES	6
	1. Current Approach	6
	2. Proposed Analysis Methods	7
II.	RECIPROCATING MACHINERY ANALYSIS	9
A.	DISCUSSION	9
B.	COMPRESSION CYCLE AND MECHANICS OF A RECIPROCATING AIR COMPRESSOR	11
	1. Compressor Cycle	11
	2. Compressor Timing	12
C.	DATA COLLECTION FOR VIBRATION ANALYSIS . . .	13
	1. Transducer Placement	13
	2. Overview of Reciprocating Vibration Patterns	14
III.	TIME DOMAIN AND FREQUENCY SPECTRUM REPRESENTATION OF VIBRATION MEASUREMENT DATA	17

A.	RECIPROCATING AIR-COMPRESSOR VIBRATION	
	MEASUREMENT DATA	17
B.	DATA ACQUISITION AND PROCESSING	24
C.	TIME DOMAIN AND FREQUENCY SPECTRUM	
	REPRESENTATIONS	29
D.	ARTIFICIAL FAULT SIMULATION	54
	1. Impulse Disturbance	54
	2. Transient Vibration Signals	62
IV.	TIME-FREQUENCY DOMAIN REPRESENTATION	68
A.	PSEUDO WIGNER-VILLE DISTRIBUTION (PWVD)	68
	1. History of PWVD	68
	2. PWVD of Measured Vibration Data	69
	3. PWVD of Artificial Fault Simulation	97
B.	WAVELET ANALYSIS	110
	1. History of Wavelet Analysis	110
	2. Wavelet Analysis of Artificial Fault	
	Simulation	111
V.	CONCLUSIONS AND RECOMMENDATIONS	114
	APPENDIX. MATLAB PROGRAM CODE FOR FFT	116
	LIST OF REFERENCES	118
	INITIAL DISTRIBUTION LIST	122

LIST OF FIGURES

Figure 1:	Breakdown of Machine Data	18
Figure 2:	Vibration Test and Analysis Guide, MID 115	20
Figure 3:	Vibration Test and Analysis Guide, MID 524	22
Figure 4:	MID 115 Vibration Measurement Data Organization	25
Figure 5:	MID 524 Vibration Measurement Data Organization	26
Figure 6:	MID 115 Compressor Component Sampled at 750 HZ, Tangential Direction	30
Figure 7:	MID 115 Compressor Component FFT, Sampled at 750HZ, Tangential Direction	31
Figure 8:	MID 115 Compressor Component Sampled at 750 HZ, Axial Direction	32
Figure 9:	MID 115 Compressor Component FFT, Sampled at 750HZ, Axial Direction	33
Figure 10:	MID 115 Compressor Component Sampled at 750 HZ, Radial Direction	34
Figure 11:	MID 115 Compressor Component FFT, Sampled at 750HZ, Radial Direction	35
Figure 12:	MID 115 Compressor Component Sampled at 7500 HZ, Tangential Direction	36
Figure 13:	MID 115 Compressor Component FFT, Sampled at 7500 HZ, Tangential Direction	37

Figure 14:	MID 115 Compressor Component Sampled at 7500 HZ, Axial Direction	38
Figure 15:	MID 115 Compressor Component FFT, Sampled at 7500 HZ, Axial Direction	39
Figure 16:	MID 115 Compressor Component Sampled at 7500 HZ, Radial Direction	40
Figure 17:	MID 115 Compressor Component FFT, Sampled at 7500 HZ, Radial Direction	41
Figure 18:	MID 524 Compressor Component Sampled at 400 HZ, Tangential Direction	42
Figure 19:	MID 524 Compressor Component FFT, Sampled at 400 HZ, Tangential Direction	43
Figure 20:	MID 524 Compressor Component Sampled at 400 HZ, Axial Direction	44
Figure 21:	MID 524 Compressor Component FFT, Sampled at 400 HZ, Axial Direction	45
Figure 22:	MID 524 Compressor Component Sampled at 400 HZ, Radial Direction	46
Figure 23:	MID 524 Compressor Component FFT, Sampled at 400 HZ, Radial Direction	47
Figure 24:	MID 524 Compressor Component Sampled at 3950 HZ, Tangential Direction	48
Figure 25:	MID 524 Compressor Component FFT, Sampled at 3950 HZ, Tangential Direction	49
Figure 26:	MID 524 Compressor Component Sampled at 3950 HZ, Axial Direction	50

Figure 27:	MID 524 Compressor Component FFT, Sampled at 3950 HZ, Axial Direction	51
Figure 28:	MID 524 Compressor Component Sampled at 3950 HZ, Radial Direction	52
Figure 29:	MID 524 Compressor Component FFT, Sampled at 3950 HZ, Radial Direction	53
Figure 30:	Artificial Fault Simulation, Tangential Direction	56
Figure 31:	Artificial Fault Simulation FFT, Tangetial Direction	57
Figure 32:	Artificial Fault Simulation, Axial Direction	58
Figure 33:	Artificial Fault Simulation FFT, Axial Direction	59
Figure 34:	Artificial Fault Simulation, Radial Direction	60
Figure 35:	Artificial Fault Simulation FFT, Radial Direction	61
Figure 36:	Typical Transient Vibration, Single Impact	64
Figure 37:	Typical Transient Vibration FFT, Single Impact	65
Figure 38:	Typical Transient Vibration, Dual Impact	66
Figure 39:	Typical Transient Vibration FFT, Dual Impact	67
Figure 40:	PWVD Results, MID 115 Compressor Sampled at 750 HZ, Tangential Direction . .	72

Figure 41:	PWVD Contour Map, MID 115 Compressor	
	Sampled at 750 HZ, Tangential Direction . . .	73
Figure 42:	PWVD Results, MID 115 Compressor	
	Sampled at 750 HZ, Axial Direction	74
Figure 43:	PWVD Contour Map, MID 115 Compressor	
	Sampled at 750 HZ, Axial Direction	75
Figure 44:	PWVD Results, MID 115 Compressor	
	Sampled at 750 HZ, Radial Direction	76
Figure 45:	PWVD Contour Map, MID 115 Compressor	
	Sampled at 750 HZ, Radial Direction	77
Figure 46:	PWVD Results, MID 115 Compressor	
	Sampled at 7500 HZ, Tangential Direction .	78
Figure 47:	PWVD Contour Map, MID 115 Compressor	
	Sampled at 7500 HZ, Tangential Direction .	79
Figure 48:	PWVD Results, MID 115 Compressor	
	Sampled at 7500 HZ, Axial Direction	80
Figure 49:	PWVD Contour Map, MID 115 Compressor	
	Sampled at 7500 HZ, Axial Direction	81
Figure 50:	PWVD Results, MID 115 Compressor	
	Sampled at 7500 HZ, Radial Direction . . .	82
Figure 51:	PWVD Contour Map, MID 115 Compressor	
	Sampled at 7500 HZ, Radial Direction . . .	83
Figure 52:	PWVD Results, MID 524 Compressor	
	Sampled at 400 HZ, Tangential Direction . .	84
Figure 53:	PWVD Contour Map, MID 524 Compressor	
	Sampled at 400 HZ, Tangential Direction . .	85

Figure 54:	PWVD Results, MID 524 Compressor	
	Sampled at 400 HZ, Axial Direction	86
Figure 55:	PWVD Contour Map, MID 524 Compressor	
	Sampled at 400 HZ, Axial Direction	87
Figure 56:	PWVD Results, MID 524 Compressor	
	Sampled at 400 HZ, Radial Direction	88
Figure 57:	PWVD Contour Map, MID 524 Compressor	
	Sampled at 400 HZ, Radial Direction	89
Figure 58:	PWVD Results, MID 524 Compressor	
	Sampled at 3950 HZ, Tangential Direction .	90
Figure 59:	PWVD Contour Map, MID 524 Compressor	
	Sampled at 3950 HZ, Tangential Direction .	91
Figure 60:	PWVD Results, MID 524 Compressor	
	Sampled at 3950 HZ, Axial Direction	92
Figure 61:	PWVD Contour Map, MID 524 Compressor	
	Sampled at 3950 HZ, Axial Direction	93
Figure 62:	PWVD Results, MID 524 Compressor	
	Sampled at 3950 HZ, Radial Direction	94
Figure 63:	PWVD Contour Map, MID 524 Compressor	
	Sampled at 3950 HZ, Radial Direction	95
Figure 64:	PWVD Results, Artificial Fault	
	Simulation, Tangential Direction	98
Figure 65:	PWVD Contour Map, Artificial Fault	
	Simulation, Tangential Direction	99
Figure 66:	PWVD Results, Artificial Fault	
	Simulation, Axial Direction	100

Figure 67:	PWVD Contour Map, Artificial Fault	
	Simulation, Axial Direction	101
Figure 68:	PWVD Results, Artificial Fault	
	Simulation, Radial Direction	102
Figure 69:	PWVD Contour Map, Artificial Fault	
	Simulation, Radial Direction	103
Figure 70:	PWVD Results, Typical Transient	
	Vibration, Single Impact	106
Figure 71:	PWVD Contour Map, Typical Transient	
	Vibration, Single Impact	107
Figure 72:	PWVD Results, Typical Transient	
	Vibration, Dual Impact	108
Figure 73:	PWVD Contour Map, Typical Transient	
	Vibration, Dual Impact	109
Figure 74:	Wavelet Transform Results, Artificial	
	Fault Simulation, Tangential Direction .	112
Figure 75:	Wavelet Transform Contour Map, Artificial	
	Fault Simulation, Tangential Direction .	113

LIST OF ABBREVIATIONS

BDC	-	Bottom Dead Center
DET	-	Detachment
FFT	-	Fast Fourier Transform
HZ	-	Hertz
MHZ	-	Mega Hertz
MID	-	Machine Identification Number
PC	-	Personal Computer
PERA(CV)	-	Planning and Engineering for Repairs and Alterations, aircraft carriers
PWVD	-	Pseudo Wigner-Ville Distribution
RMS	-	Root Mean Square
RPM	-	Revolutions Per Minute
TDC	-	Top Dead Center
VTAG	-	Vibration Testing and Analysis Guide
WD	-	Wigner Distribution

ACKNOWLEDGEMENT

I would like to express my sincere appreciation to my advisor, Professor Young S. Shin, for his guidance throughout the course of my thesis research. I would also like to thank Dr. Joung J. Kim for his assistance with the computer programs used in this study. Additionally, I would like to thank Mr. Lynn Hampton of NAVSEADDET PERA (CV) for providing the machine data.

I dedicate this work to my loving wife Susan, and to my son Steven James.

I. INTRODUCTION

A. GENERAL BACKGROUND

1. Rational For Maintenance and Monitoring Programs

There are many reasons for conducting analysis and assessment of machine operating condition and performance. The principal influence for an organization to accurately assess the operation of its engineering plant is financial. In almost every application, cost is a major driving factor in maintaining equipment in proper operating condition. This practice not only reduces the associated repair time, but ensures optimal performance is achieved. The importance of maintaining equipment at its optimal level is readily apparent in the commercial industry. Costs for equipment operation and repairs are directly linked to a company's profit margin. Simply put, non-operating or poorly operating equipment consume more resources and produce less work. For this reason, many organizations have realized the importance of machinery analysis and some have entire teams dedicated to machine health and condition monitoring.

In military applications where profit margins are not a motivating factor, machinery analysis can still lend itself to the benefit of the organization. This is especially true in surface ship engineering plants [Refs. 1-2]. In the unique application of shipboard engineering plants, there is intense

pressure to ensure machinery and equipment is ready for a particular mission or maneuver, and is available upon demand. Using an aircraft carrier for example, it is readily apparent why there cannot be a delay in response due to equipment malfunction or lack of machine output during aircraft launching or recovering operations. To ensure a prudent response, surface ship engineering plants have designed redundancies. The critical equipment is usually duplicated or has some type of backup system to ensure the required output is continuously delivered.

Because surface ship engineering plants consist of overly redundant systems, optimal performance may not appear to be a worthwhile crusade. As long as a particular system is producing the required output, whether or not it is the most economical or the actual designed output, the demand is being met and therefore it is performing at an acceptable level. The associated input required for this level of operation is seldom a consideration. Machine function is more important than the energy constraints. However, the maintenance time associated with this type of equipment arrangement becomes a significant factor. The duplication and backup of systems increases the number of machinery components requiring support. To assist engineers in the planning, scheduling, and actual performance of maintenance activities for these complex systems, many organizations have adopted varying maintenance practices to manage their engineering plants. Most current

maintenance procedures have fallen under these three types; Preventive Maintenance (also referred to as Planned Maintenance), Casualty Control, and a practice some refer to as Fly to Failure. A brief explanation of each of these practices will be given to emphasize the magnitude of resources, inherent problems, and shortcomings associated with these antiquated practices.

2. Current Maintenance and Repair Practices

In Preventive Maintenance equipment is overhauled based on time (calendar based) and/or usage (operating hours). Plant engineers plan and schedule maintenance regardless of the actual operating condition of the machine. This provides the convenience of predictable logistics support and resource requirements, but it also has many drawbacks. Although this maintenance practices ensures availability, it is very expensive both in actual dollars spent and time available for maintenance. This practice diverts valuable resources from more efficient use, and in today's economic environment, manpower constraints are becoming more strained and less maintenance hours are available. In addition, premature tear downs increase costs and degrade reliability. More often than would be expected, routine open and inspect procedures and unwarranted tear downs result in reassembly problems and failed machinery which had been in good condition prior to undergoing repairs [Ref. 1]. On top of these shortcomings,

many of these same units will have to undergo some type of casualty control measures during operations.

Under Casualty Control procedures, equipment is operated until a fault is detected either by alarm or by decline in performance and then is repaired as required. As long as the equipment is fully functional no other maintenance is performed. It should be noted here that without proper or accurate diagnostics, troubleshooting the fault in the equipment can consume numerous man-hours. Casualty control is usually not used as a primary means to maintain equipment. It is intended for emergency situations to prevent catastrophic failure and degradation of the engineering plant. Mission requirements are usually not severely affected due to the nature of the system design for naval surface ships. However, in the commercial industry where systems may not be as redundant, required output may be severely hampered by the loss of just one piece of gear.

Fly to Failure is probably the least used practice both in commercial industry and in naval surface ship application. Fly to Failure is a concept where equipment is used until complete failure and then replaced. After a faulty condition is first detected, a determination is made as to the significance of the fault and any hazardous conditions that may result by the continued operation of the equipment. Once again without proper and accurate diagnostic procedures any equipment assessment can contain many uncertainties. If a

hazard is determined not to exist to surrounding equipment, personnel, or mission requirements the equipment is allowed to operate until complete failure occurs. In this case equipment is usually monitored but no corrective actions are taken. In some instances naval ships are forced into the fly to failure predicament due to demands on the machinery that are so great as to not allow for proper casualty control.

3. Predictive Maintenance

All of these methods are costly in the realm of manpower, time, and dollar expenditures. With the increasing costs of associated with current maintenance practices and the desire for higher operational availability and extended operating cycles, organizations have sought better ways to manage maintenance requirements. This trend has brought a need to accurately predict and define machinery repairs based on knowledge of system and component performance. One method which provides such information is vibration analysis. Vibration and noise generated by machines is now commonly used to diagnosis machinery conditions, predict failures based on wear related degradation, and to prevent unexpected catastrophic failures [Refs. 1-3]. With accurate assessment of machinery conditions, resources can be more efficiently assigned. In May of 1988 it was published that as many as seven different simultaneous efforts of utilizing vibration measurement and analysis for machinery health determination and maintenance planning existed in the United States surface

Navy program [Ref. 1]. However, a common thread with all of these efforts was the lack of success with the analysis and trending of reciprocating components [Refs. 1-2].

B. DEVELOPMENT OF VIBRATION ANALYSIS TECHNIQUES FOR RECIPROCATING MACHINES

1. Current Approach

Many of the programs developed for surface ships primarily focused the attention on rotating equipment even though reciprocating machinery is a major player in most shipboard engineering plants. Analysis was focused on machine data displayed in the frequency domain. Throughout the commercial industry and specifically in naval surface ship programs, reciprocating machinery has posed additional problems in forming a consensus of opinion as to the validity of applying average data as acceptable criteria [Ref. 1,3]. Averaging data was developed to measure signals in the presence of noise and to measure noise itself. The most common technique used in vibration analysis of machine data is RMS averaging. This averaging technique determines the average magnitude of the signal, ignoring any phase difference that may exist between the spectra. The lack of consensus promoted an unevenness in the analysis of the different types of equipments. Since there was an agreed upon procedure for rotating machinery, that portion of the program marched forward with little consideration for the specific requirements for accurate reciprocating machinery analysis

[Ref. 2]. By approaching the task from one side, analysts developed proven frequency domain techniques for rotating machinery analysis which they then applied to reciprocating machinery. Current shipboard machinery vibration monitoring and diagnostic procedures use this frequency domain spectra to identify possible faults and problem areas.

2. Proposed Analysis Methods

Frequency domain analysis implies that the vibration data is assumed to be stationary and even time independent. This method has proven to be inadequate for reciprocating machinery analysis. In reciprocating machinery the vibration signal is no longer a stationary, ergodic process, but is time-dependent and in some cases transient. These techniques do have value with reciprocating machinery for certain machine components, but they cannot accomplish the total analysis that is required and expected [Ref. 3]. Because of these shortcomings, the surface Navy programs for the analysis of reciprocating machinery have not yielded complete analysis results.

To conduct a total analysis and gain an accurate assessment of the operating condition of a reciprocating machine, advanced analysis techniques need to be employed. Wavelet analysis and Pseudo Wigner-Ville Distribution (PWVD) technique use a time-frequency domain distribution for detection of fault location and severity level and may fill the gap between rotating and reciprocating machinery. By

providing a time-frequency domain distribution the detection of fault locations and severity are based on the signal displacement and timing of the event. Wavelet analysis and PWVD technique are both being explored due to the strong implications that one type of analysis may not cover all possible cases of reciprocation and transient machines. It is proposed that Wavelet analysis will play a complementary role to the PWVD technique.

II. RECIPROCATING MACHINERY ANALYSIS

A. DISCUSSION

To understand how a time-frequency domain distribution analysis can fill the gap between rotating and reciprocation machinery, we must first understand the mechanics of reciprocating machines. The subject of engine vibration can be divided into two categories: vibration of the engine parts relative to each other, called internal vibration, and movement of the engine as a whole, called external vibration [Ref. 4]. With the use of various machinery mounting systems and other isolation techniques, external vibration can be reduced from being a factor in the analysis. That is not to say that external sources will never be a major contributor to machine vibrations, but that external effects will not be studied here. The focus of this investigation has been limited to high-pressure air compressors although it can be equally applied to any reciprocating type machine with few modifications.

As mentioned earlier, there are some benefits of monitoring reciprocating machinery using frequency domain spectra. By viewing the vibration signatures in the frequency domain, information on some of the major components can be gained. The frequency domain should produce indications of crankshaft unbalance, reciprocating unbalance, torsional

unbalance, misalignment, improper gear mesh, and worn or bad bearings. There are other possible components in addition to those listed above that would lend themselves to be analyzed in the frequency domain. The entire frequency span of the machine is related to the rpm of the components. For example, the crankshaft is rotating at a known rpm and establishes the baseline running speed frequency. As the crankshaft makes one revolution, the piston assembly makes two distinct movements. These two distinct movements and the assembly weight is what creates the two times running speed frequency [Ref. 3].

However, reciprocating components such as piston rings, wrist pins, and valves cannot be analyzed in the frequency domain. With frequency domain analysis, the action of these components is lost in noise. In addition, frequencies produced by mechanical faults can not be distinguished from other contributors such as combustion noise, port flow, injection noise and a host of many other factors. The recognition and separation of this noise has left many excellent analysts dismayed [Ref. 3]. For this type of analysis we have to look at timing relationships between mechanical events. Time relates to something that is happening in relationship to the mechanical events or rotational speed or crank-angle position. Knowing how these components act in conjunction with other components of the reciprocating machine, each component frequency can be separated by the use of relative phase comparison measurements

[Ref. 3]. By conducting the analysis in the time-frequency domain, information required to separate component frequencies can be obtained.

B. COMPRESSION CYCLE AND MECHANICS OF A RECIPROCATING AIR COMPRESSOR

1. Compressor Cycle

High pressure air compressors allow mechanical events to be related based on cylinder pressures and crank angle. Just like a two-cycle engine, a compressor repeats its cycle every 360 degrees. Understanding how the cycle of events that happen with a compressor is important in interpreting the data that will be subject to analysis. Simplifying the basic process of a single-stage compressor [Ref. 5], a compressor cycle can be viewed in three steps. Starting in the top dead center (TDC) position where the piston is in the farthest position from the crankshaft, the sequence of events begin. In this position the pressure inside the cylinder is approximately equal to the that of the discharge line. Both the suction valve and discharge valve are closed with the piston in this position.

The second stage of the compressor cycle has the piston assembly drawing back down the cylinder creating a vacuum in the cylinder. The suction valve opens at this point and with the negative pressure gradient between the cylinder and the suction line, gas or air enters the cylinder. Theoretically once the piston reaches bottom dead center (BDC)

the pressure inside the cylinder is the same as that of the suction line and spring action allows the suction valve to close. The piston assembly now begins its movement up or towards TDC starting the final stage of the compressor cycle.

In the final stage of the compressor cycle pressure inside the cylinder increases with the upward movement of the piston assembly and creates a positive pressure gradient between the cylinder and the discharge line. Once the pressure inside the cylinder becomes great enough to overcome the spring tension of the discharge valve, the discharge valve opens and the volume of gas displaces to the discharge line. The displacement of the gas inside the cylinder decreases the pressure required to hold the discharge valve open causing the valve to close. From this point the cycle repeats itself.

2. Compressor Timing

The knowledge of what takes place during the compressor cycle is only a small portion of the information that is needed to establish a relationship between mechanical events. In order to accurately assess the reciprocating components, the compression stage for the cylinder of interest in relation to the vibration signatures taken at a specific point in time in relation to rotational speed must be established. This can be determine based on crank-angle and crankshaft rpm. Piston position can be obtained by knowing the displaced cylinder volume. To calculate displaced cylinder volume, the ratio of the length of the piston

connecting rod and the radius of the circle created by the crank shaft throw to the connecting rod is required [Ref. 5]. Each major timing event within the cylinder is also required. As an example, we need to know when each valve opens and closes in relation to TDC. Obviously for multi-cylinder compressors we would need this information for each cylinder. The compressor manufacturer can provide this information along with other important machine data such as bore, stroke, suction/discharge pressures, cylinder clearance, and rod loading that will be required to conduct a thorough analysis. This study will not discuss all of the analysis required for a complete assessment of a high-pressure air compressor. At this point, identifying frequency components to mechanical events and their relationship in the time-frequency domain is of interest.

C. DATA COLLECTION FOR VIBRATION ANALYSIS

1. Transducer Placement

Understanding what causes specific events to create vibrations at different frequencies, as well as knowing where they should occur in the time trace relative to the crank-angle degree, enables one to pinpoint, predict and trend reciprocating machinery. By knowing the crankshaft rpm, crank-angle and cylinder events can easily be converted to time. In order to gather this information it is important that the analysis equipment is setup correctly. Repeatability

is extremely important. Since frequency responses of mechanical events of individual cylinders is of interest, placement of the vibration transducers is a governing element. To gather vibration information for the reciprocating components, the transducer should be moved around the cylinder frame to allow the analyst the opportunity to observe the highest response area for different mechanical problems [Ref. 3]. Vibration signals for the rotating components are taken in the same manner as rotating machine analysis - in the axial, tangential, and radial directions of the compressor crankshaft and the drive shaft of the powering unit.

2. Overview of Reciprocating Vibration Patterns

Reciprocating components create distinct vibration patterns which allow them to be separated from machine noise. Looking at each cylinder, vibration signals created by worn valves, atypical valve opening and closing events, worn piston rings, cylinder scoring, and mechanical knocking can be seen. Mechanically driven vibrations such as wrist pin looseness, or piston slap, or even the valve events themselves usually create low frequency vibration. However, there are some mechanical events that create high frequency signals. Examples of a mechanical high frequency might be a scored cylinder liner or rings rubbing along the cylinder walls or through the port area [Ref. 3]. The intensity of a fault condition will determine the amplitude of the vibration pattern. The duration of the vibration signal created by a

fault condition will assist in determining its cause. A time-frequency representation will allow both elements of the data to be displayed simultaneously for accurate assessment of the compressor's operating condition.

There are three basic types of noise that will represent different actions within the cylinder; friction, mechanical knocks, and gas blow. Friction creates high frequency wave forms that are long in duration but in reciprocating machines may not be time-independent. Sharp mechanical impacts create wave forms that will always be time-dependent and in some cases transient. As an example, a valve opening event will appear as an impact as the valve opens fully or to the maximum of the stroke. Loose bearings will also create an impact knock at the time of pressure reversal, and when rings go through the port opening or a step in the cylinder wall, a very fast clip or knock will take place. In the case of multiple knocks spaced closely together, the faults may be spring bounce or many rings hitting the same fault as they go by it. Gas blow or vacuum leak patterns are caused by events which increase the velocity of gases or air going over a very small area. Examples that could create this type of pattern include; leaking head gasket, blow-by, and valve opening/closing events. Knowing where the action occurs in relationship to the crank-angle degree is key to interpretation. Again, amplitude of the vibration pattern will depend on the severity of the event.

Once the fault condition can be located, assessed, and diagnosed, the root cause(s) can be traced back and determined. Common problems with valves range from a slight leak to the loss of the valve plate. Valve failure can be caused from wear, impacting, corrosion, or a combination of the three. Valve component wear is often caused by the introduction of foreign materials, incorrect design or modification, or incorrect lubrication. Impacting of the valve plates, seats, and guards may be caused from weak or broken springs as well as excessively strong springs. Piston problems can be caused by incorrect assembly, incorrect machining, improper positioning, as well as broken or leaking rings. Cylinder problems usually result from boring or resizing the cylinder cavity. Detection of inadequate repair and modification type problems can usually be verified by checking the compressor repair history. Regardless of the cause, time-frequency domain analysis will assist in troubleshooting the equipment and expedite the required repairs. The long term benefits of this advance analysis techniques may even be to correct flawed maintenance practices and procedures.

III. TIME DOMAIN AND FREQUENCY SPECTRUM REPRESENTATION OF VIBRATION MEASUREMENT DATA

A. RECIPROCATING AIR-COMPRESSOR VIBRATION MEASUREMENT DATA

Machine data was received from NAVSEA DET PERA(CV) (Planning and Engineering for Repairs and Alterations, aircraft carriers) for two different high-pressure air compressors [Ref. 6]. Each compressor was designated by an assigned Machine Identification (MID) number. The five stage reciprocating high-pressure air compressor was designated MID 115. The six stage reciprocating high-pressure air compressor was designated MID 524. Included in the machine data was a six channel recording of analog vibration measurements, and a Vibration Testing and Analysis Guide (VTAG) for each compressor type. The recorded tape log contained approximately twenty seconds of vibration measurement signals for each data set. Figure 1 shows the breakdown of the machine data that was analyzed during this study. As shown in this figure, three recordings were selected for each compressor type. The recordings captured tri-directional vibration measurement signals for the driving unit (motor) and tri-directional vibration measurement signals for the driven unit (compressor). Each recording was then analyzed at two sampling frequency levels to ensure a broad bandwidth of the vibration measurements was captured.

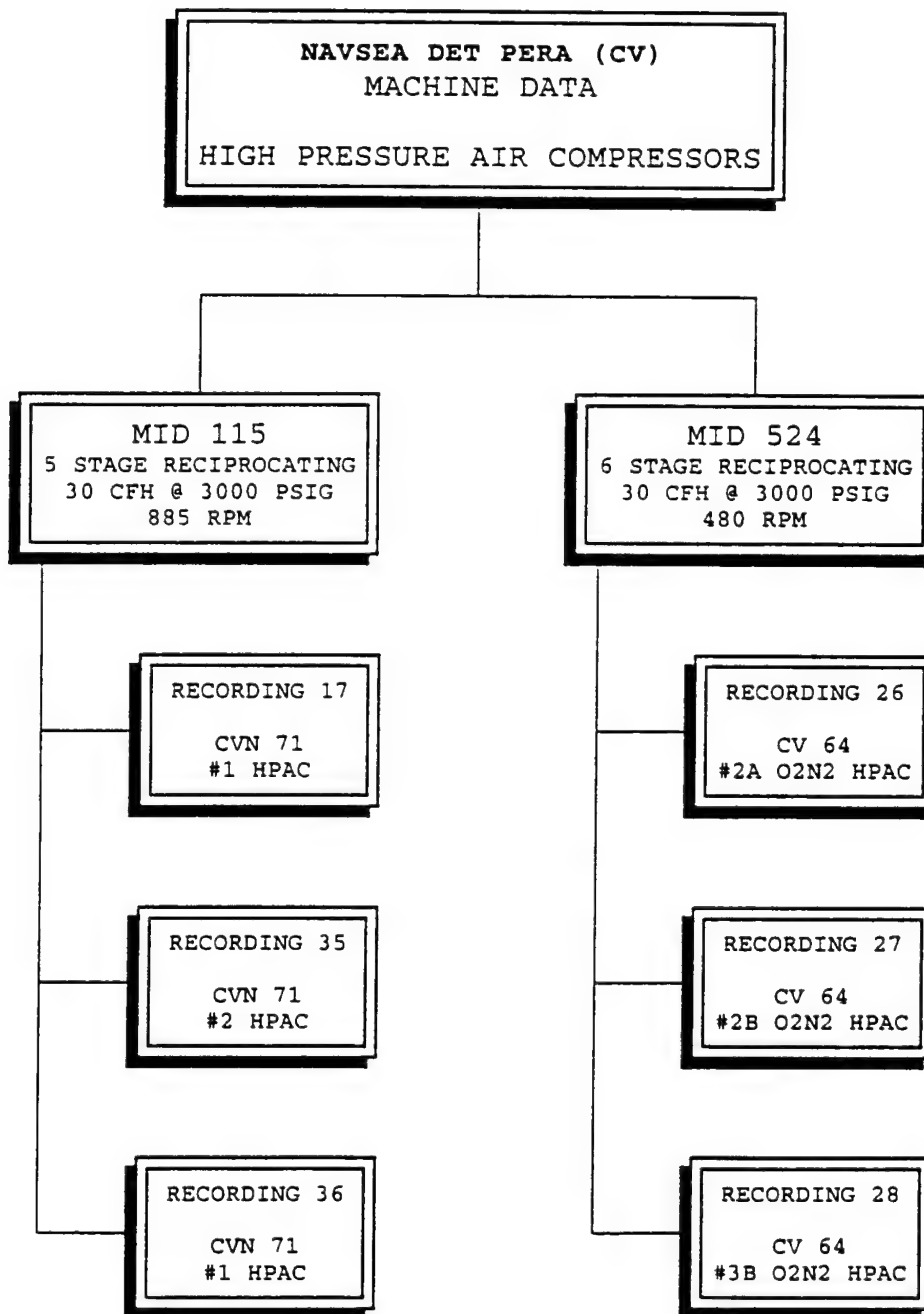


FIGURE 1: Breakdown of Machine Data

The transducers used to measure the vibration levels were positioned on the free end of the motor and on the free end of the compressor for the MID 115 type high-pressure air compressor. For the MID 524 type compressor the transducers were position on the coupling end of the motor and on the free end of the compressor. The transducers were oriented in the traditional axial, tangential, and radial directions that is common place in rotating machinery analysis. Unfortunately vibration data was not captured for individual cylinder actions as previously discussed in Chapter II. Figures 2 and 3 are the VTAGs for the MID 115 type compressor and MID 524 type compressor respectively. The VTAGs clearly show the different compressor and motor arrangements and the transducer placements for the two reciprocating machines.

"AIRCRAFT CARRIER MACHINERY VIBRATION TEST & ANALYSIS GUIDE" PERA (CV) PUB 1822-207

MACHINE: HIGH PRESSURE AIR COMPRESSOR SHIP APPLICABILITY: 70.71 CVN71 UNITS: 1,2,3,4		SWAB: 551-5 MID: 115 DATE: AUGUST 1992
DRIVER		DRIVEN
CID#: 175505340 TECH MANUAL: S6220-AP-MM0-010 MFR: GENERAL ELECTRIC HP: 75 INPUT: Voltage: 440 AC Current: 100 A RPM: 380 FRAME: 444TNSD		CID#: 061900403 TECH MANUAL: S6220-AP-MM0-010 MFR: WORTHINGTON OUTPUT: 30 CFH @ 3000 PSIG RPM: 385 TYPE: FIVE STAGE. VERTICAL. RECIPROCATING
TEST RPMs AND OPERATING CONDITIONS MOTOR: 390		ANALYSIS RANGES REF RPM: 1 X MOTOR ORDERS: 10, 100 FREQ HZ: 150, 1500
<div style="display: flex; justify-content: space-around; align-items: flex-start;"> <div style="text-align: center;"> <div style="border: 1px solid black; padding: 2px; margin-bottom: 5px;">MOTOR 1 ART</div> <p>ELEVATION</p> </div> <div style="text-align: center;"> <div style="border: 1px solid black; padding: 2px; margin-bottom: 5px;">CPRSR 4 ART</div> <p>VIEW A-A</p> </div> </div>		
HIGH PRESSURE AIR COMPRESSOR		551-5 - 115

FIGURE 2: Vibration Test and Analysis Guide, MID 115
page 1 of 2

21

"AIRCRAFT CARRIER MACHINERY VIBRATION TEST & ANALYSIS GUIDE" PERA (CV) PUB 1822-207

MACHINE: HIGH PRESSURE AIR COMPRESSOR (O2N2)SWAB: 553-2 MID: 524SHIP APPLICABILITY: 41,43,59,60,61,62,64,65,67,69DATE: DECEMBER 1992

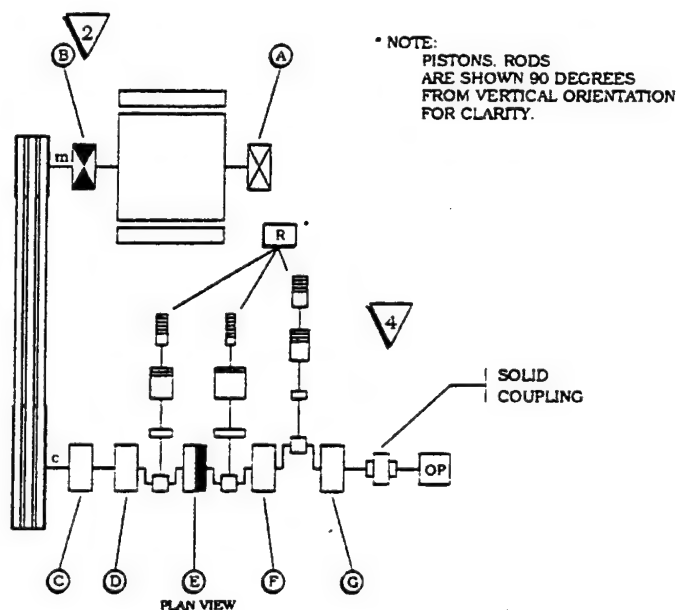
DRIVER		DRIVEN
<u>CID#:</u> 175504979 <u>TECH MANUAL:</u> S6220-BE-MMA-010 <u>MFR:</u> GENERAL ELECTRIC <u>HP:</u> 75 <u>INPUT:</u> Voltage: 440 AC Current: 98.5 A <u>RPM:</u> 1200 <u>FRAME:</u> 405TN		<u>CID#:</u> 061430253 <u>TECH MANUAL:</u> S6220-BE-MMA-010 <u>MFR:</u> INGERSOLL RAND <u>OUTPUT:</u> 30 CFH @ 3000 PSIG <u>RPM:</u> 480 <u>TYPE:</u> 6 STAGE. RECIPROCATING
<u>TEST RPMs AND OPERATING CONDITIONS</u> MOTOR: 1180 COMPRESSOR: 472		<u>ANALYSIS RANGES</u> <u>REF RPM:</u> 1 X CPRSR <u>ORDERS:</u> 10, 100 <u>FREQ HZ:</u> 30, 790
<div style="text-align: right;">HBRCPR2F</div> <p style="text-align: center;">PLAN VIEW</p> <p style="text-align: center;">ELEVATION</p>		
HIGH PRESSURE AIR COMPRESSOR (O2N2)		553-2 - 524

FIGURE 3: Vibration Test and Analysis Guide, MID 524
 page 1 of 2

VIBRATION SOURCE COMPONENTS												19921214	
DRIVER				INTERMEDIATE OR AUXILIARY SHAFTS				DRIVEN					
ITEM	DESCRIPTION	ELEM	ORDER	ITEM	DESCRIPTION	ELEM	ORDER	ITEM	DESCRIPTION	ELEM	ORDER		
m	Motor Shaft		2.50c					c	Compressor Shaft (Ref)		1.00c		
	Slois	72	180.00c					R	Pistons, Rods	3	3.00c		
	Bars	84	210.00c					OP	Oil Pump	12	12.00c		
	Pores:	6	15.00c										

VIBRATION SOURCE DIAGRAM

HSH PACX1



HIGH PRESSURE AIR COMPRESSOR (O2N2)

553-2 - 524

FIGURE 3: Vibration Test and Analysis Guide, MID 524
page 2 of 2

B. DATA ACQUISITION AND PROCESSING

Each vibration measurement recording selected for the two compressors was first analyzed in the time domain and then in the frequency domain (spectrum) using a 486-50MHZ personal computer. **EASYEST™ LX** software, developed by Keithley Asyst, was used to convert the analog data from the tape log to digital format. This PC-based data acquisition system digitized the analog signal, converted the units from voltage to velocity, and finally stored the velocity data sequences in ASCII form into the hard disk of the personal computer. The data was filed separately based on MID number, recording number, sampling frequency, machine component (motor or compressor), and sampling direction (tangential, axial, or radial). The digitized data was comprised of 2048 data points. Figures 4 and 5 depict how the vibration measurement data was broken down and stored into the various files. Although the figures show only one machine record for each compressor type, the same format was utilized for each recorded vibration measurement data set.

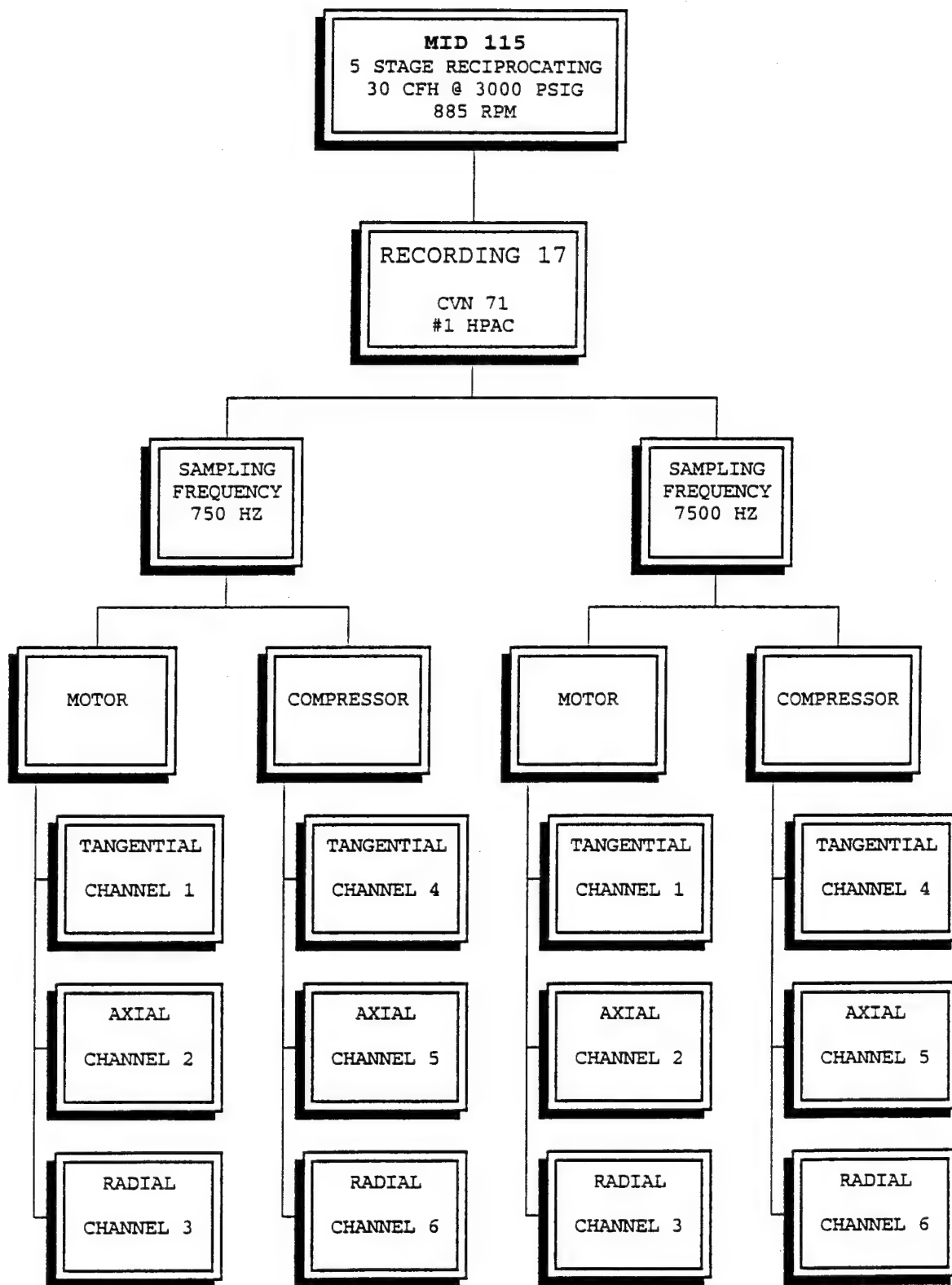


FIGURE 4: MID 115 Vibration Measurement Data Organization

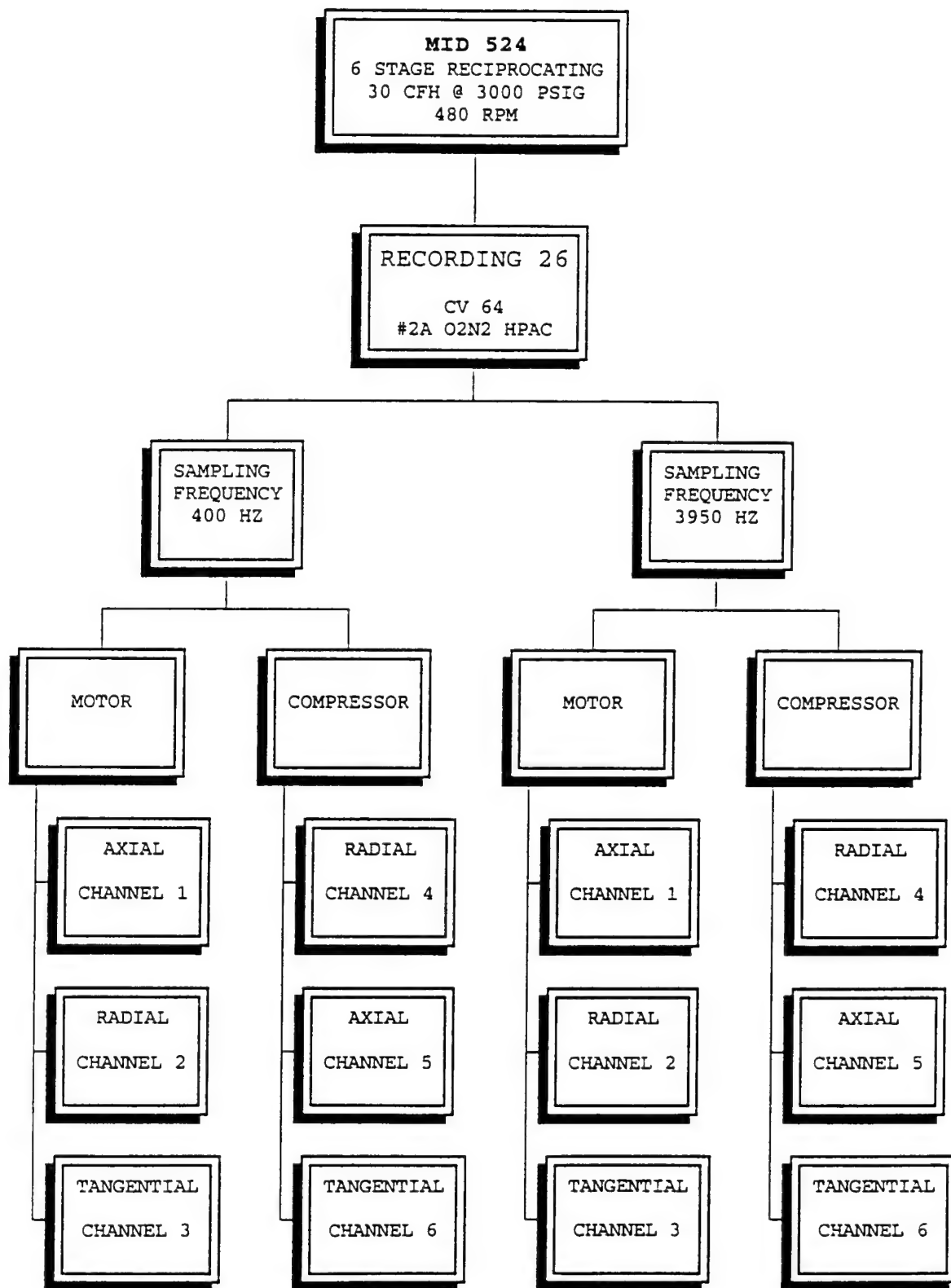


FIGURE 5: MID 524 Vibration Measurement Data Organization

Sampling frequencies were selected based on the information provided in the VTAGs for each machine. In order to prevent aliasing, five times the analysis range for the machine frequencies was used as the sampling frequencies during the data acquisition process. For the MID 115 type compressor sampling frequencies of 750HZ (5 X 150HZ) for the low end and 7500HZ (5 X 1500HZ) for the high end were used. The MID 524 type compressor had a much lower analysis range. Thus frequencies of 400HZ (5 X 80HZ) and 3950HZ (5 X 790HZ) were used for the low and high sampling frequencies respectively.

The data was then loaded into the **MATLAB**[®] software environment to display the time domain information and to transform that information to display the frequency spectrum. Using the data obtained from the analog tape through **EASYEST**[™] **LX**, time domain representations of the vibration signals were then plotted from the **MATLAB**[®] environment via a Hewlett-Packard Laserjet 4 printer. The Fast Fourier Transform (FFT) was calculated by using a program written using **MATLAB**[®] to obtain the frequency domain representation. The program code for the FFT can be found in the Appendix.

The Graphical representations for the time domain and the spectrum of the measured vibration signals were compared for each machine type to establish general machine trending. For example, two vibration records for the MID 115 type compressor were compared at both low and high sampling frequency in each

sampling direction against each other. Signal sampling directions (i.e. tangential, axial, and radial) were established in the tape log provided by PERA(CV). It was felt that by comparing time and frequency domain representations of the vibration measurements the transducer orientation and locations could be verified. As previously established, reciprocating machine vibration signals are time dependent thus no two signals were identical. However, signal trends could be mapped to correlate data between like machines for different sampling periods. After mapping like graphical displays, no conclusive evidence was found to discount the information provided in the tape log. The transducer pick-up directions were assumed to be correct and general vibration trends for the two types of compressor units were able to be established.

C. TIME DOMAIN AND FREQUENCY SPECTRUM REPRESENTATIONS

Figures 6 through 11 show the time domain and spectrum for a MID 115 type compressor taken on the compressor component of the unit at the established low sampling frequency. The figures are arranged in a sequence to allow the time domain representation to be viewed first followed by the corresponding frequency spectrum. The first pair of figures show the data collected in the tangential direction. The next pair of figures display the data in the axial direction with the data collected in the radial direction immediately following. Figures 12 through 17 show the same vibration measurement signals but at the established high sampling frequency. These figures are also presented in the same sequence as established above. Although the tape log provided a continuous record from the compressor and motor components of the high-pressure air compressor units during the period data was collected, the process to convert the vibration measurement signals from analog to digital format created discontinuities in the actual time periods displayed in the figures. A direct comparison between the time periods of the vibration measurement signals captured at different sampling frequencies cannot be made. The signals in this case have been shifted by a finite time differential between the low sampling frequency data and the high sampling frequency data. Figures 18 through 29 apply to a MID 524 type compressor.

MID 115 COMPRESSOR COMPONENT

Number of Sampling Data Points = 2048

Mean Value = -0.0122

Standard Deviation = 0.1108

REC17CT7.ASC

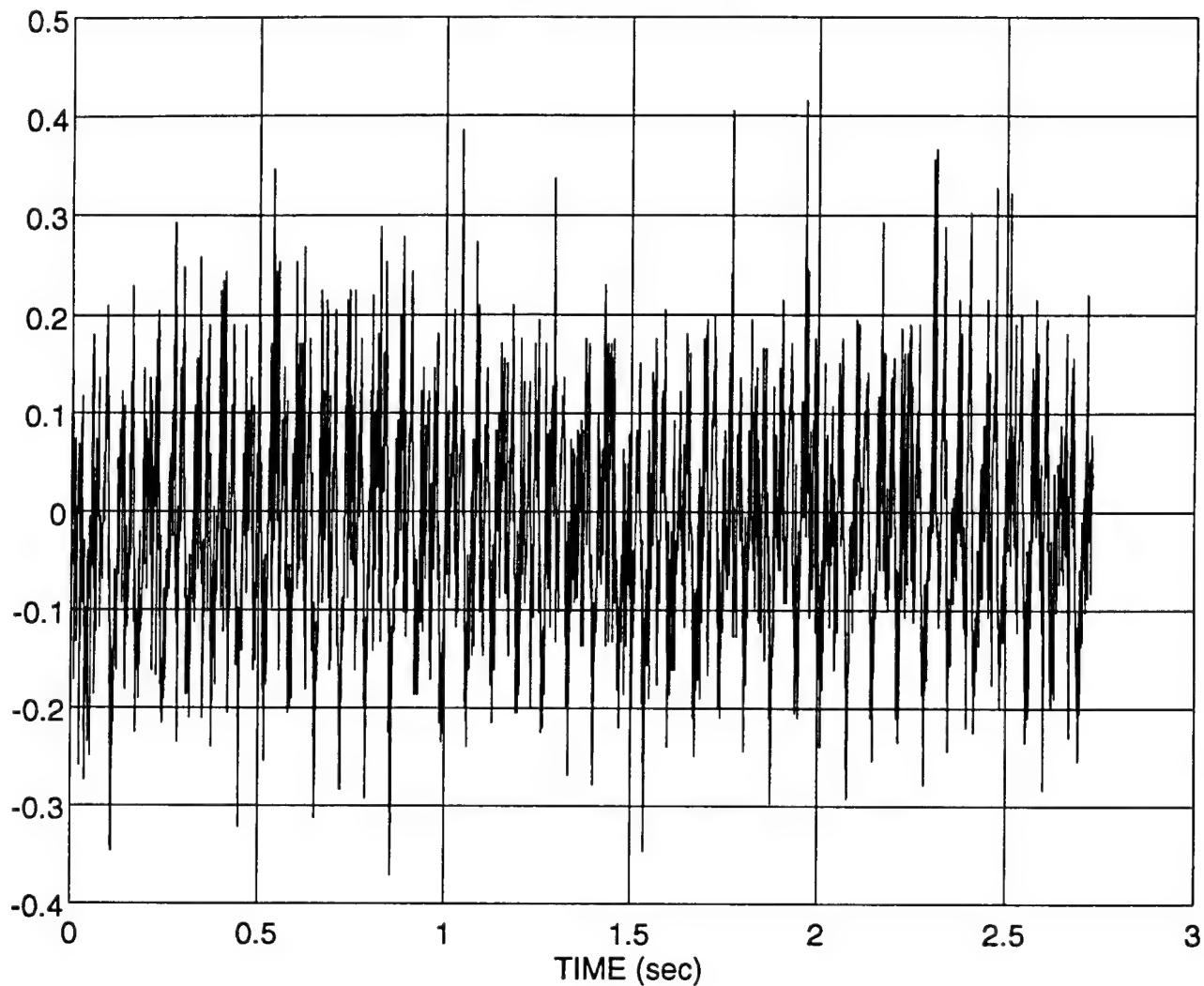
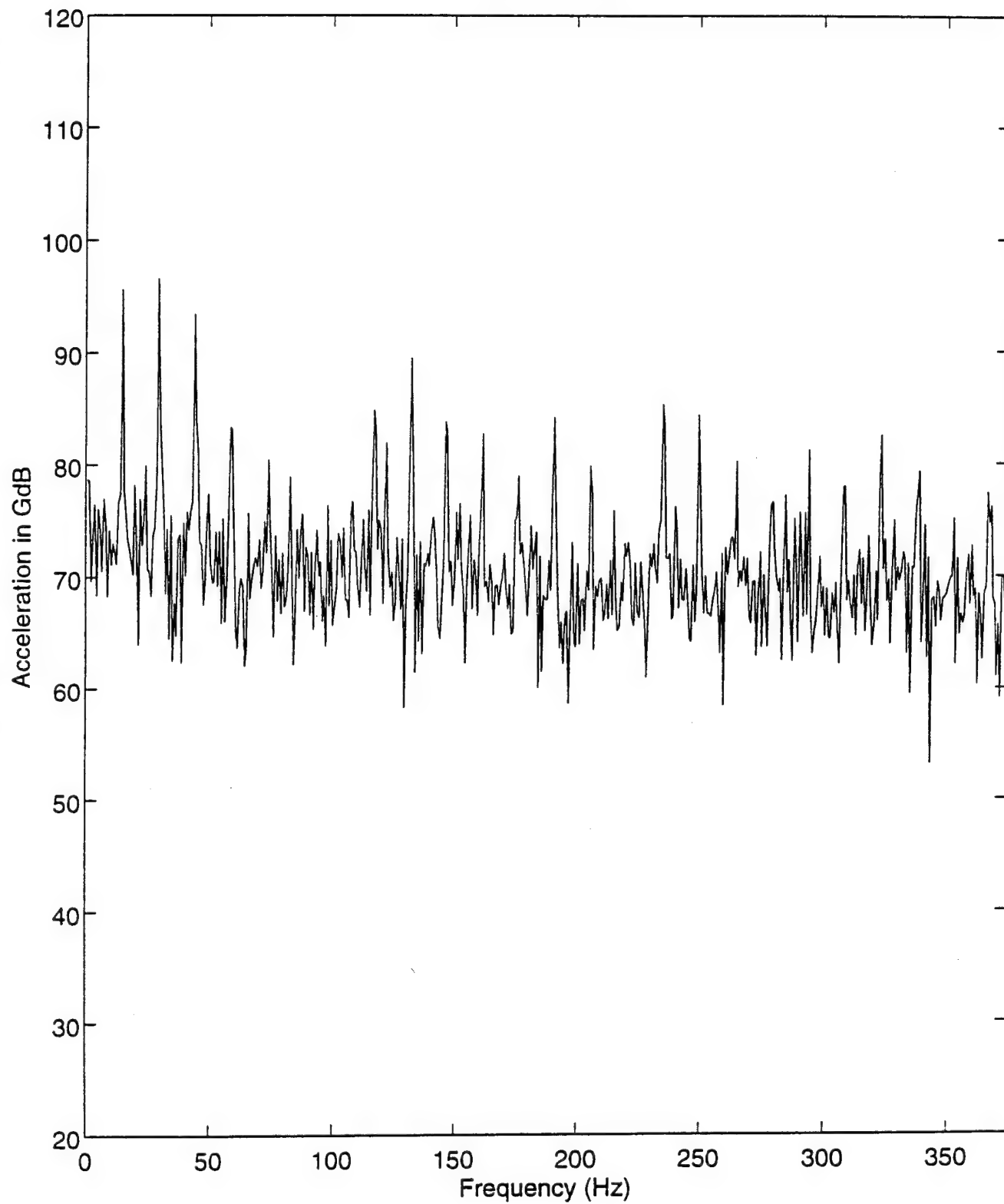


FIGURE 6: MID 115 Compressor Component Sampled at 750 HZ
Tangential Direction

REC17CT7



**FIGURE 7: MID 115 Compressor Component FFT
Sampled at 750 HZ, Tangential Direction**

MID 115 COMPRESSOR COMPONENT

Number of Sampling Data Points = 2048

Mean Value = -0.0577

Standard Deviation = 0.1083

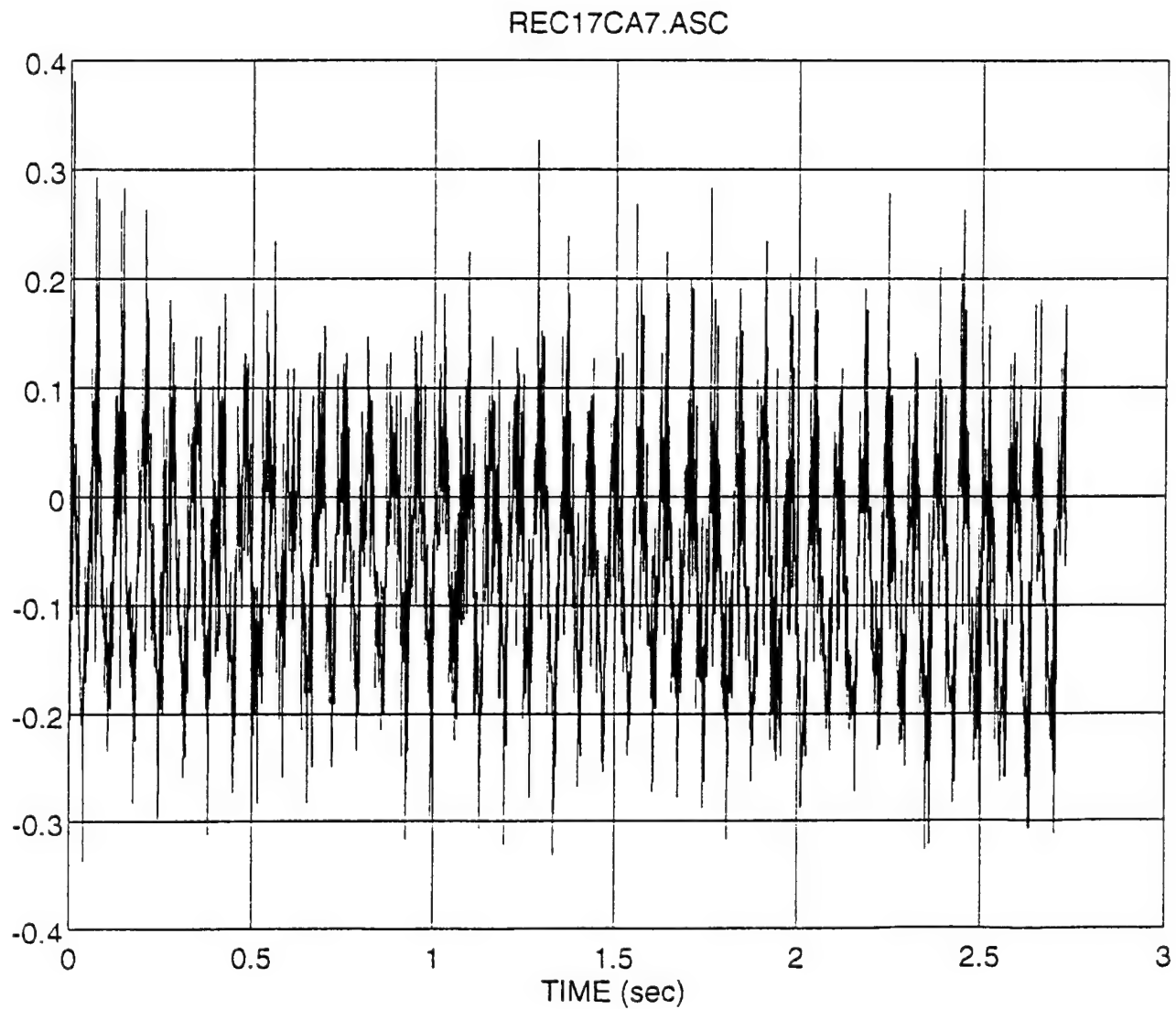


FIGURE 8: MID 115 Compressor Component Sampled at 750 HZ
Axial Direction

REC17CA7

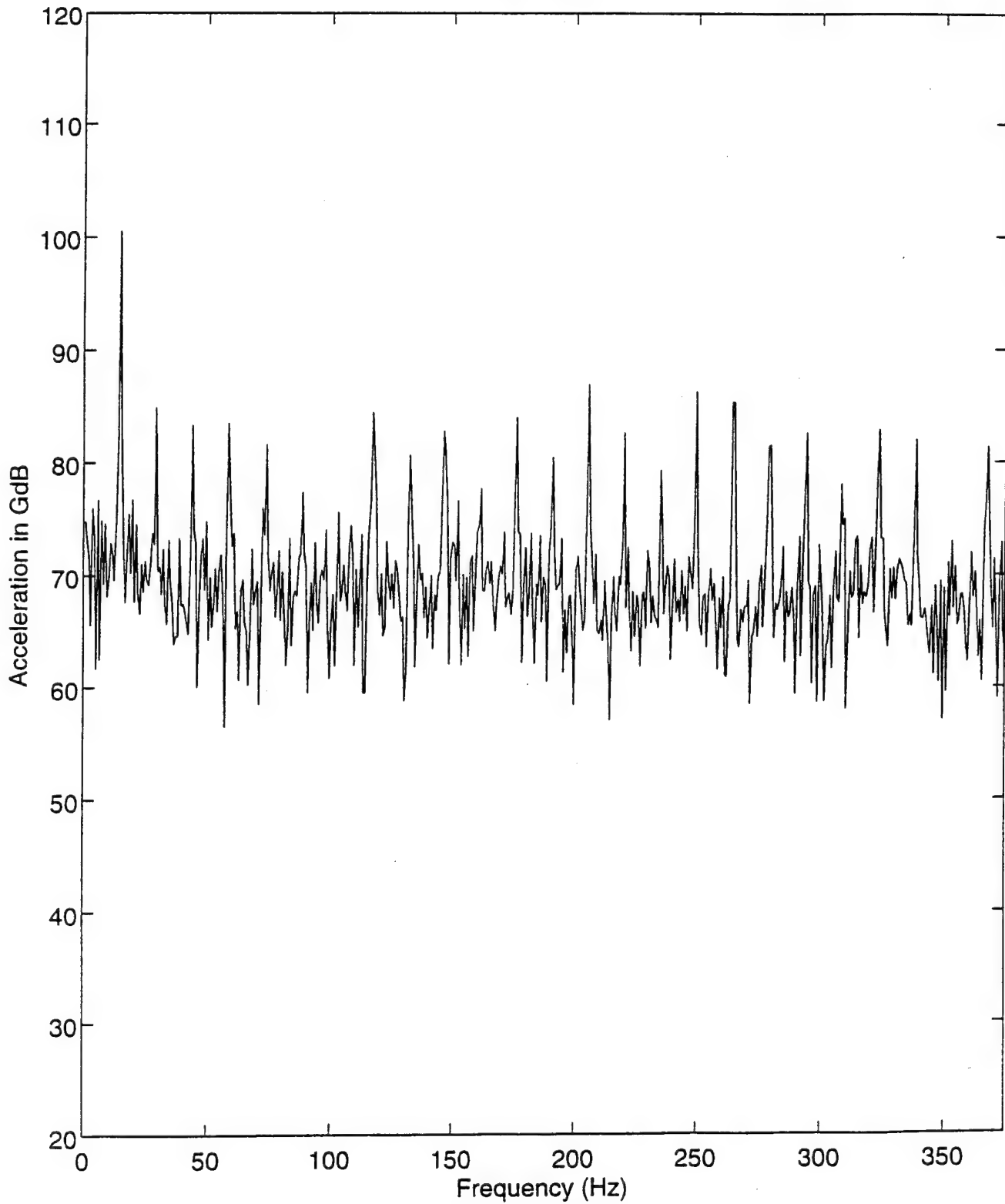


FIGURE 9: MID 115 Compressor Component FFT
Sampled at 750 HZ, Axial Direction

MID 115 COMPRESSOR COMPONENT

Number of Sampling Data Points = 2048

Mean Value = -0.0420

Standard Deviation = 0.1641

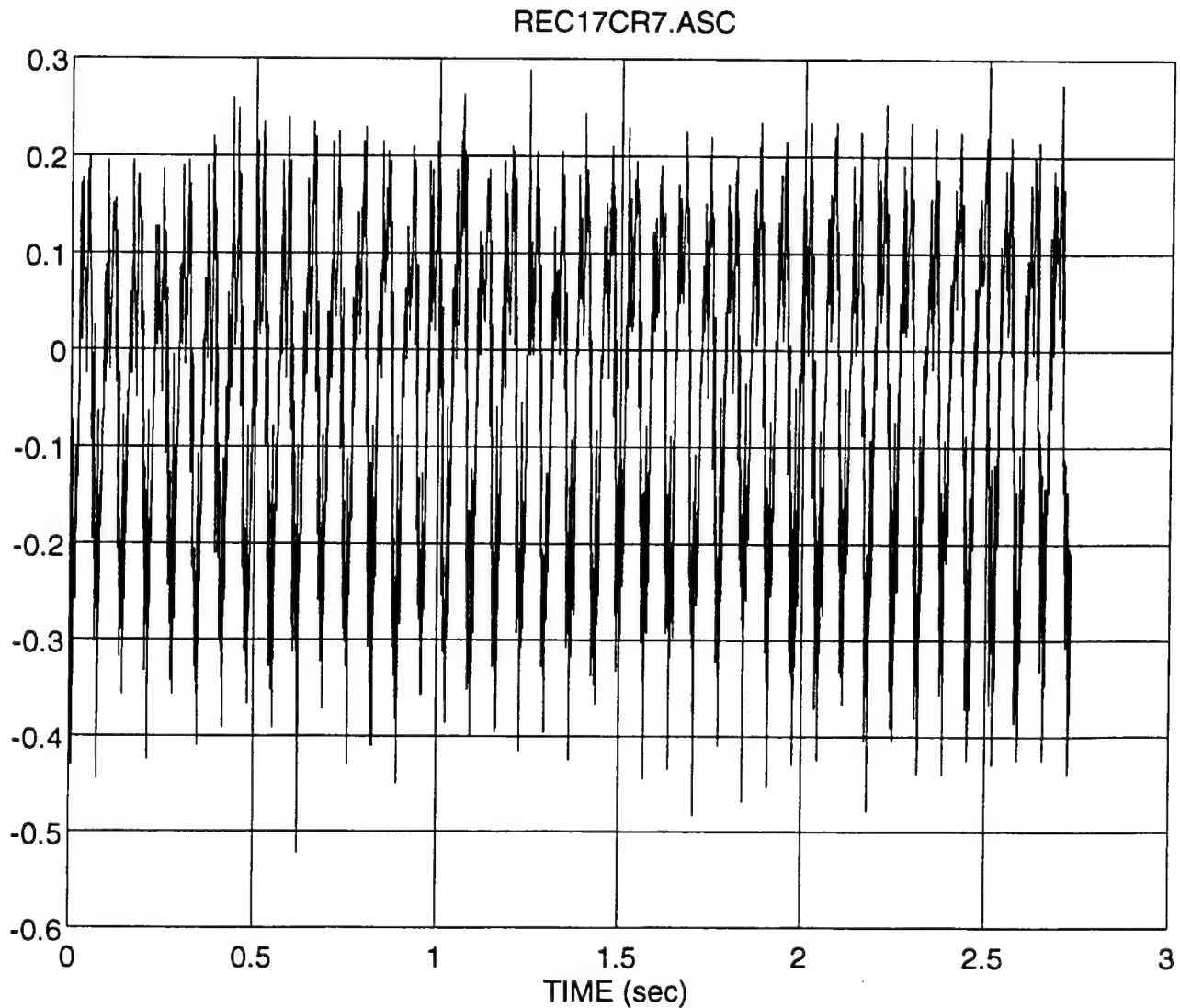
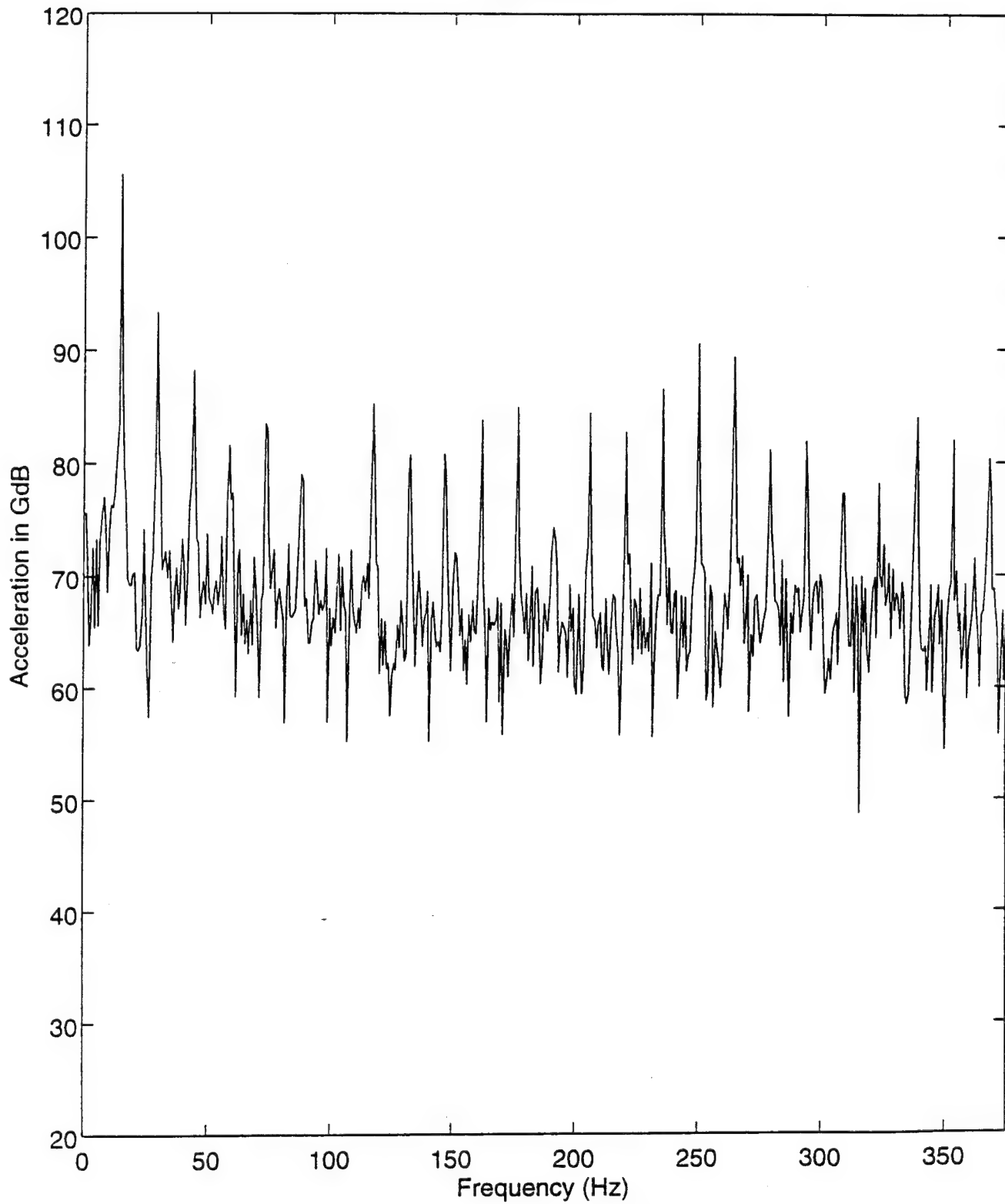


FIGURE 10: MID 115 Compressor Component Sampled at 750 HZ
Radial Direction

REC17CR7



**FIGURE 11: MID 115 Compressor Component FFT
Sampled at 750 HZ, Radial Direction**

MID 115 COMPRESSOR COMPONENT

Number of Sampling Data Points = 2048

Mean Value = -0.0174

Standard Deviation = 0.1159

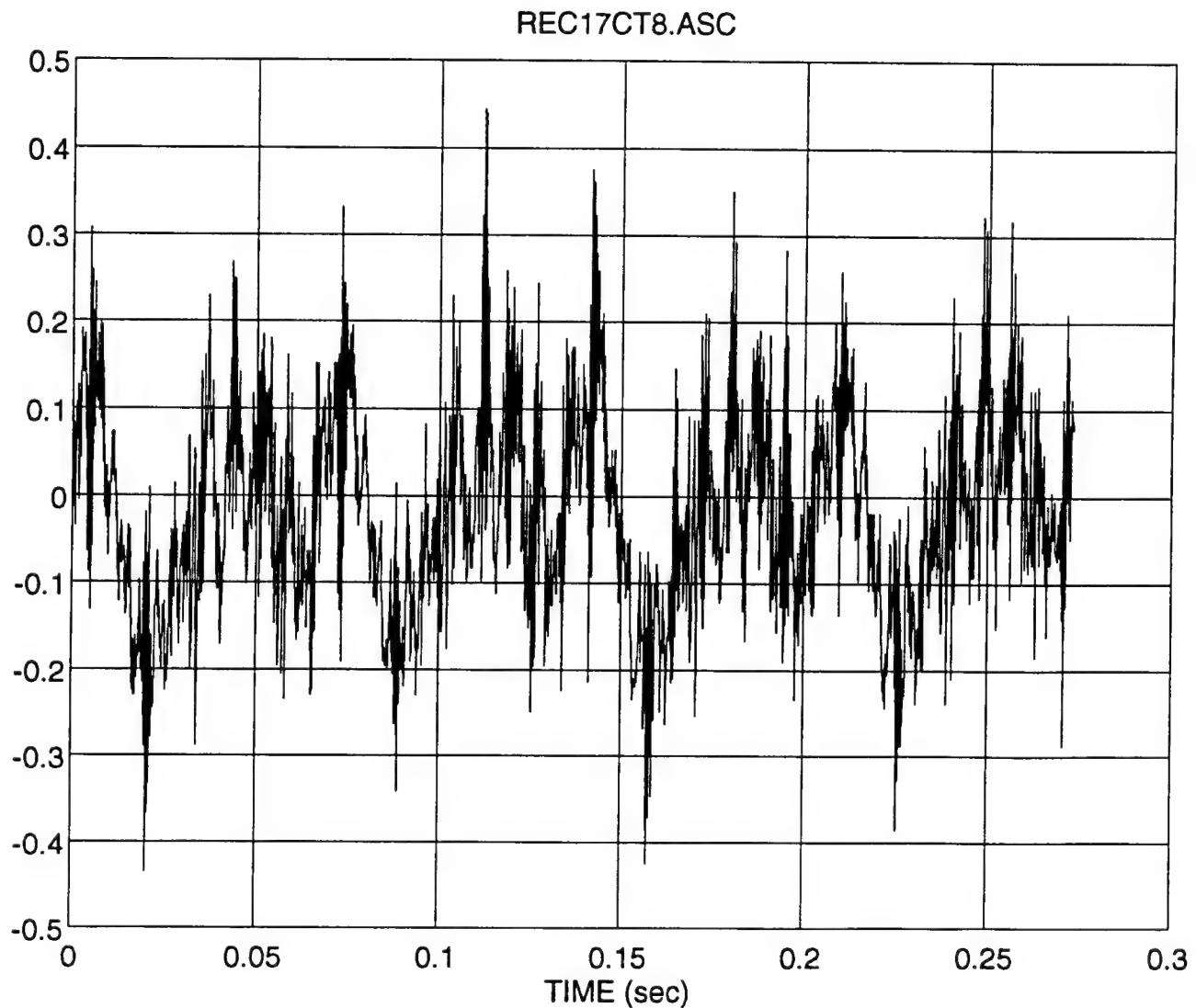
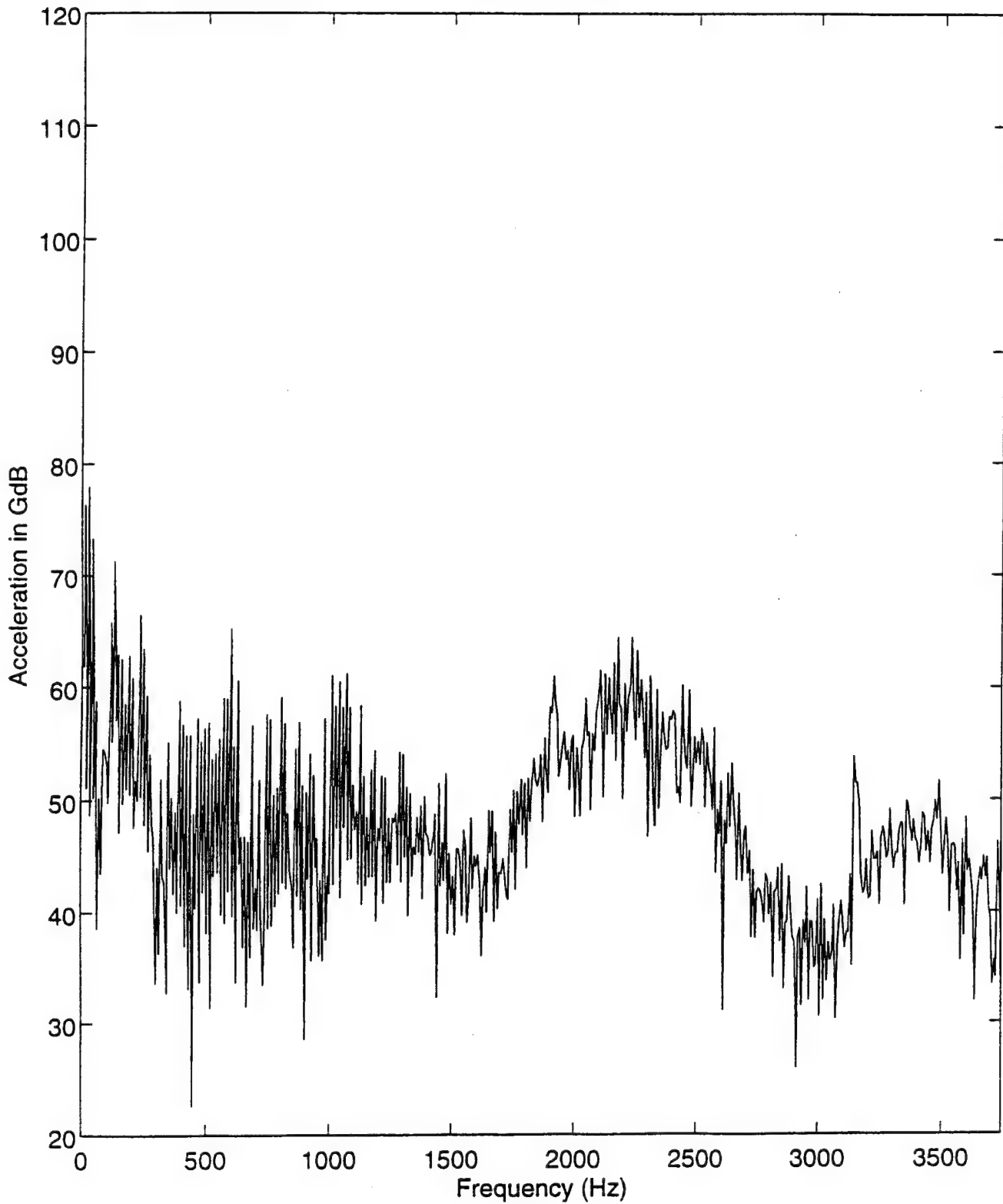


FIGURE 12: MID 115 Compressor Component Sampled at 7500 HZ
Tangential Direction

REC17CT8



**FIGURE 13: MID 115 Compressor Component FFT
Sampled at 7500 HZ, Tangential Direction**

MID 115 COMPRESSOR COMPONENT

Number of Sampling Data Points = 2048

Mean Value = -0.0608

Standard Deviation = 0.1127

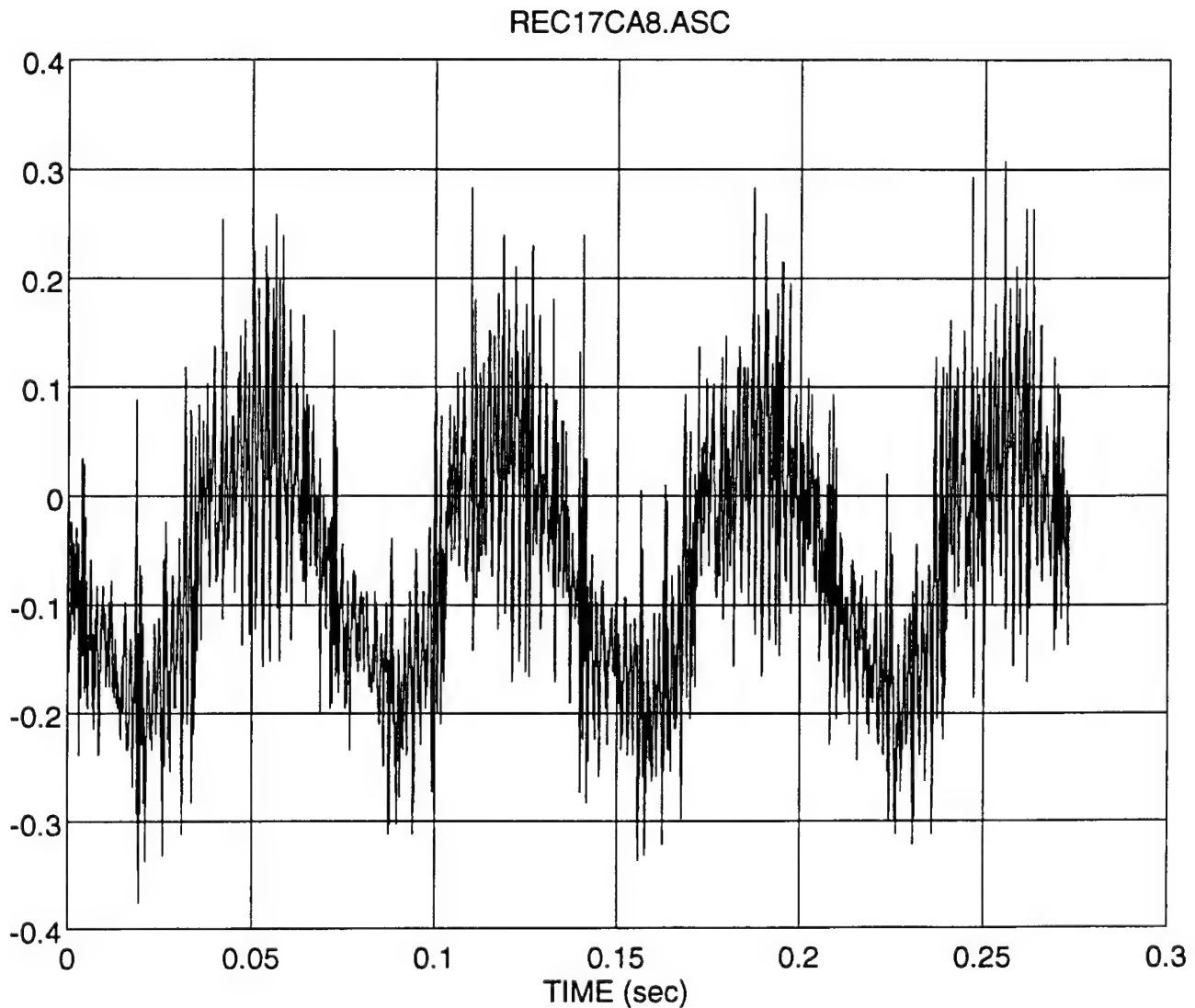
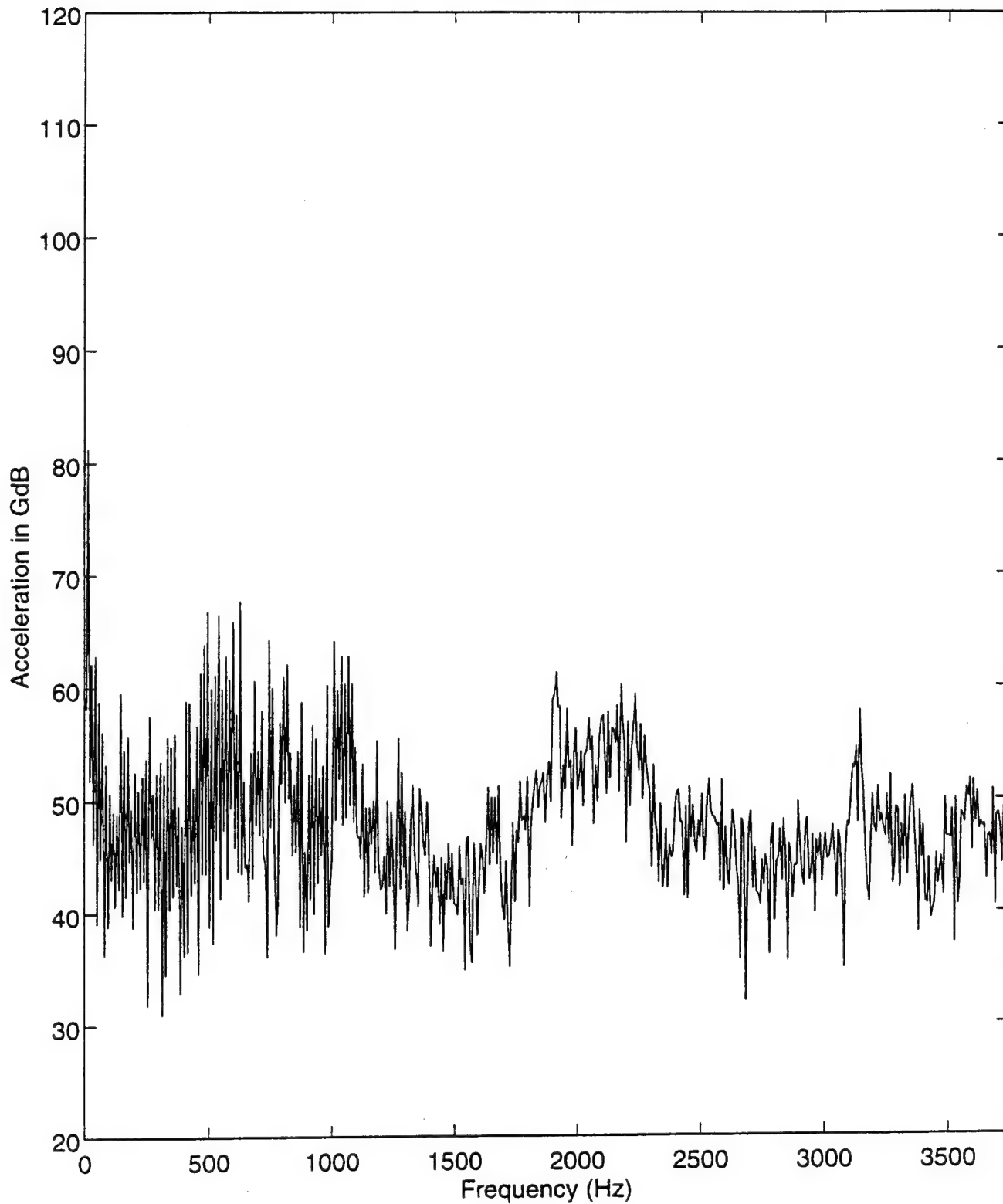


FIGURE 14: MID 115 Compressor Component Sampled at 7500 HZ
Axial Direction

REC17CA8



**FIGURE 15: MID 115 Compressor Component FFT
Sampled at 7500 HZ, Axial Direction**

MID 115 COMPRESSOR COMPONENT

Number of Sampling Data Points = 2048

Mean Value = -0.0445

Standard Deviation = 0.1653

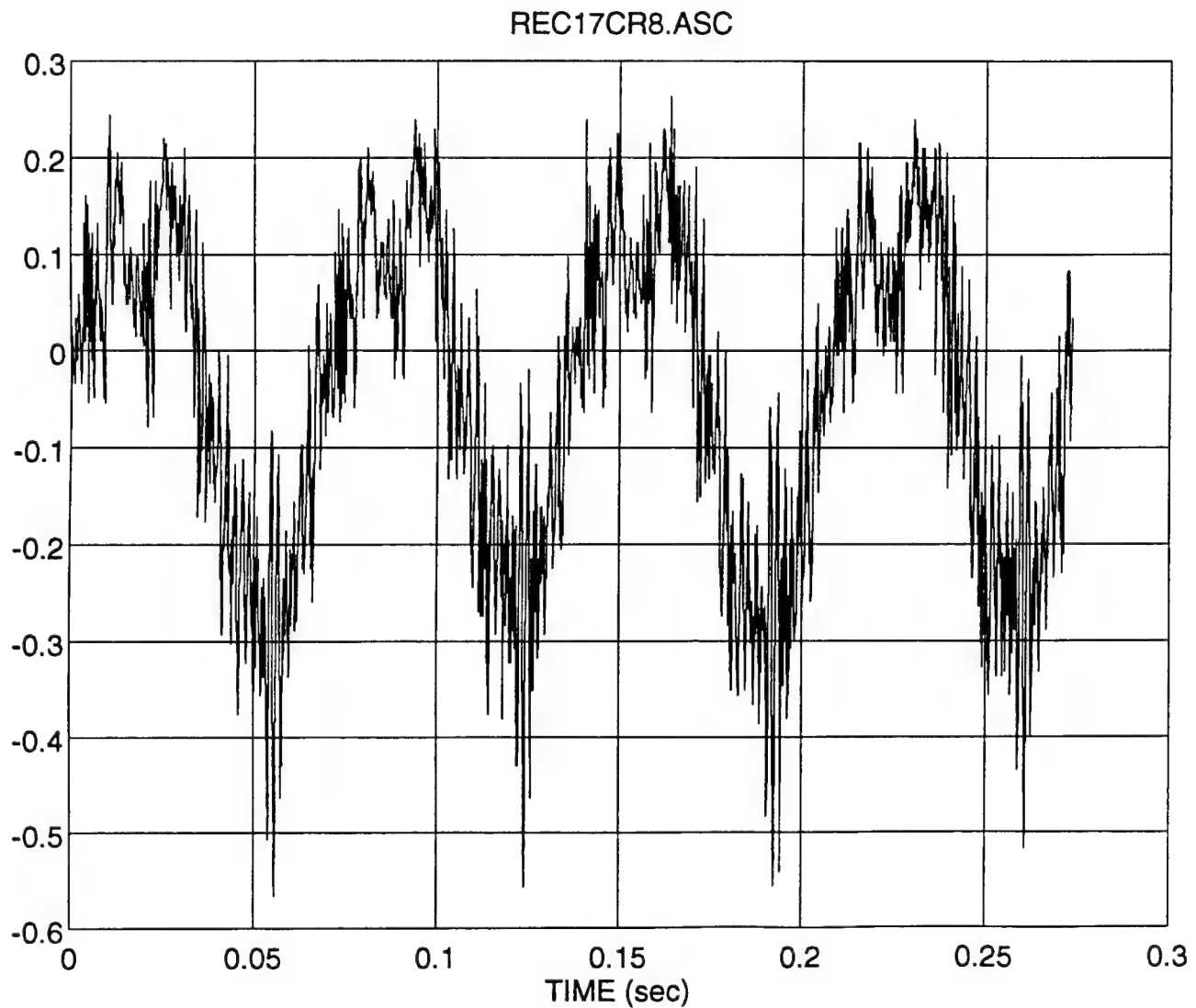
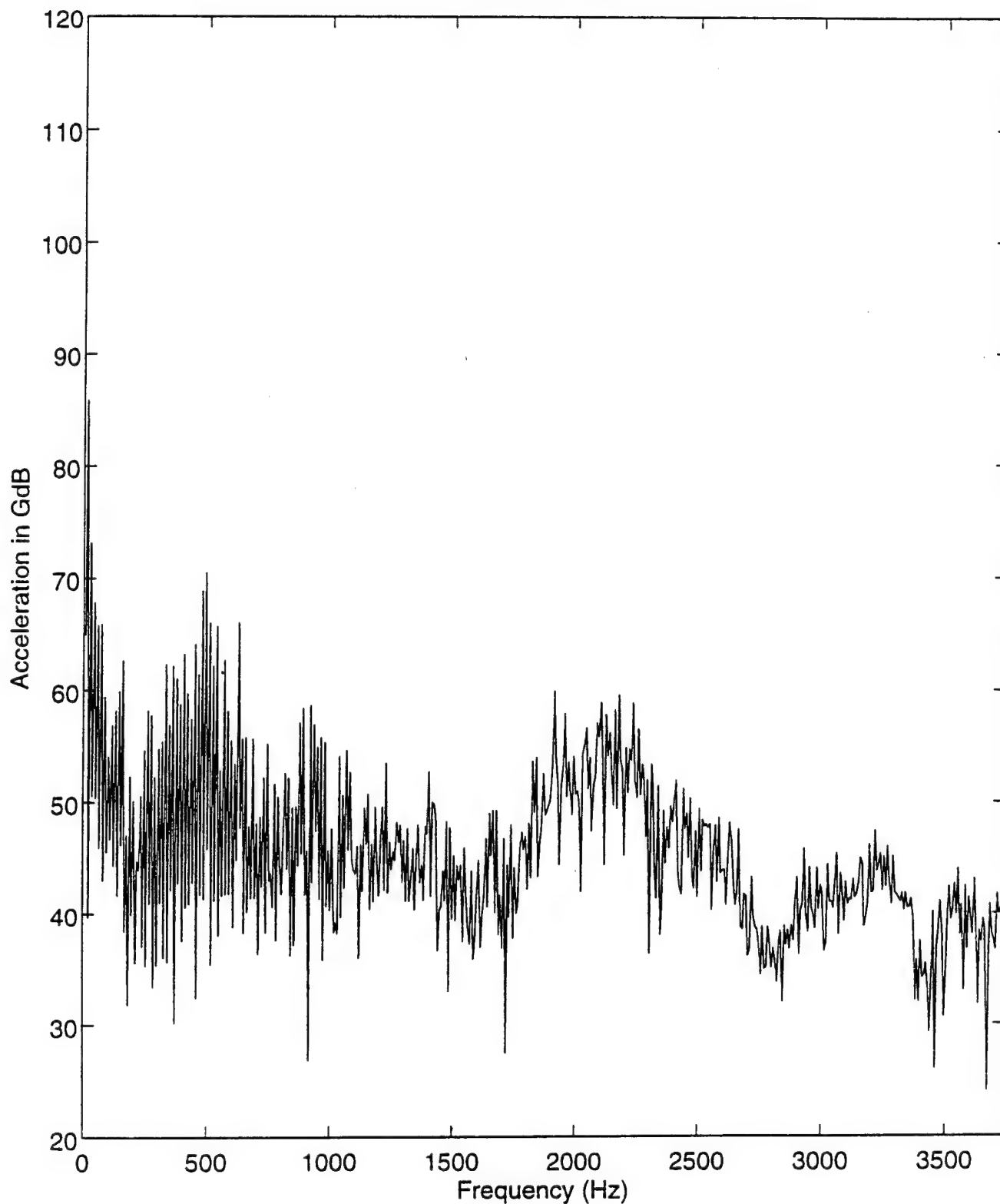


FIGURE 16: MID 115 Compressor Component Sampled at 7500 HZ
Radial Direction

REC17CR8



**FIGURE 17: MID 115 Compressor Component FFT
Sampled at 7500 HZ, Radial Direction**

MID 524 COMPRESSOR COMPONENT

Number of Sampling Data Points = 2048

Mean Value = -0.0151

Standard Deviation = 0.0810

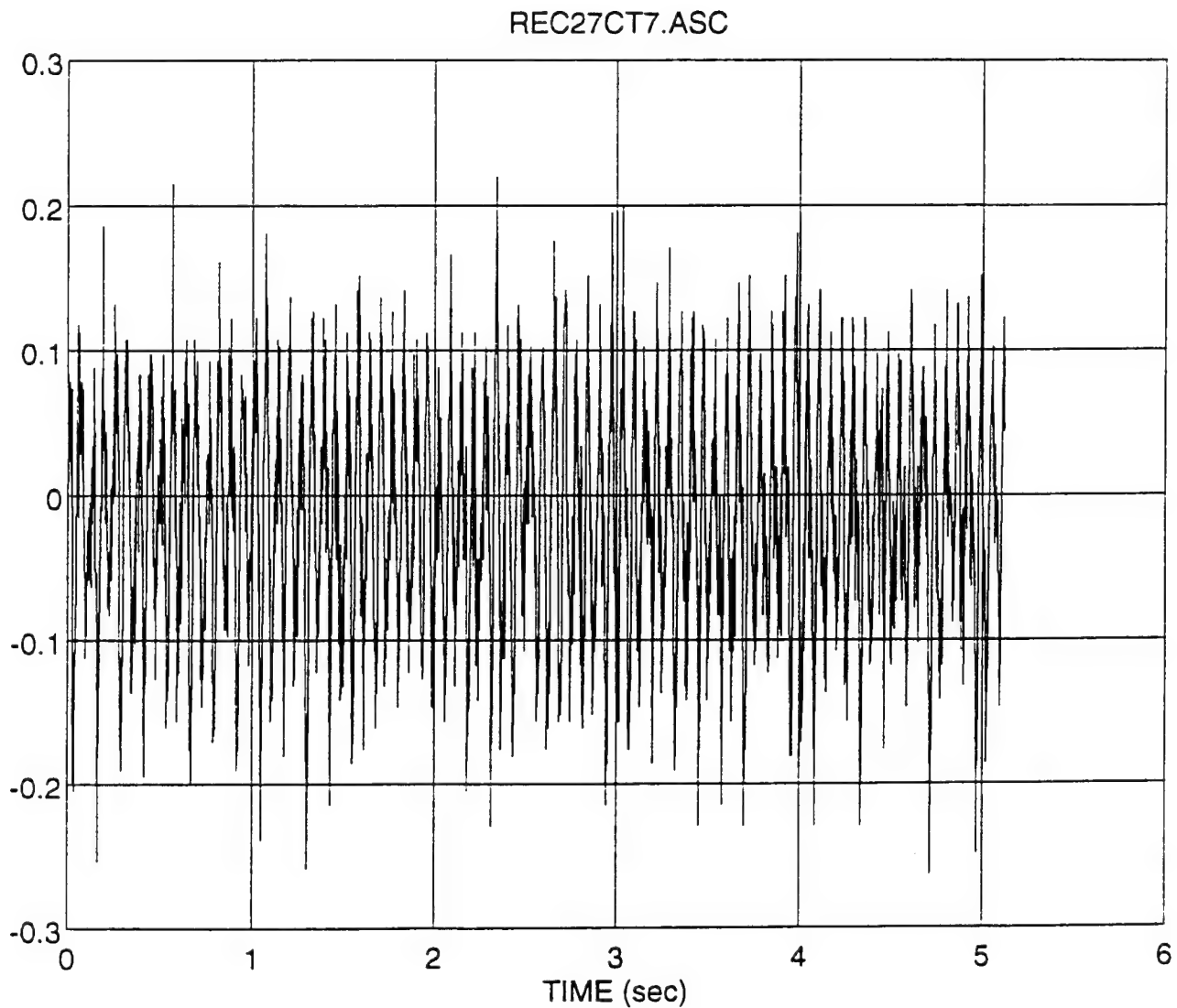
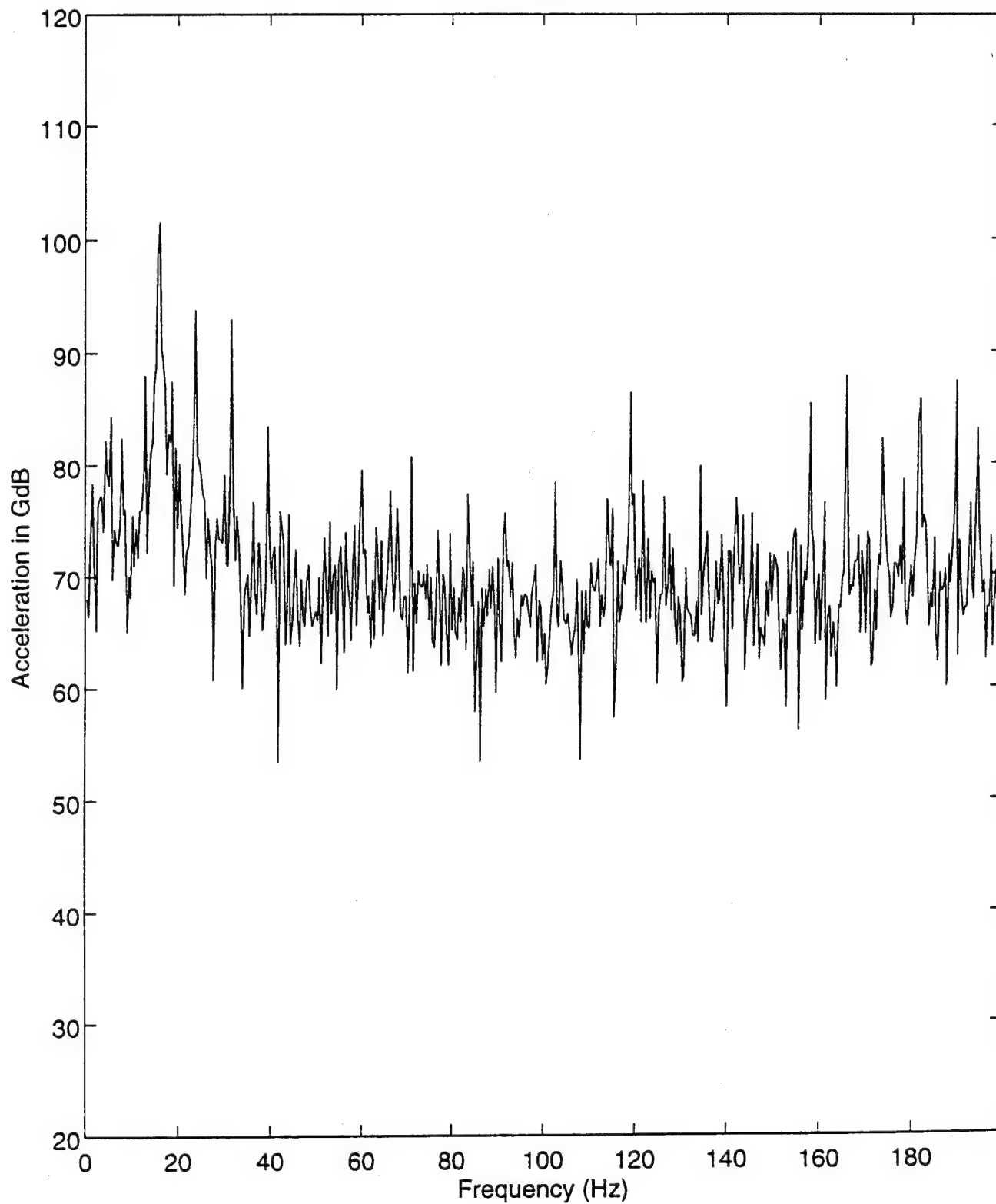


FIGURE 18: MID 524 Compressor Component Sampled at 400 HZ
Tangential Direction

REC27CT7



**FIGURE 19: MID 524 Compressor Component FFT
Sampled at 400 HZ, Tangential Direction**

MID 524 COMPRESSOR COMPONENT

Number of Sampling Data Points = 2048

Mean Value = -0.0125

Standard Deviation = 0.0753

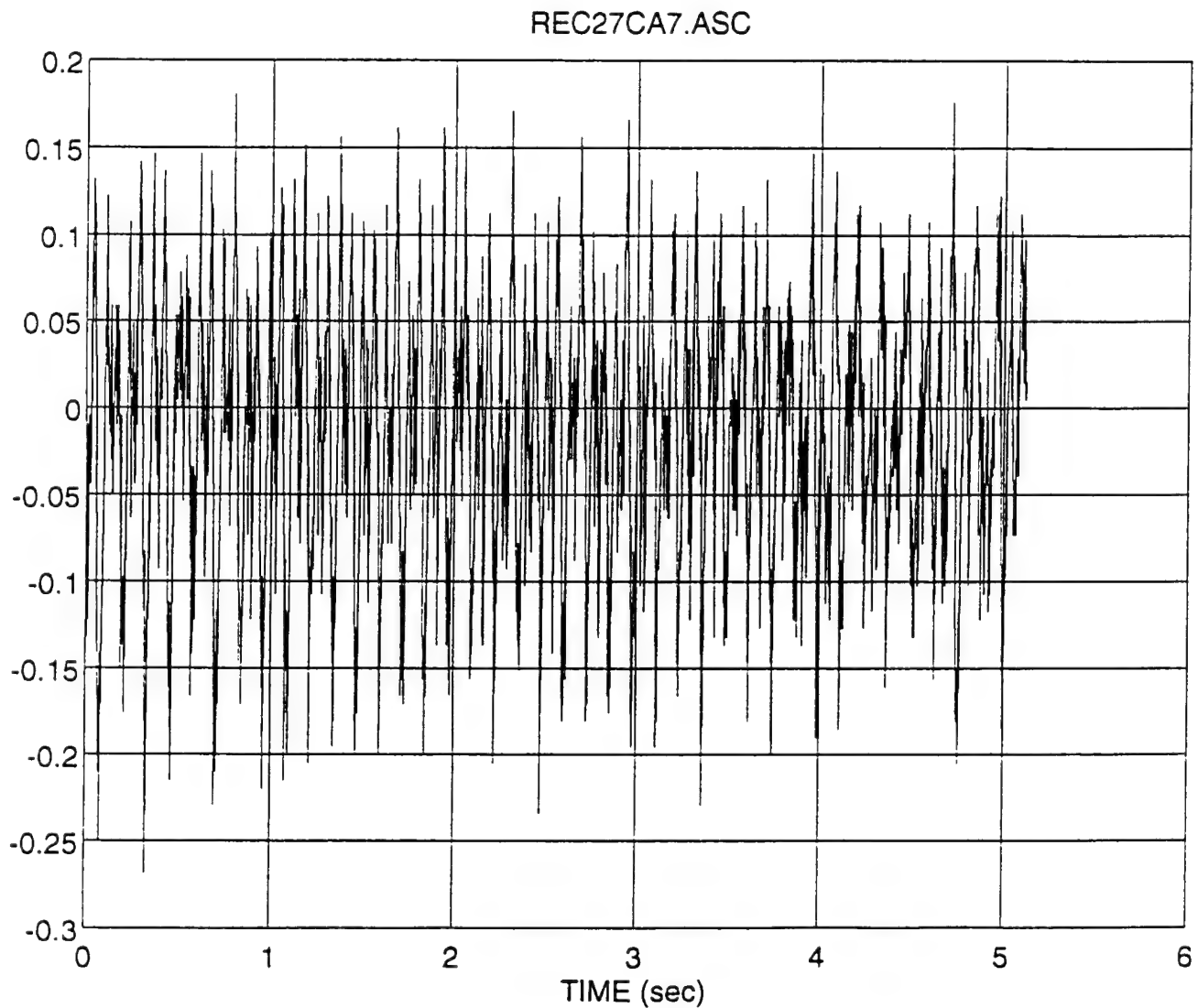


FIGURE 20: MID 524 Compressor Component Sampled at 400 HZ
Axial Direction

REC27CA7

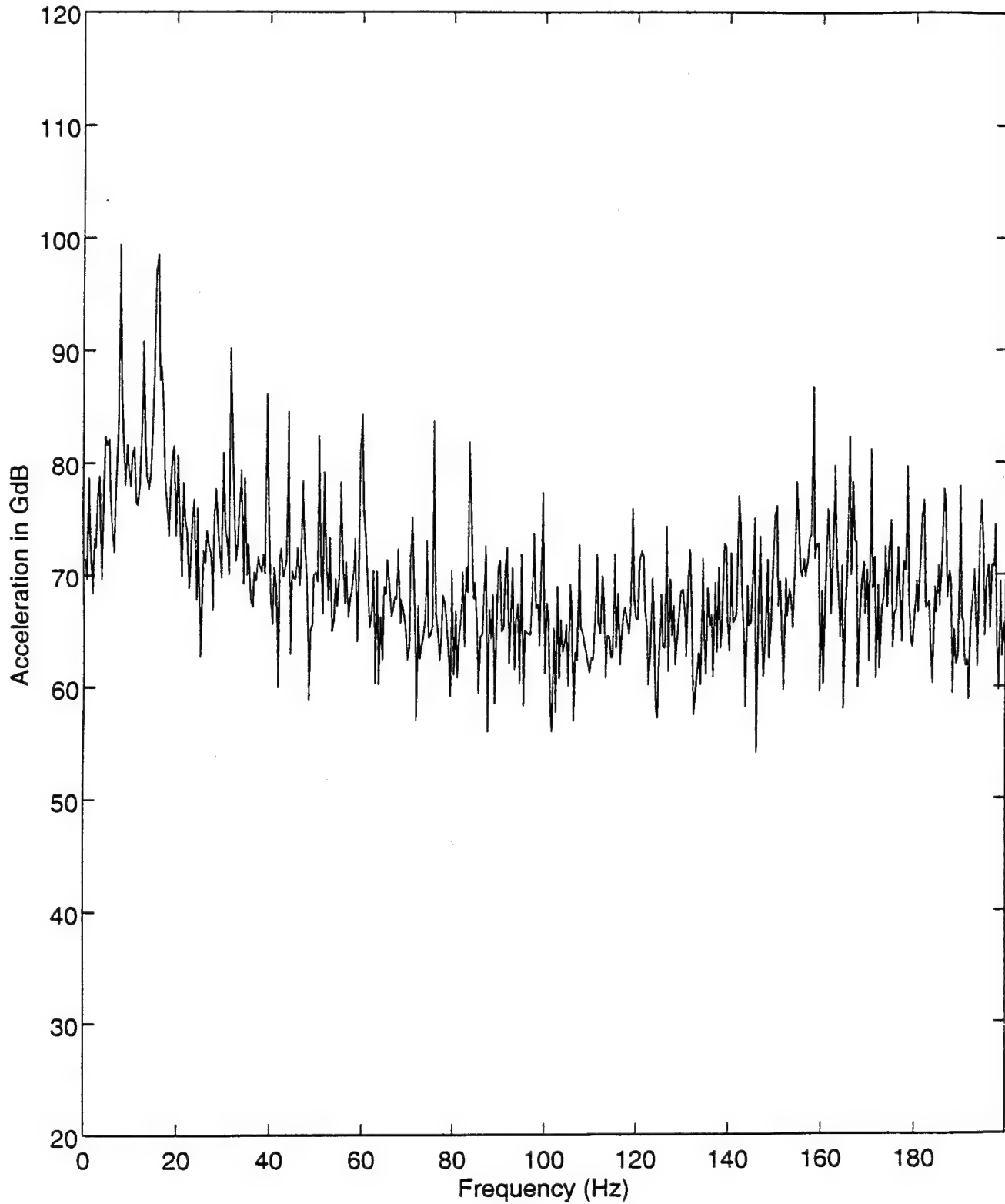


FIGURE 21: MID 524 Compressor Component FFT
Sampled at 400 HZ, Axial Direction

MID 524 COMPRESSOR COMPONENT

Number of Sampling Data Points = 2048

Mean Value = -0.0130

Standard Deviation = 0.0721

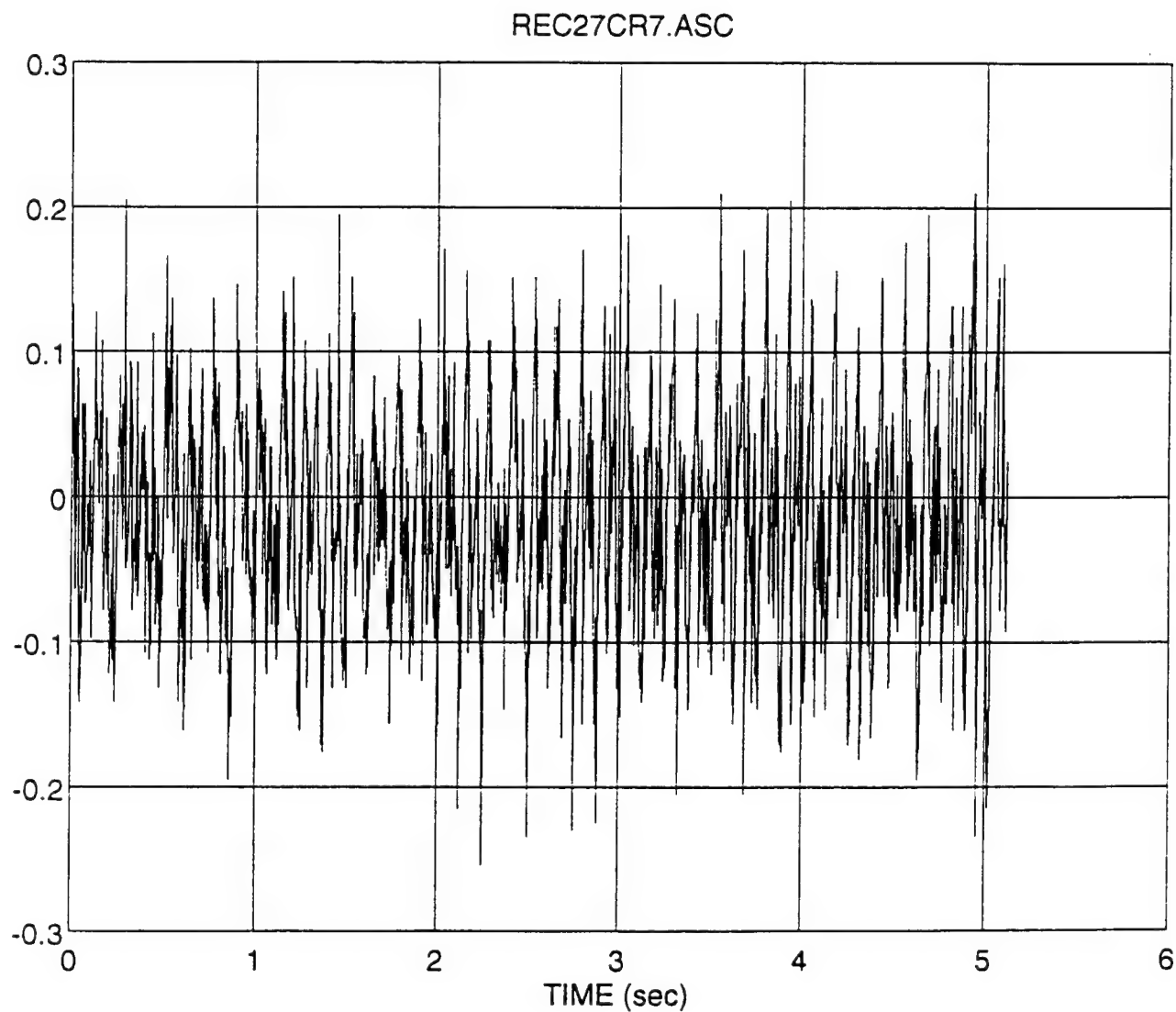
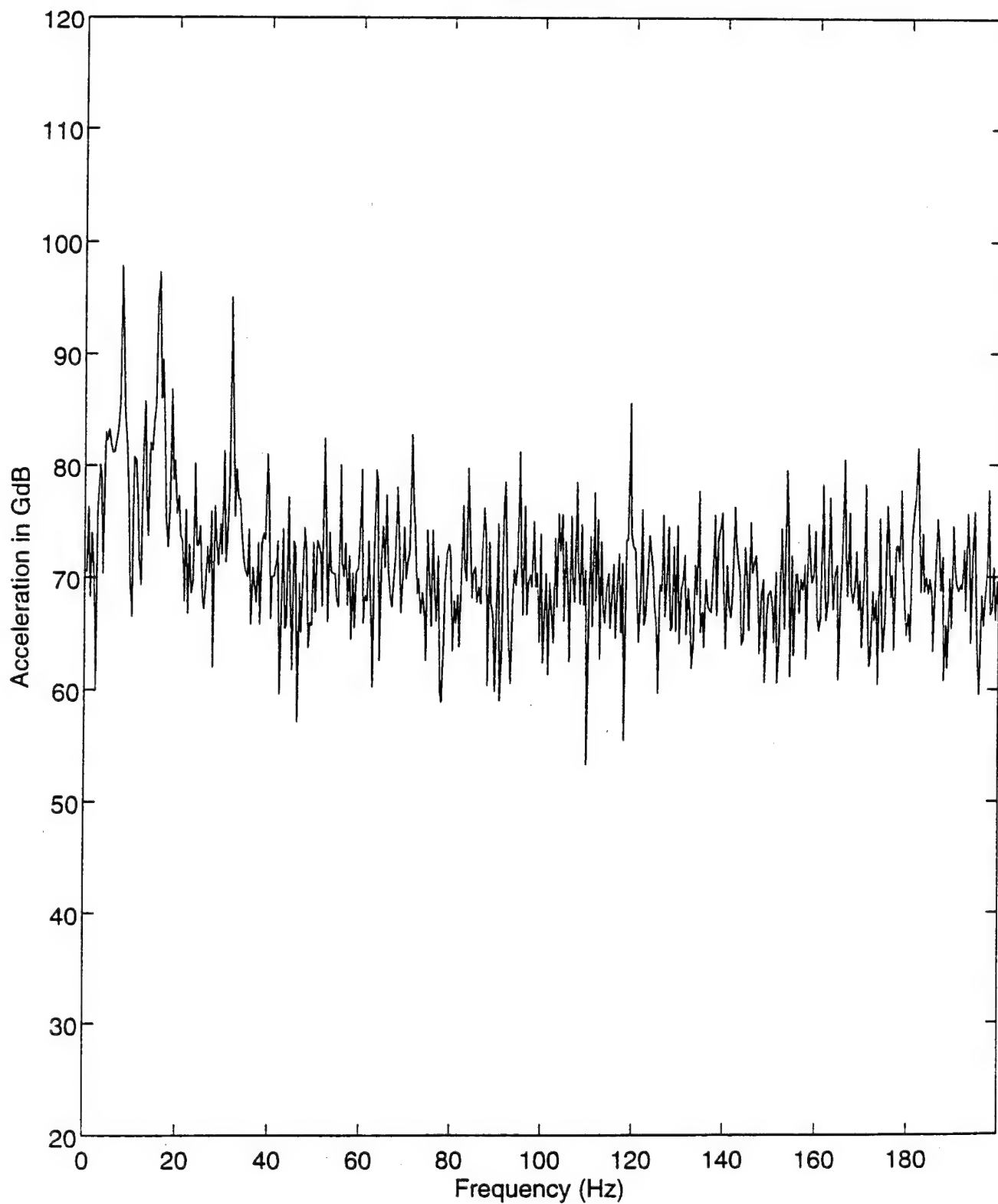


FIGURE 22: MID 524 Compressor Component Sampled at 400 HZ
Radial Direction

REC27CR7



**FIGURE 23: MID 524 Compressor Component FFT
Sampled at 400 HZ, Radial Direction**

MID 524 COMPRESSOR COMPONENT

Number of Sampling Data Points = 2048

Mean Value = -0.0171

Standard Deviation = 0.0811

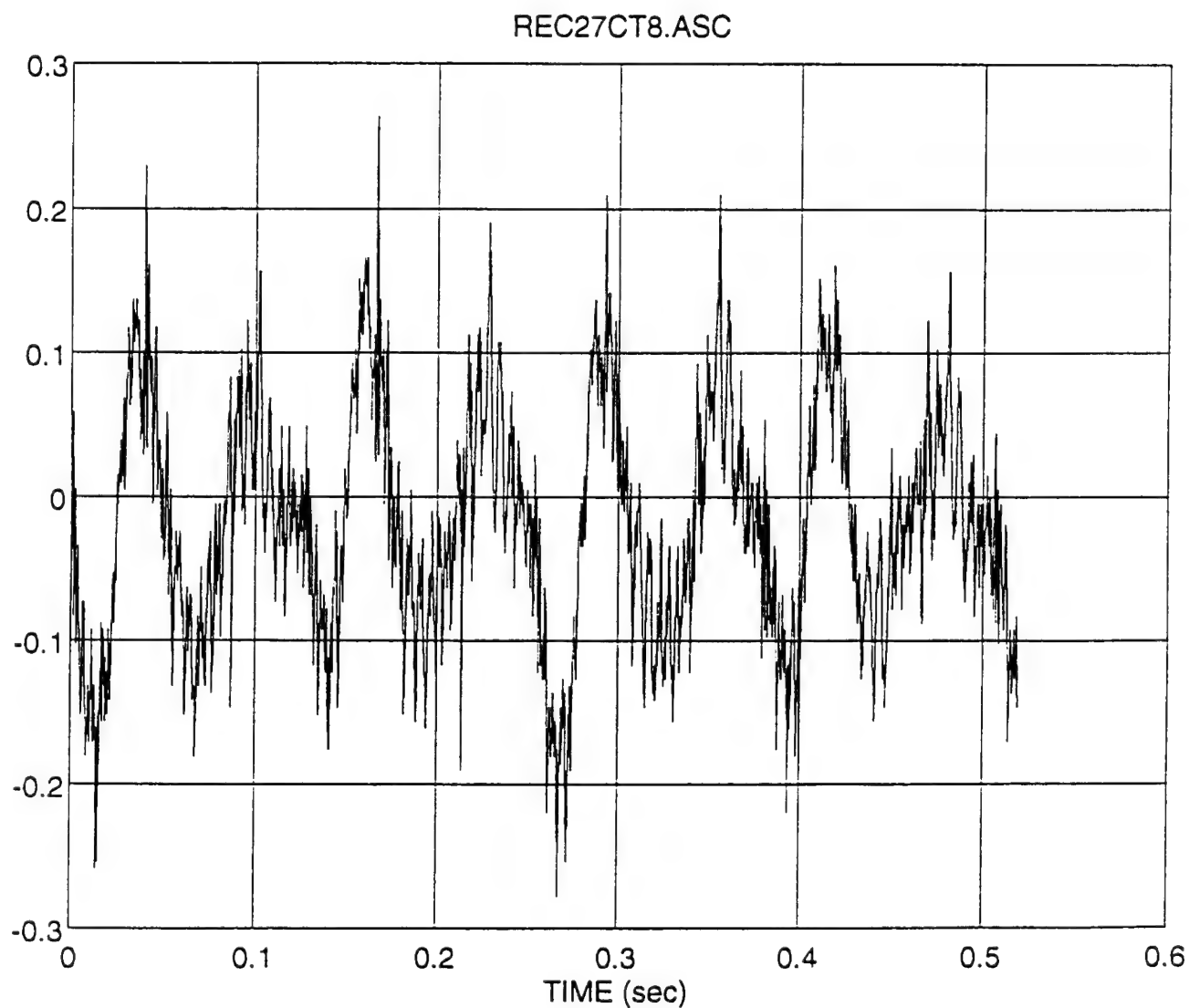
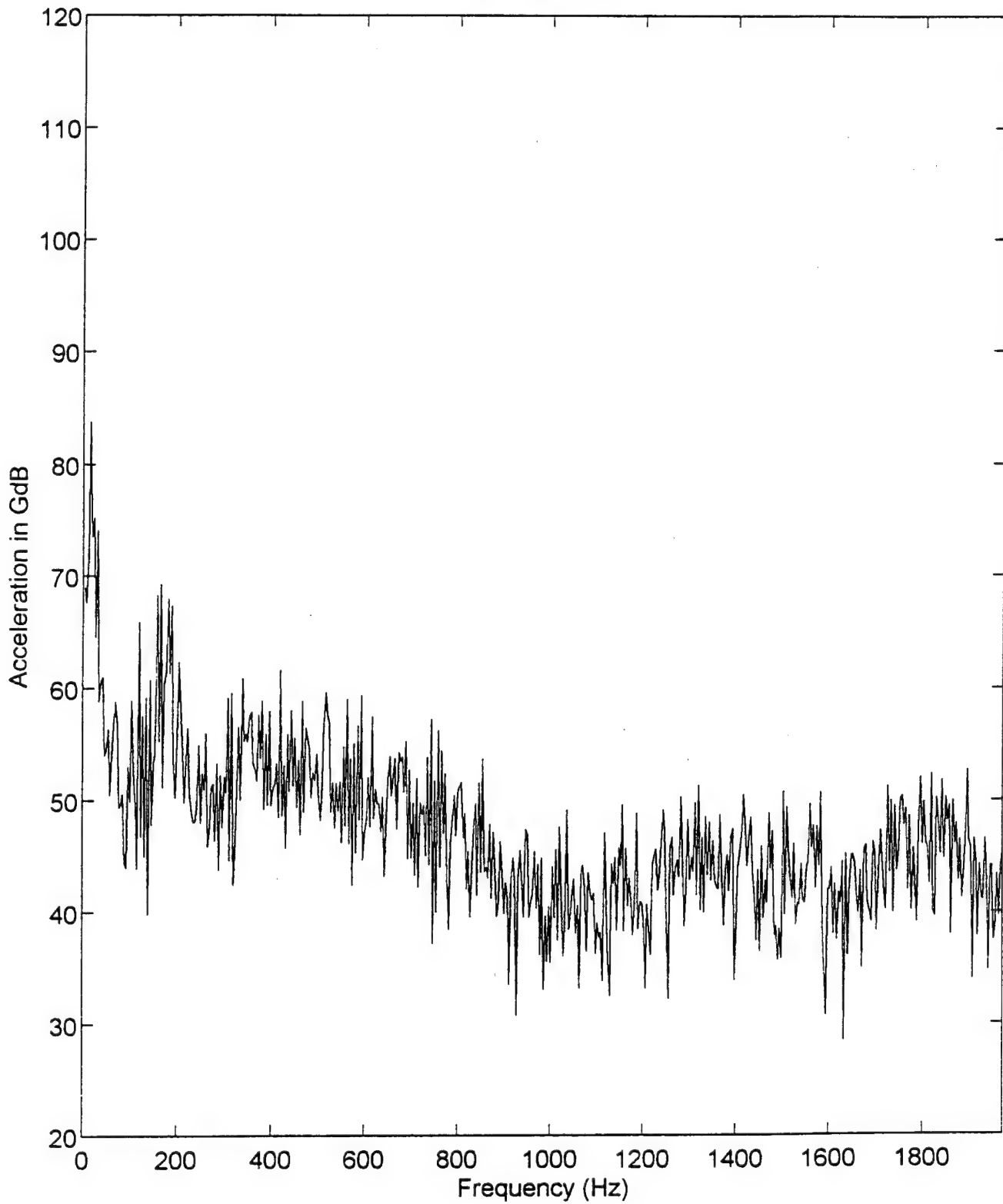


FIGURE 24: MID 524 Compressor Component Sampled at 3950 HZ
Tangential Direction

REC27CT8



**FIGURE 25: MID 524 Compressor Component FFT
Sampled at 3950 HZ, Tangential Direction**

MID 524 COMPRESSOR COMPONENT

Number of Sampling Data Points = 2048

Mean Value = -0.0102

Standard Deviation = 0.0696

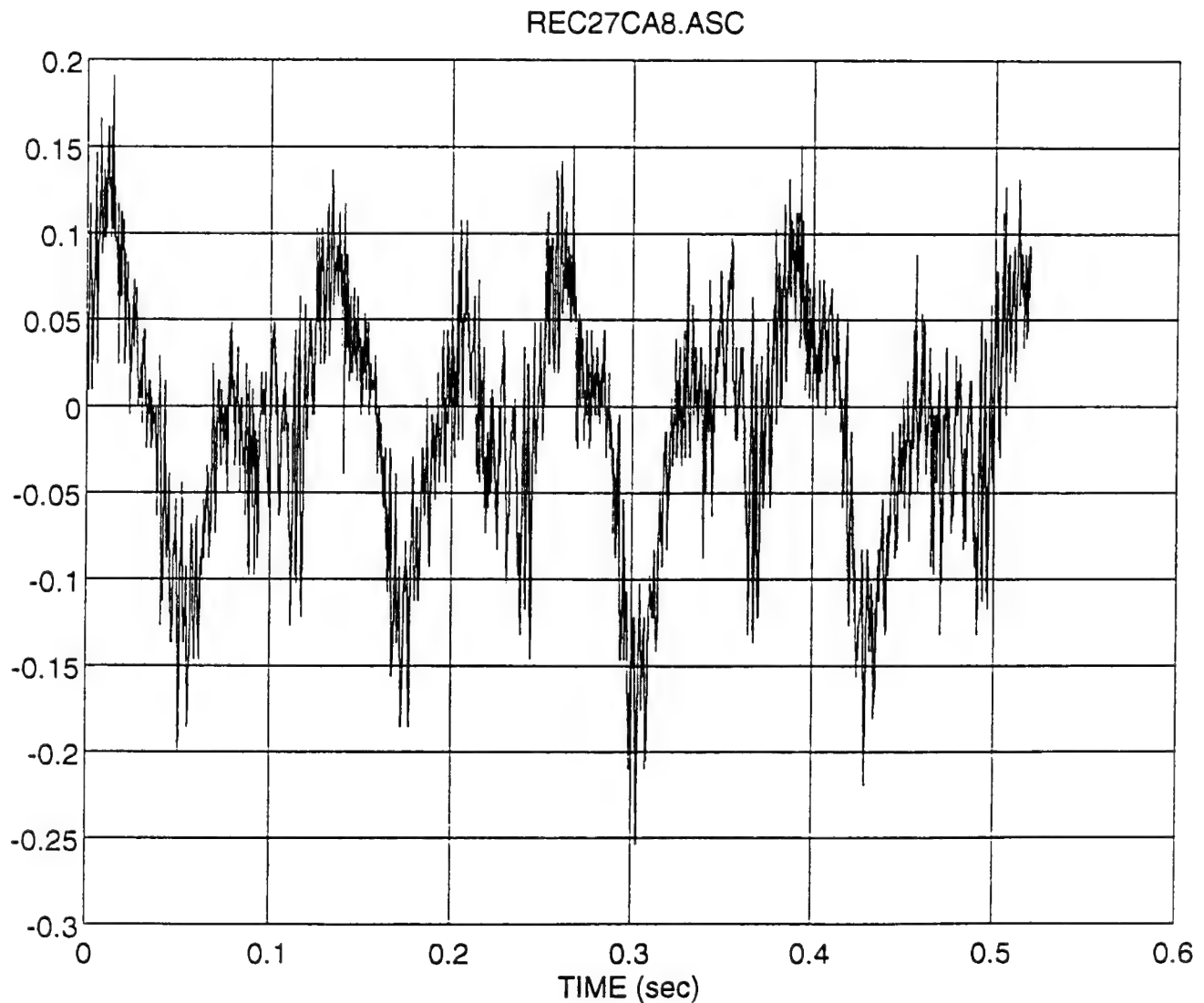


FIGURE 26: MID 524 Compressor Component Sampled at 3950 HZ
Axial Direction

REC27CA8

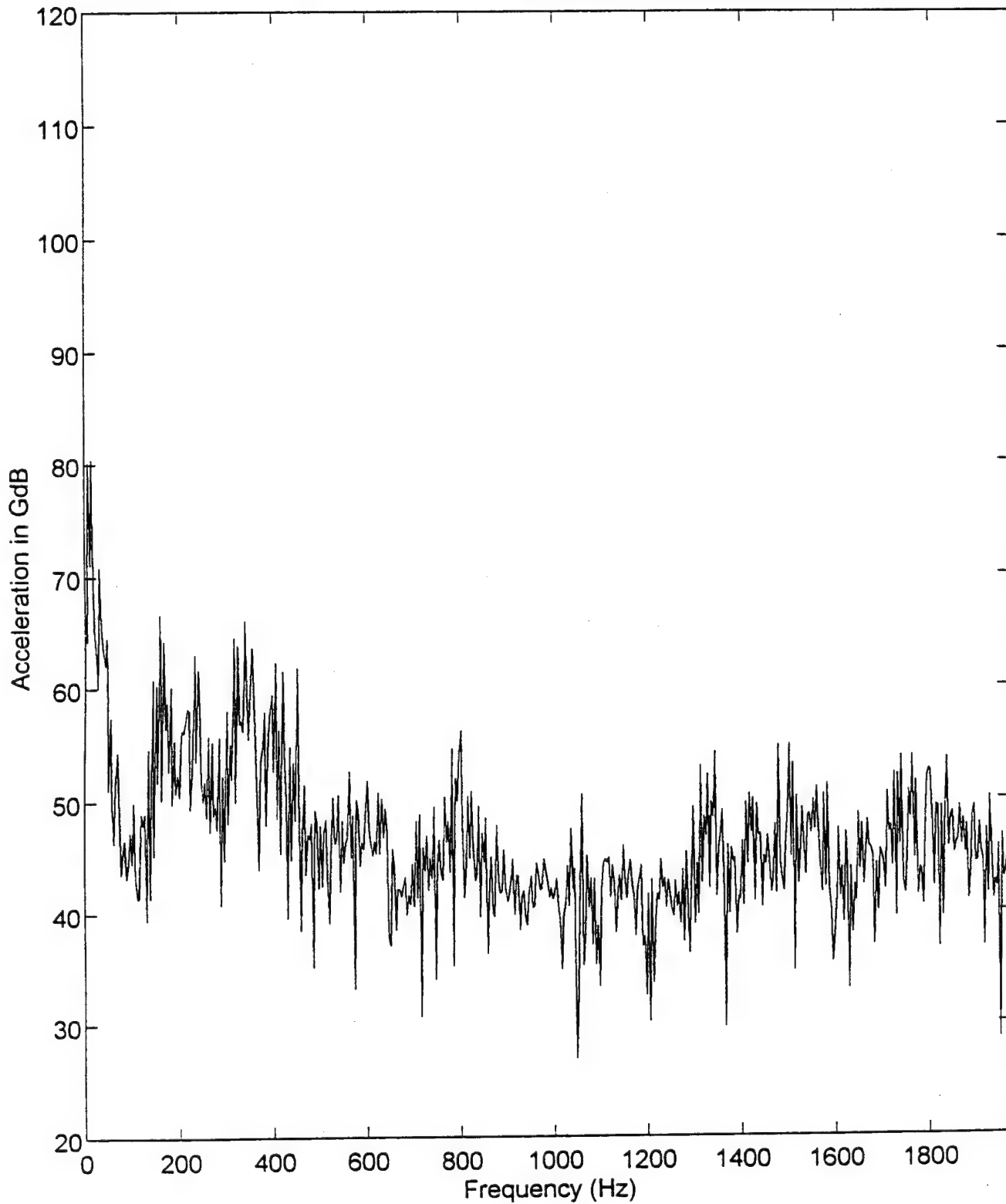


FIGURE 27: MID 524 Compressor Component FFT
Sampled at 3950 HZ, Axial Direction

MID 524 COMPRESSOR COMPONENT

Number of Sampling Data Points = 2048

Mean Value = -0.0167

Standard Deviation = 0.0706

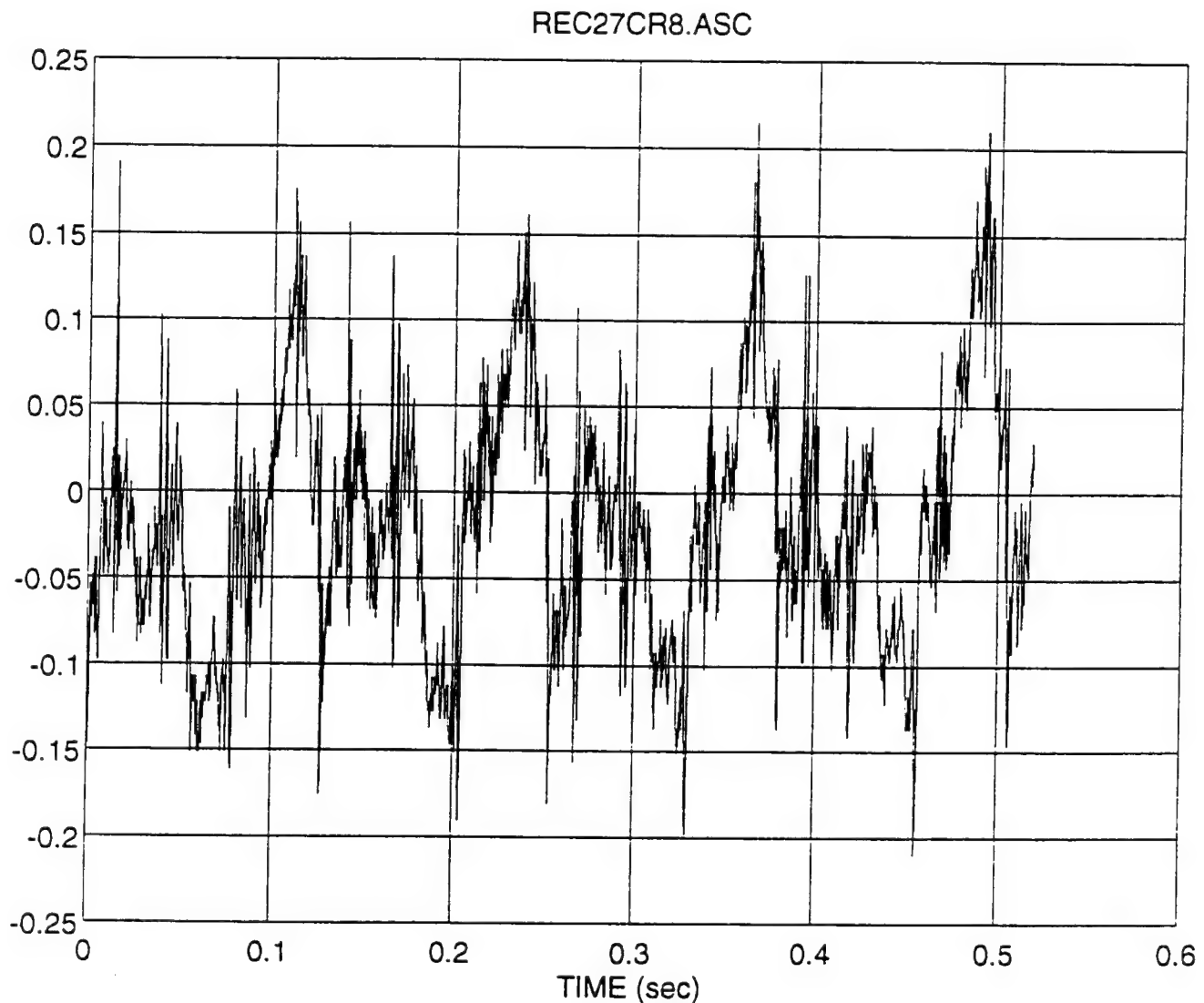
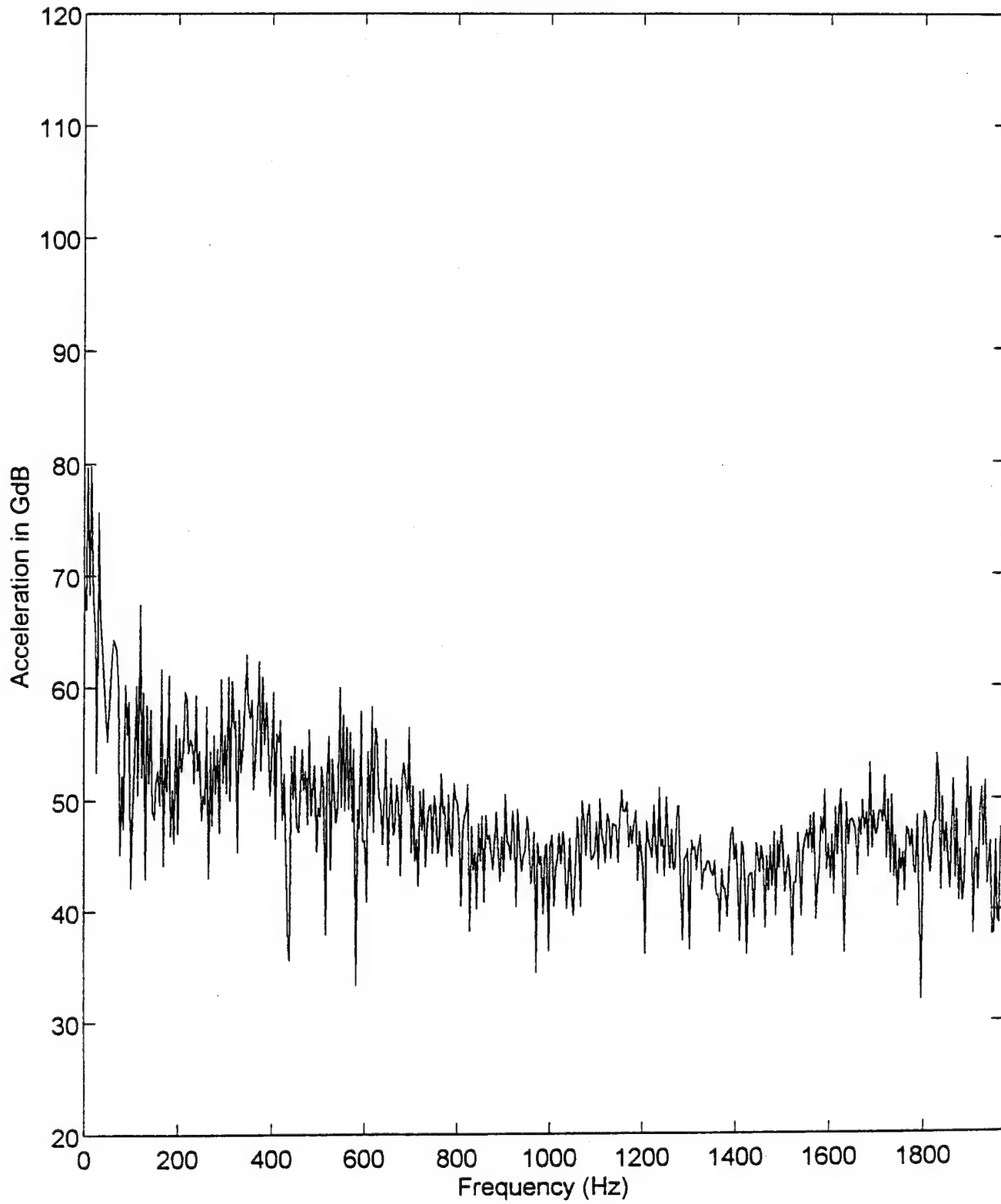


FIGURE 28: MID 524 Compressor Component Sampled at 3950 HZ
Radial Direction

REC27CR8



**FIGURE 29: MID 524 Compressor Component FFT
Sampled at 3950 HZ, Radial Direction**

To include the complete set of vibration measurement signals for all of the high-pressure air compressors considered in this study would be a tedious exercise. For clarity, only one set of vibration measurement signals for each machine type was chosen to be displayed in the body of the text. The vibration measurement signals for compressor units of the same MID number were all found to be similar in appearance. These similarities may be coincidental for the small sampling of data considered here, and may not be the general case for all compressor units. In addition, after reviewing all of the data collected and analyzed in the time domain and frequency spectrum, none of the compressor units displayed any alarming vibration patterns.

D. ARTIFICIAL FAULT SIMULATION

1. Impulse Disturbance

To create deformities in the basic waveform patterns of the vibration measurement signals an artificial fault signal was introduced. This signal was created in **MATLAB®** to correspond to the sampling size of the machine data and not to the major timing events of the compressor units. Due to the dynamic nature of the data processing using **EASYEST™ LX**, the start and stop points of the waveform could not be adequately controlled for the infinitesimal portion of the overall signal that was acquired. In addition, because the vibration measurement data was captured using traditional rotating

machine analysis techniques, the major timing events and crank-angle position were never established. These shortcomings prevented an artificial fault signal that would represent poor operating conditions of a particular compressor mechanical component, such as a loose cylinder wrist pin, to be incorporated into the measured data. The fault signals that were introduced to the measured vibration data were made up of a series of instantaneous impulses (spikes) of constant amplitude at equidistant spacing along the time axis. These simple fault signals were created to correspond to the signal time span of the high sampling frequency data for the MID 115 type compressor unit. Figures 30 through 35 show the artificial fault signal added to the vibration measurement signals for a MID 115 type compressor component (time domain followed by the corresponding frequency spectrum in the tangential, axial, and radial directions). Both time domain and frequency spectrum are presented to display the semi-arbitrary disruption to the vibration patterns of the compressor component. As can be seen in the appropriate figures, the fault signal appears as a spikes in the time-domain. In the frequency spectrum, the appearance of the fault signal is more readily noticed in the area of higher frequencies. As will be shown shortly, the true influence of the artificial fault signal will be more obvious when the manipulated vibration data is viewed in the time-frequency domain.

ARTIFICIAL FAULT SIMULATION

Number of Sampling Data Points = 2048

Mean Value = -0.0160

Standard Deviation = 0.1181

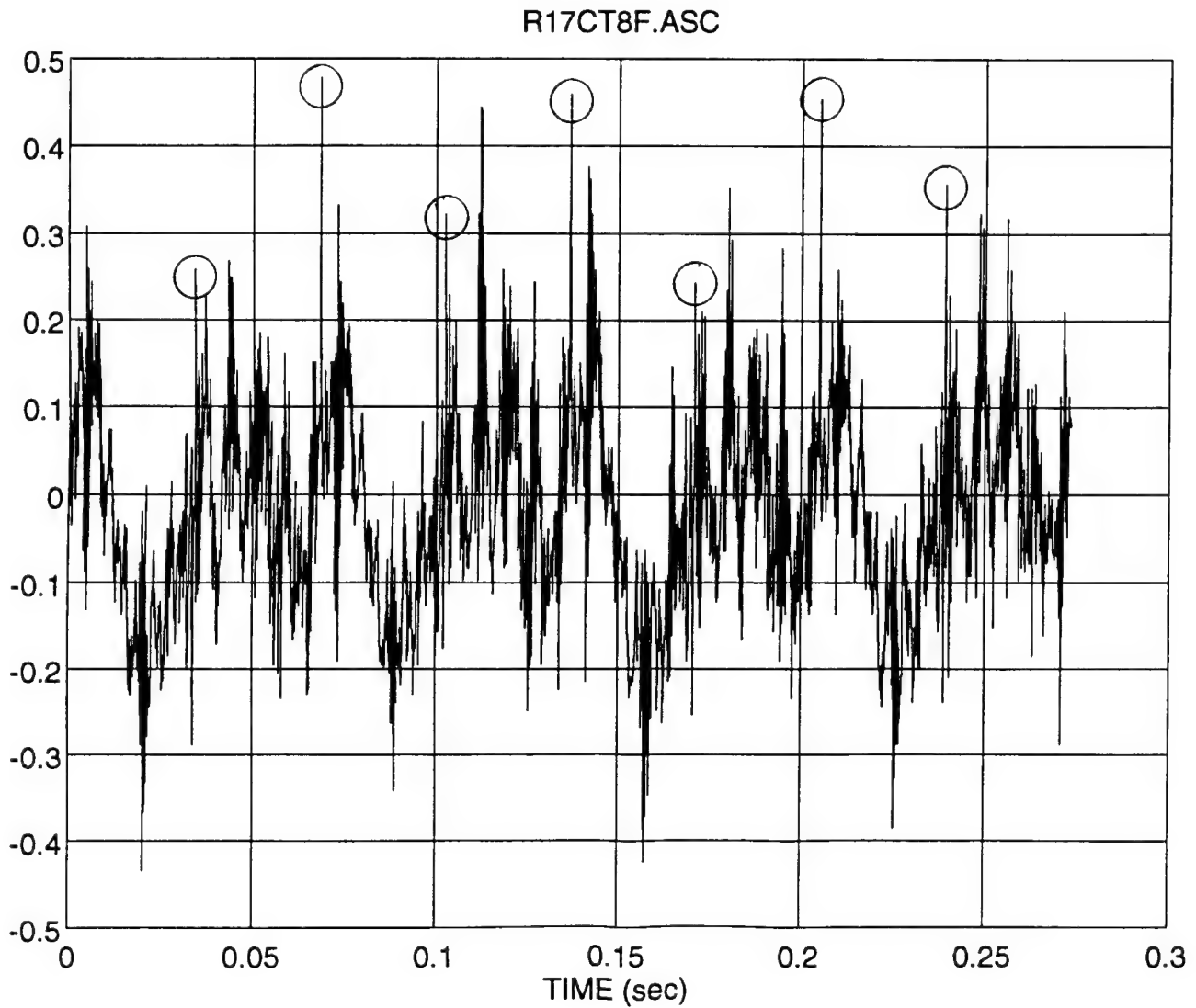


**FIGURE 30: Artificial Fault Simulation
Tangential Direction**

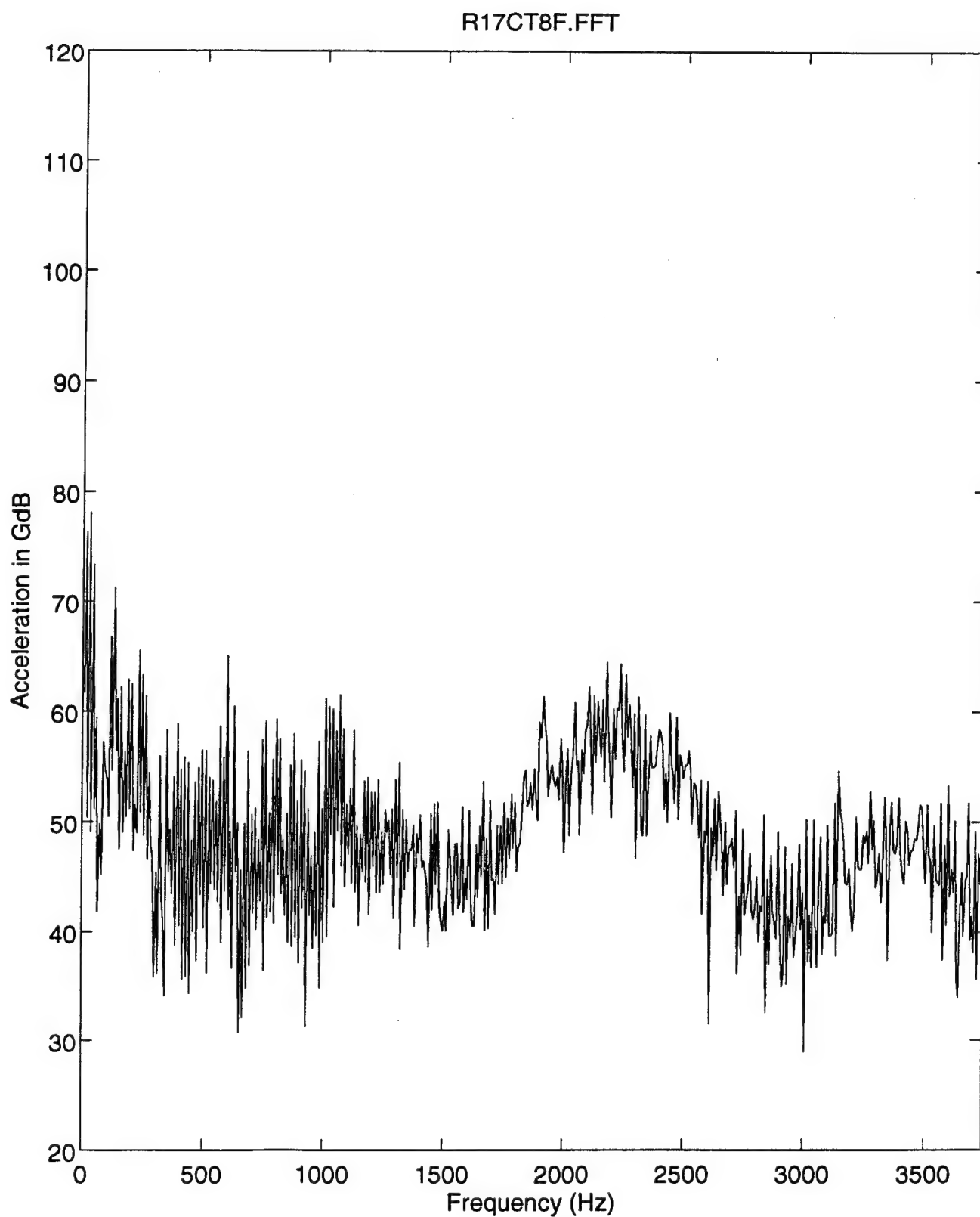


**FIGURE 31: Artificial Fault Simulation FFT
Tangential Direction**

ARTIFICIAL FAULT SIMULATION

Number of Sampling Data Points = 2048

Mean Value = -0.0595

Standard Deviation = 0.1153

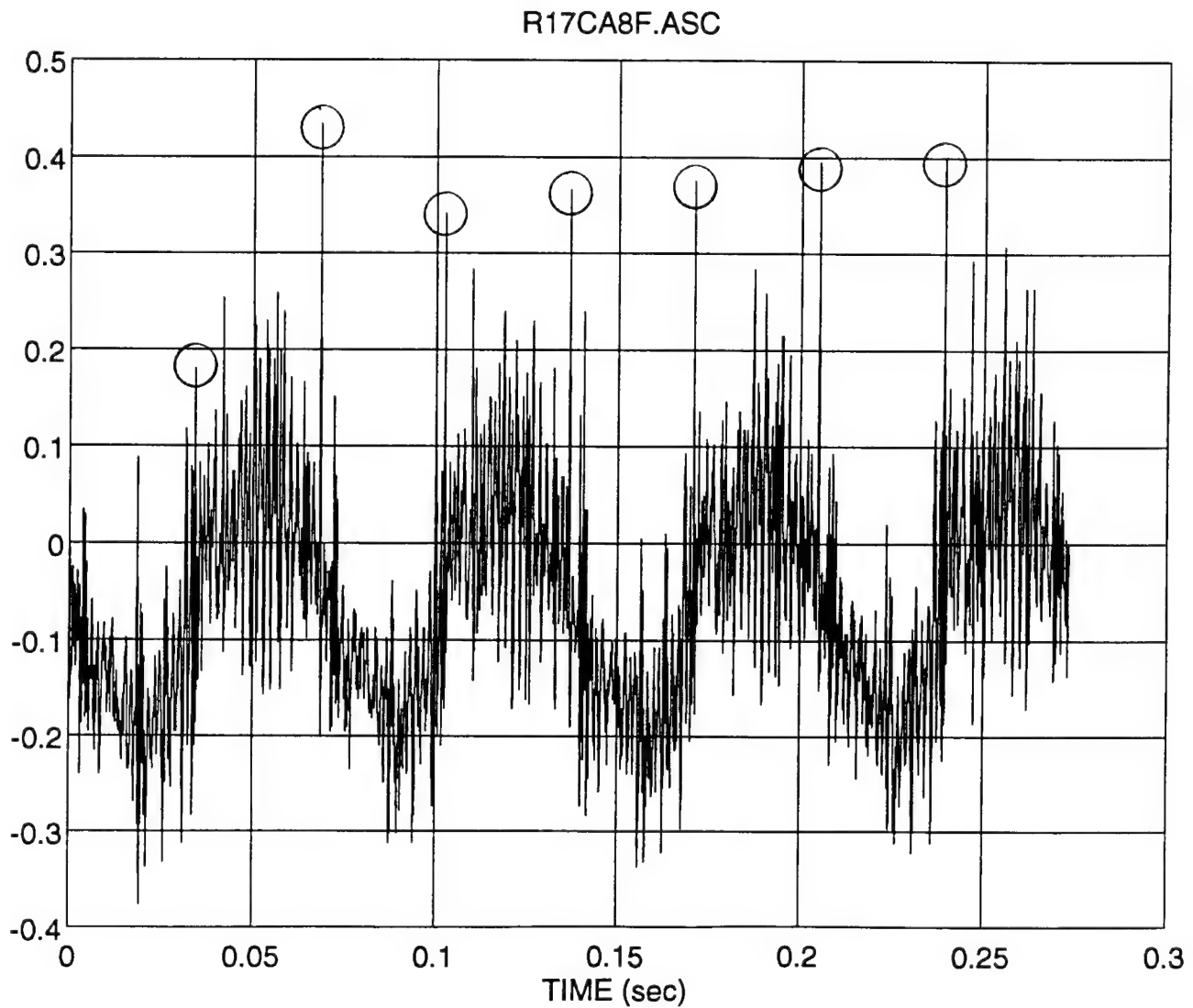


**FIGURE 32: Artificial Fault Simulation
Axial Direction**

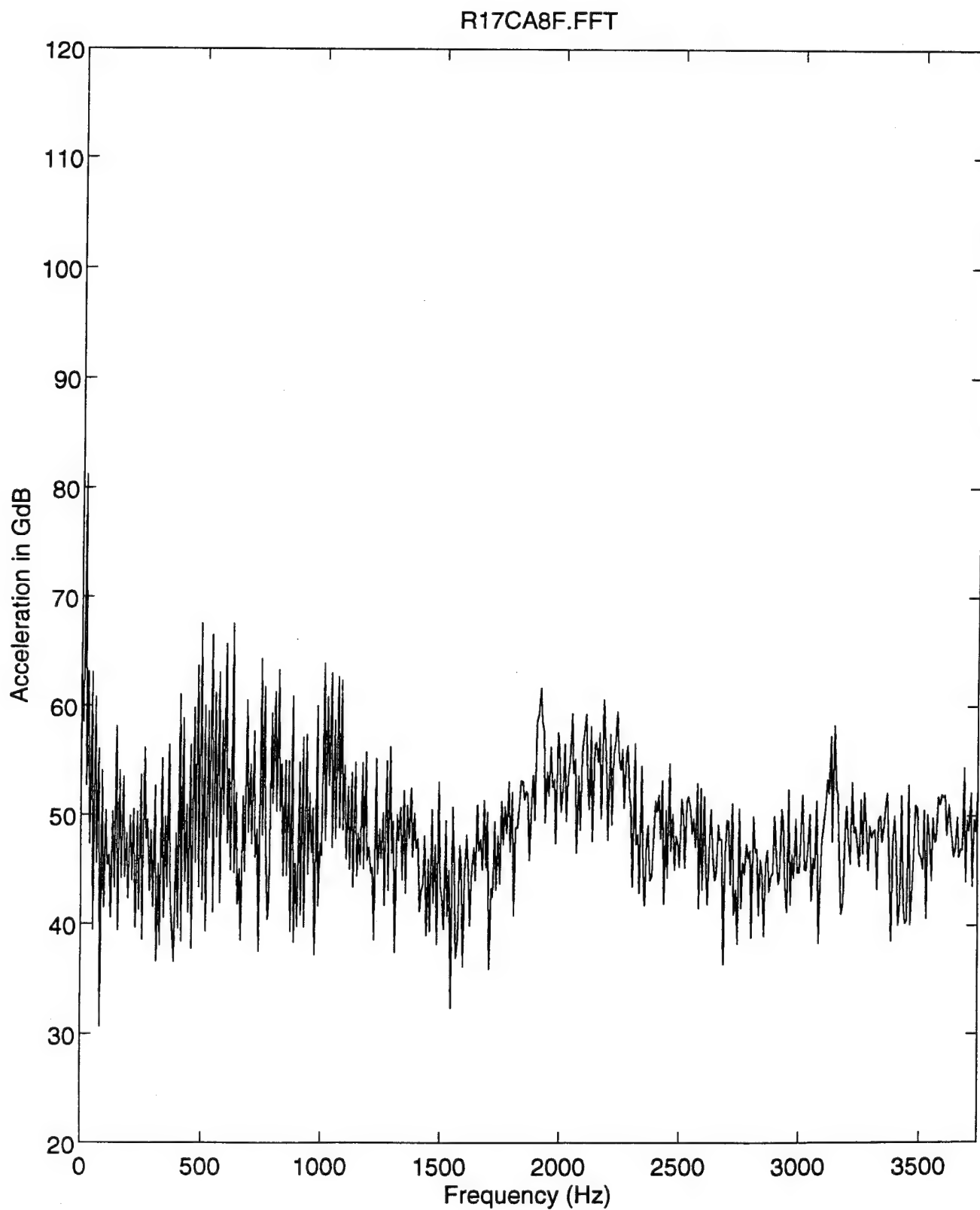


**FIGURE 33: Artificial Fault Simulation FFT
Axial Direction**

ARTIFICIAL FAULT SIMULATION

Number of Sampling Data Points = 2048

Mean Value = -0.0431

Standard Deviation = 0.1677

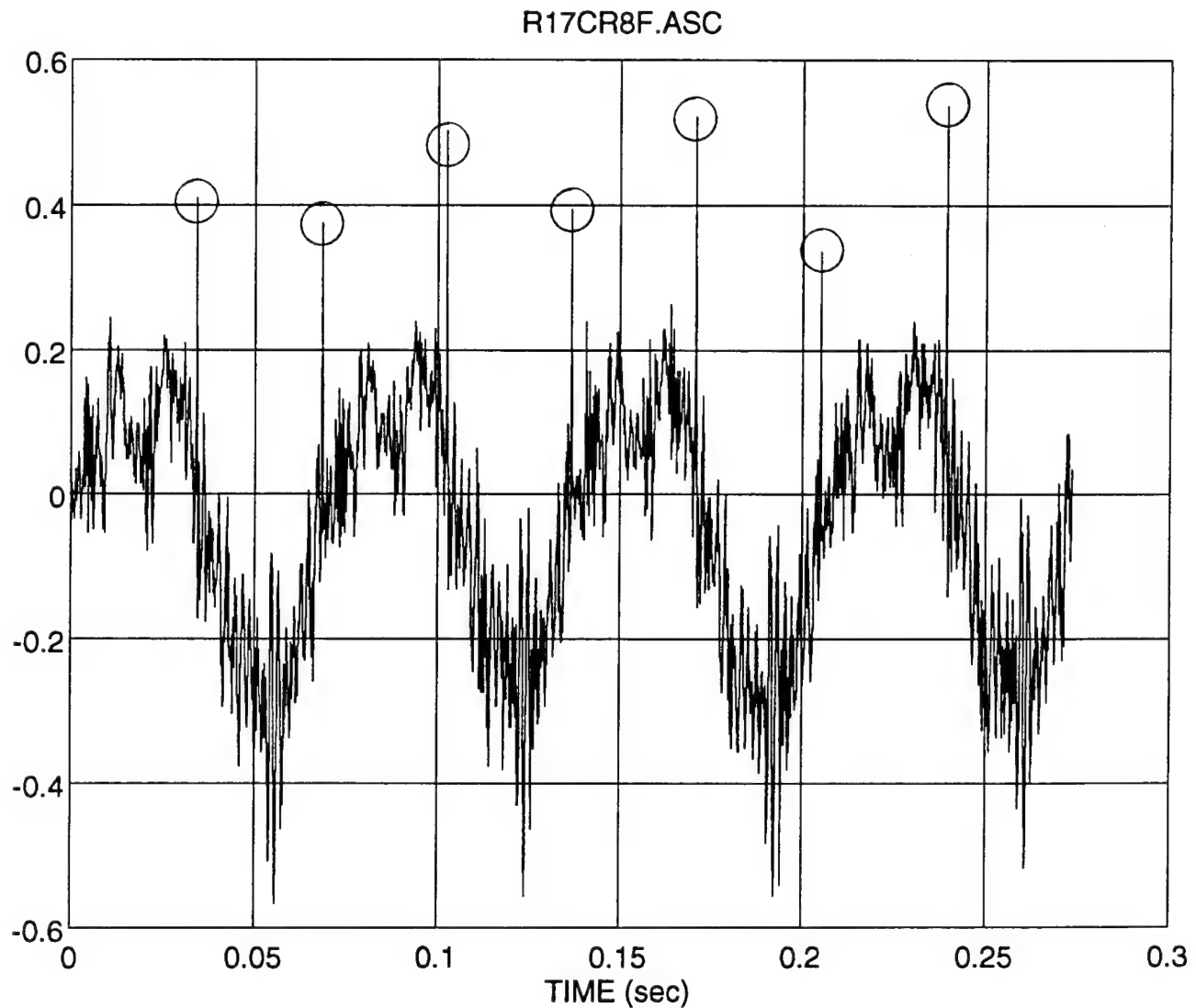


**FIGURE 34: Artificial Fault Simulation
Radial Direction**

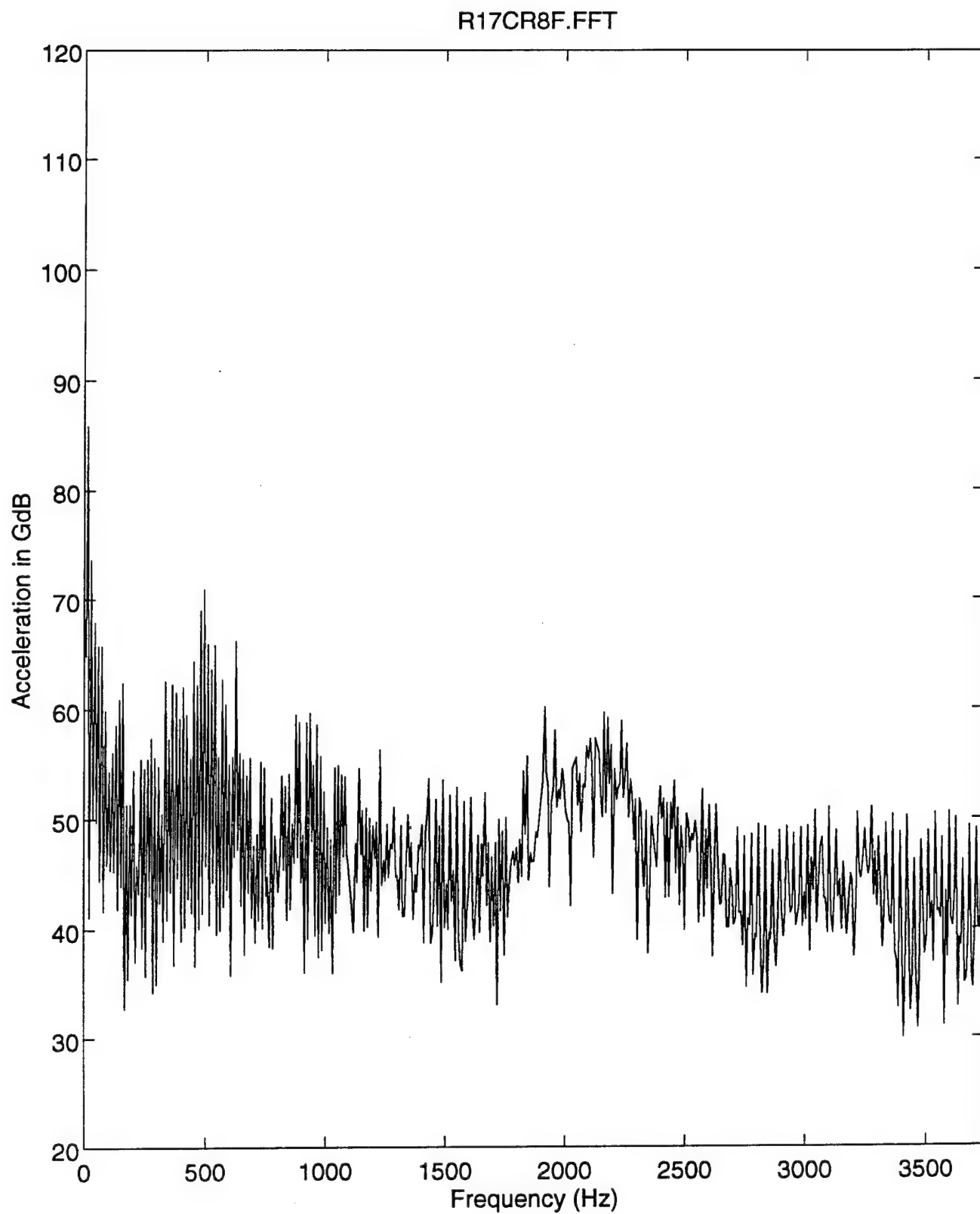


**FIGURE 35: Artificial Fault Simulation FFT
Radial Direction**

2. Transient Vibration Signals

In addition to demonstrating the effects of an simulated fault signal, transient signals were created and analyzed separately. A complete analysis of a reciprocating machine would not only produce time-dependent data, but in some cases the vibration data may also include transient vibration patterns. Vibration data collected around the cylinder frame of the compressor component would definitely display this type of transient signature. Unfortunately, the vibration measurement data analyzed in this study were absent the true effects of transient signals created by certain reciprocating components. Non-machine data was created in order to explore the transient phenomenon associated with reciprocating machines.

To create the transient signals, a thin aluminum plate, fully supported on one end and free hanging on the other, was struck with a sharp impacting motion. For the first data sample, a single impact event was imparted on the plate. The free vibration of the plate was recorded by using an accelerometer attached at the free end. A Hewlett-Packard 3562A Dynamic Signal Analyzer in conjunction with a personal computer captured, recorded, and converted the vibration signal to ASCII format. Once the signal was in ASCII form, the same analysis procedures used for the measured machine data was conducted. Figure 36 is the time domain

representation of a single impact event. Figure 37 is the corresponding frequency spectrum.

A second data sample was captured in similar fashion. However, for this data sample two impact events were conducted to demonstrate the effects of two nearly simultaneous transient events. Figures 38 and 39 display the time domain and frequency spectrum respectively.

TYPICAL TRANSIENT VIBRATION

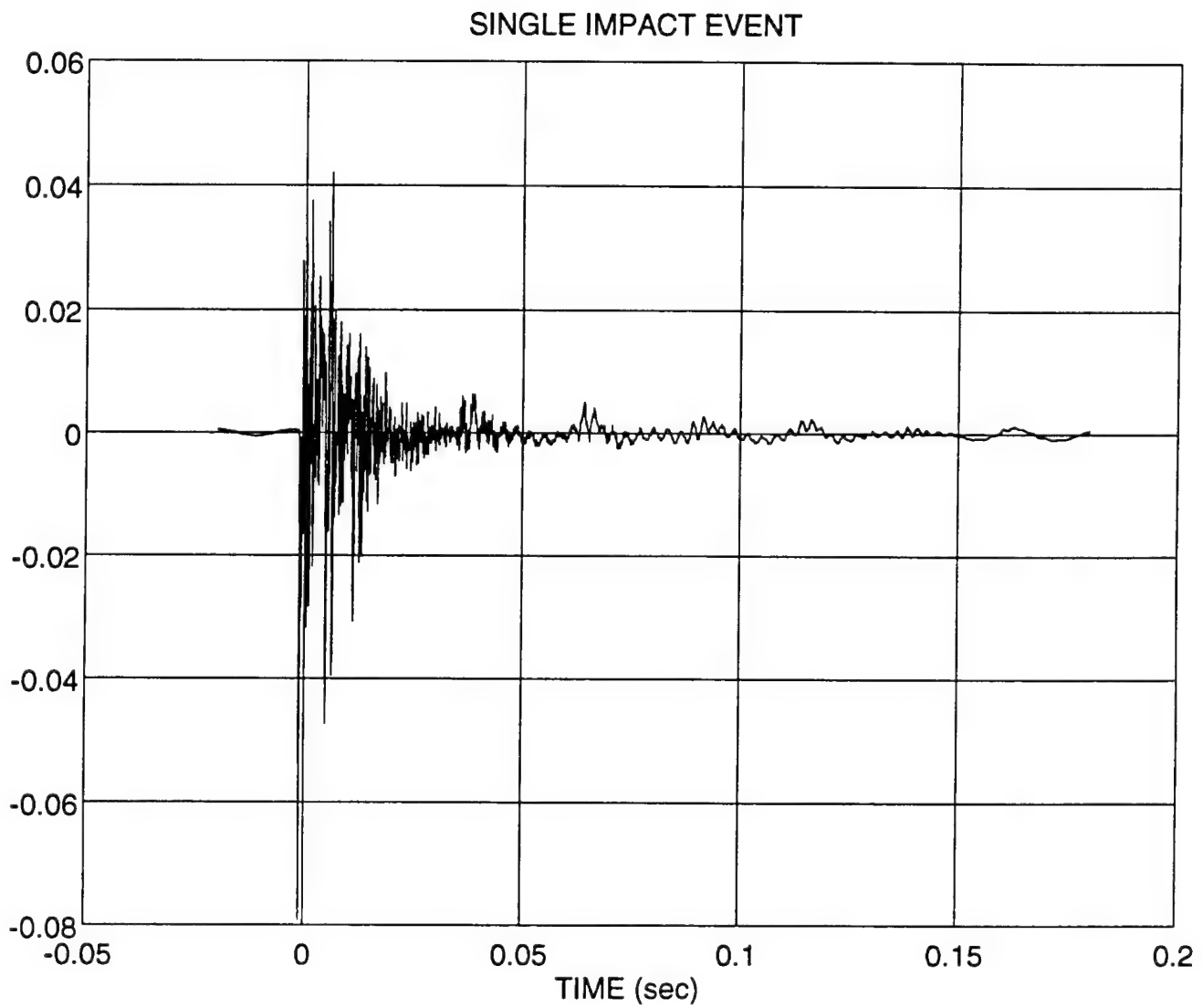


**FIGURE 36: Typical Transient Vibration
Single Impact**

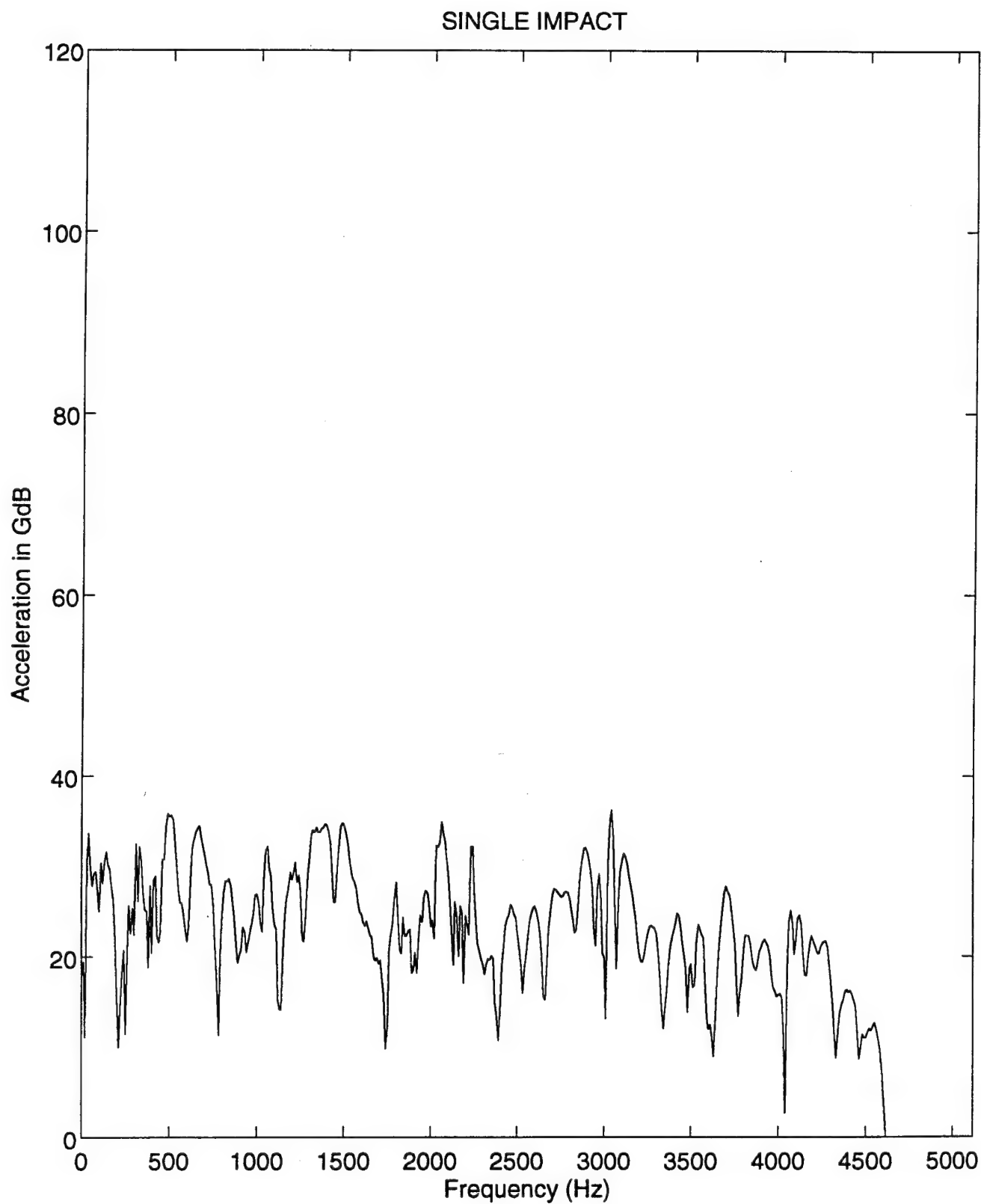


**FIGURE 37: Typical Transient Vibration FFT
Single Impact**

TYPICAL TRANSIENT VIBRATION

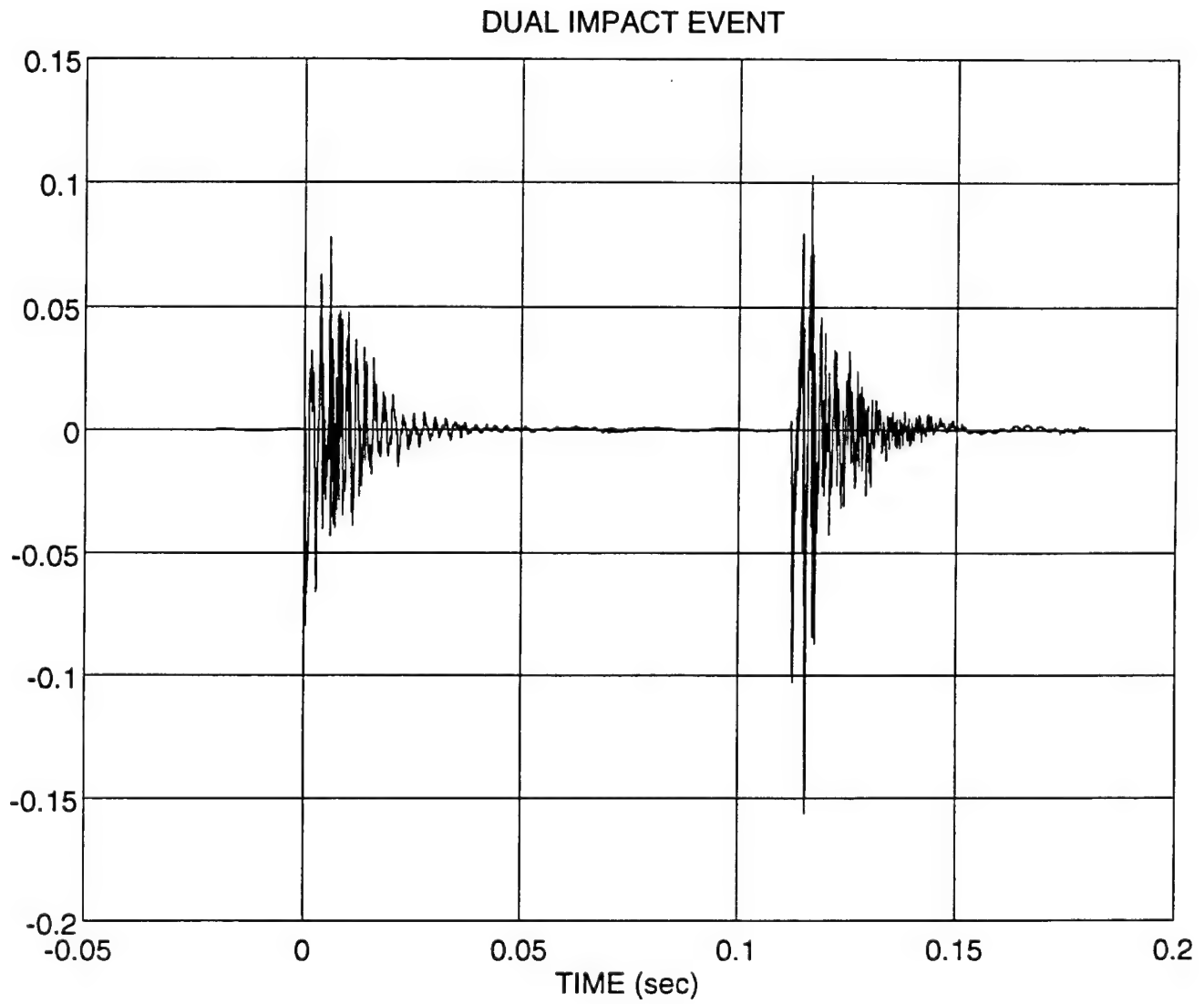


**FIGURE 38: Typical Transient Vibration
Dual Impact**

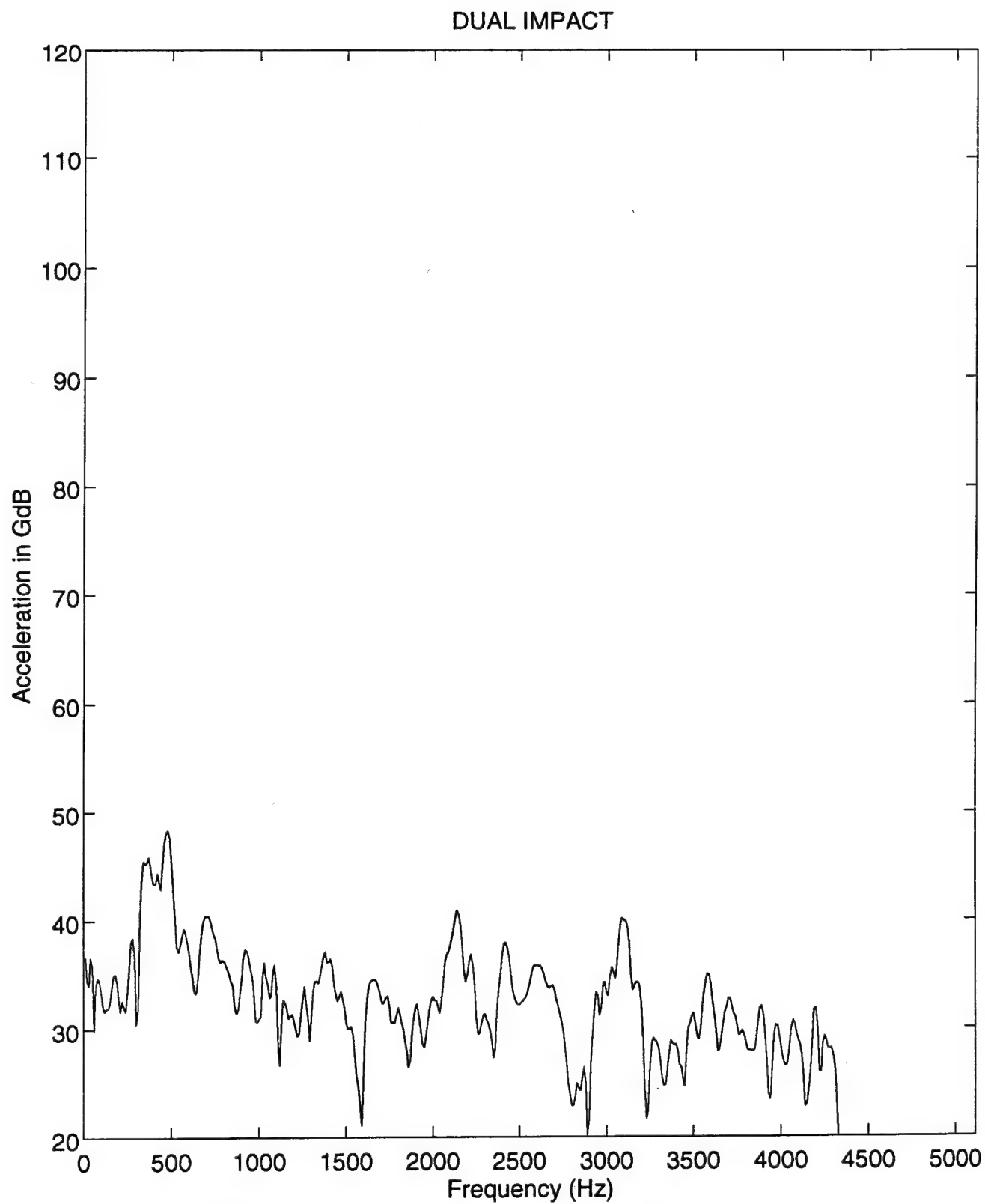


**FIGURE 39: Typical Transient Vibration FFT
Dual Impact**

IV. TIME-FREQUENCY DOMAIN REPRESENTATION

A. PSEUDO WIGNER-VILLE DISTRIBUTION (PWVD)

1. History of Pseudo Wigner-Ville Distribution

The primary advanced analysis technique considered in this study was the Pseudo Wigner-Ville Distribution (PWVD). PWVD is a three-dimensional (time, frequency, and amplitude) representation of an input signal and is particularly well suited for the analysis of transient and other non-stationary vibration signals. The capability of PWVD to evaluate the input data in three dimensions makes it a logical choice as an appropriate medium for the analysis of reciprocating machine vibration data. The application of PWVD analysis techniques for machinery condition monitoring and diagnostics is not a novel concept. The PWVD has been proposed in the past for use in machinery condition monitoring and diagnostics by Flandrin et. al. [Ref.7] and in gear fault detection by Forrester [Ref.8].

PWVD has a long history in its development for use in vibration signal analysis. Eugene Wigner [Ref.9] first introduced the Wigner distribution in 1932 to study the problem of statistical equilibrium in the area of quantum mechanics. His work was furthered in 1948 by J. Ville [Ref.10], who used the Wigner distribution in the area of harmonic signal analysis. Claasen and Mecklenbrauker [Refs.

11, 12, and 13] paved the way for many recent applications of the PWVD. Their three part paper is an all encompassing work that has served to highlight the capabilities of the Wigner Distribution (WD) and allow for greater knowledge of the subject with an emphasis on signal processing and analysis. Claasen and Mecklenbrauker described the application of a sliding window in the time domain while calculating the WD producing a smoothed version with respect to frequency. The WD obtained with a window function is called the pseudo WD. Transposing this terminology, PWVD is the application of a smoothing window to the results of a Wigner-Ville distribution [Ref.14]. The derivation of the PWVD equations and processes will not be presented in this paper. The development of the PWVD has been covered extensively in the sighted references. The purpose of this paper is to demonstrate what can be gained from a time-frequency domain analysis of reciprocating machines.

2. PWVD of Measured Vibration Data

To conduct the PWVD analysis of the reciprocating machine data presented in this study, a computer program developed by Jeon and Shin [Ref.14] was used to perform the required calculations. For each run of the PWVD program the option to remove the mean value was selected. The reduction size was selected as 128 by 128, and a square smoothing window of 26 by 26 was established to correspond to the number of

data points. The smoothed results were plotted using **CA-DISSPLA®**, release 11.0 by Computer Associates International, INC.

A 486-50MHZ personal computer in conjunction with a laser printer was used for all data processing. One of the main objectives of this study was to demonstrate that reciprocating machinery analysis can be conducted with minimal investment in any specialized analysis equipment beyond what is required to actually capture the vibration signals. Approximately twenty minutes of computation time was expended for each PWVD calculation for the digitized input signals comprised of 2048 data points. Another twenty minutes was required to output the PWVD results for both the three-dimensional display and contour map. A total of eight hours were exhausted to calculate the PWVD and output a complete set of figures for the twelve data sets of each compressor unit. A Hewlett-Packard Series 700 workstation was used in the latter stages of this study to expedite calculations and graphic outputs.

After viewing all of the vibration measurement signals from the selected compressor units, two recordings for each compressor type were selected for PWVD analysis. Once again, only one set of data for each compressor type will be presented in the body of the text for clarity. Figures 40 through 51 apply to a MID 115 type compressor unit. The figures are presented in the same directional sequence

(tangential followed by axial then radial directions), and sampling frequencies (low sampling frequency followed by the high sampling frequency) as the time domain and spectrum representations in Chapter III. The figures are arranged in pairs to allow the PWVD results in three-dimensional; time, frequency, and amplitude orientation to be viewed first followed by the two-dimensional; time and frequency contour map. Figures 52 through 63 display the PWVD results for the input data taken from a MID 524 type compressor unit.

PSEUDO WIGNER-VILLE DISTRIBUTION

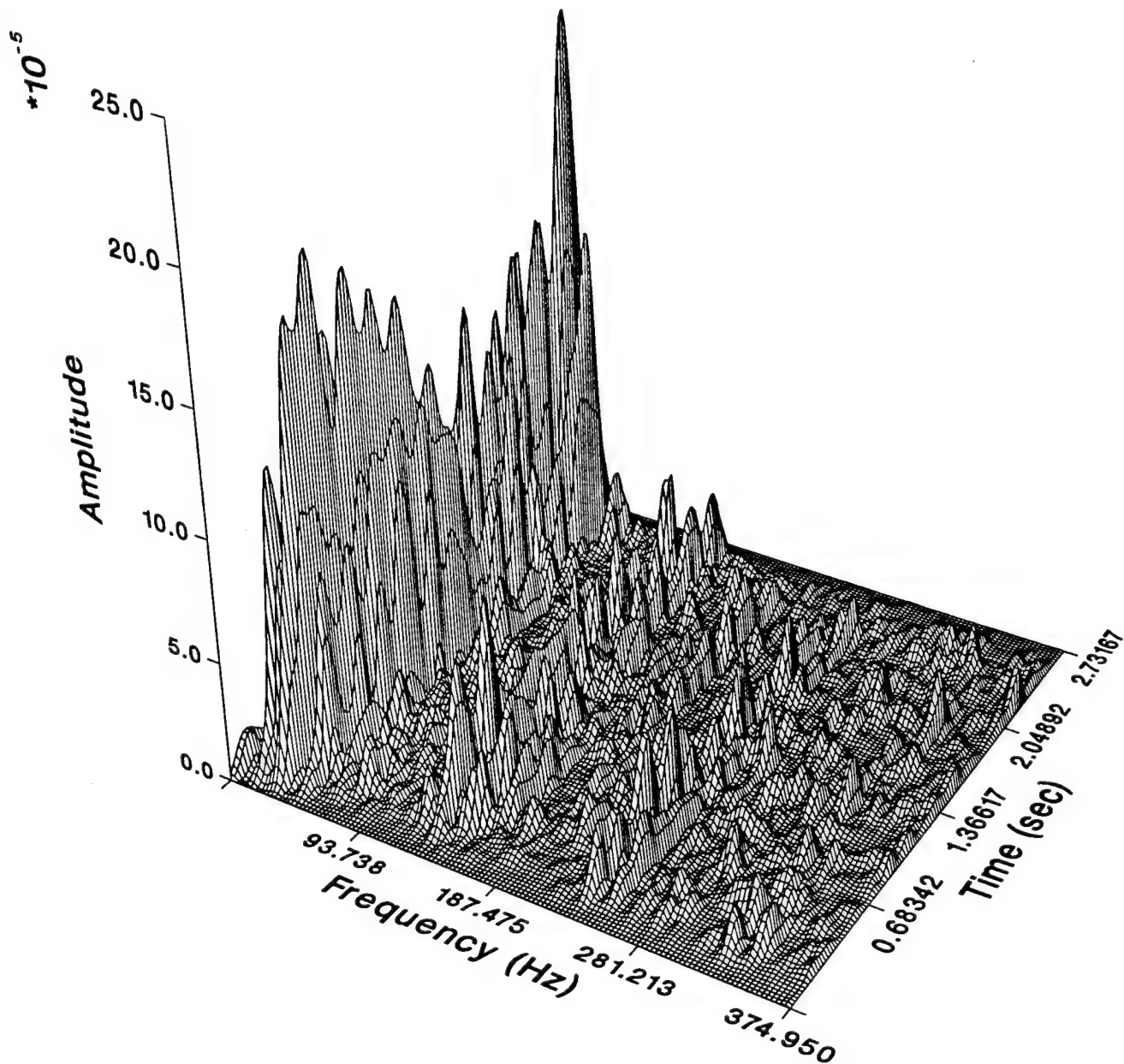


**FIGURE 40: PWVD Results, MID 115 Compressor
Sampled at 750 HZ, Tangential Direction**

PWVD CONTOUR MAP

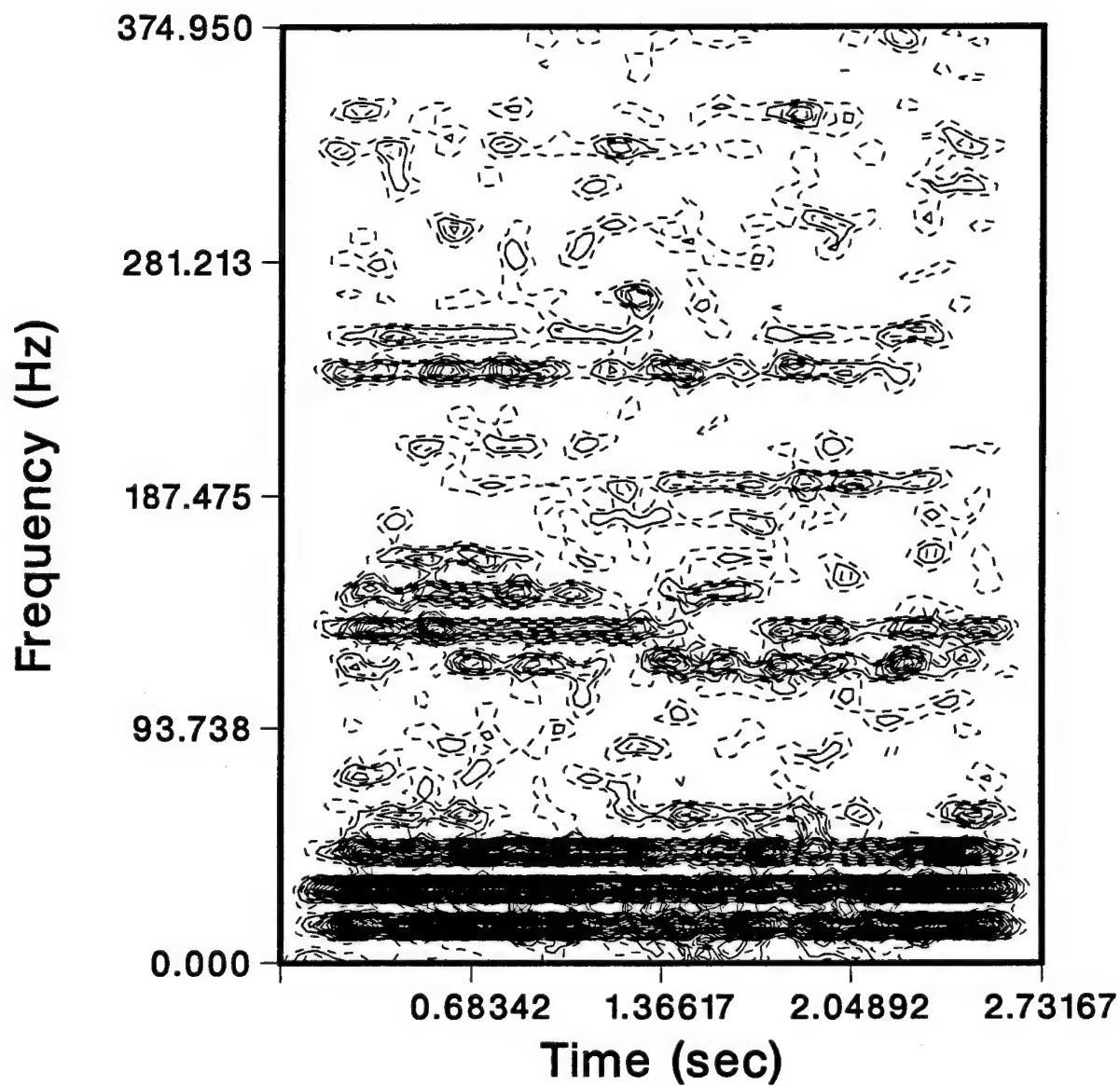


**FIGURE 41: PWVD Contour Map, MID 115 Compressor
Sampled at 750 HZ, Tangential Direction**

PSEUDO WIGNER-VILLE DISTRIBUTION

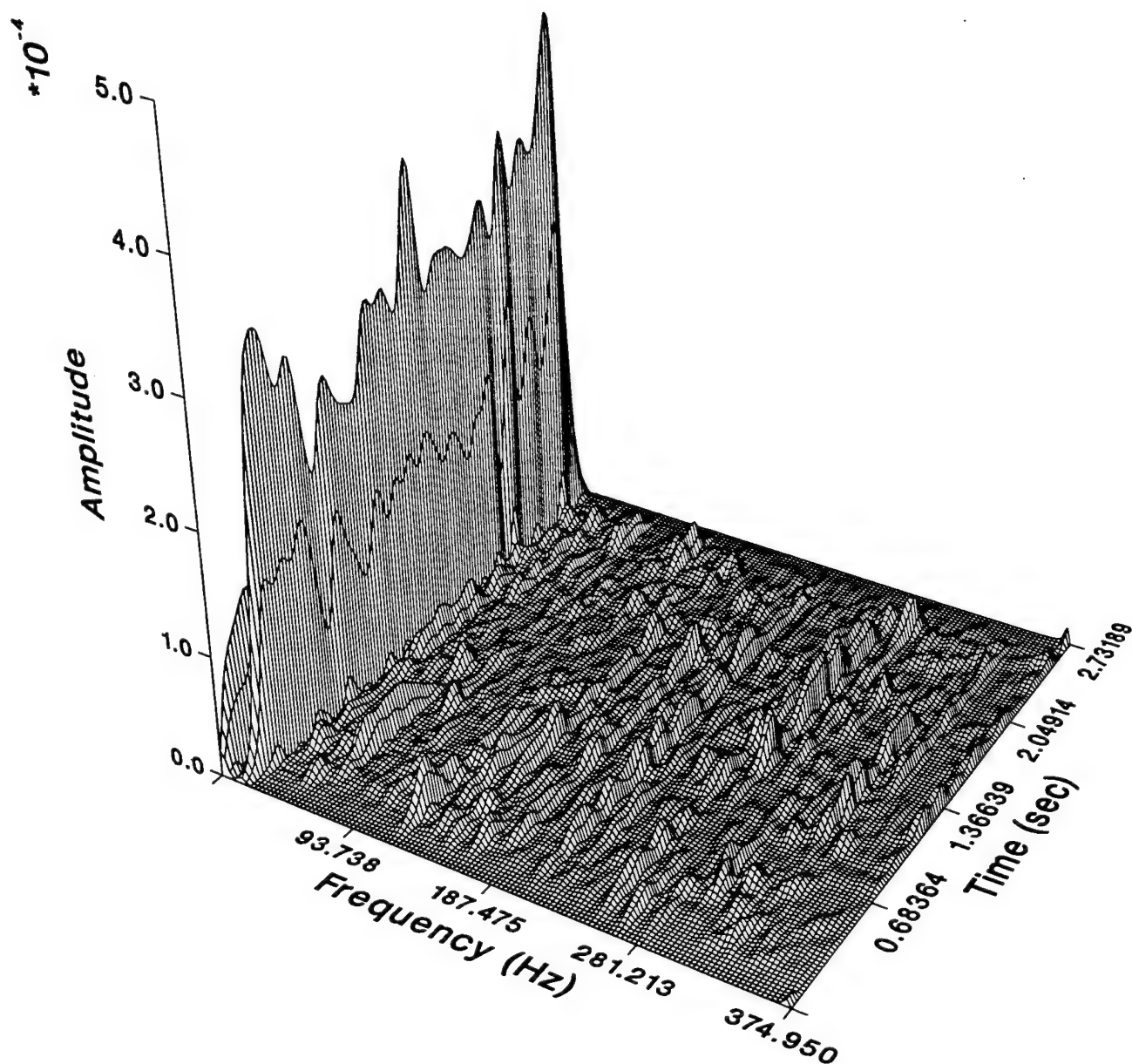
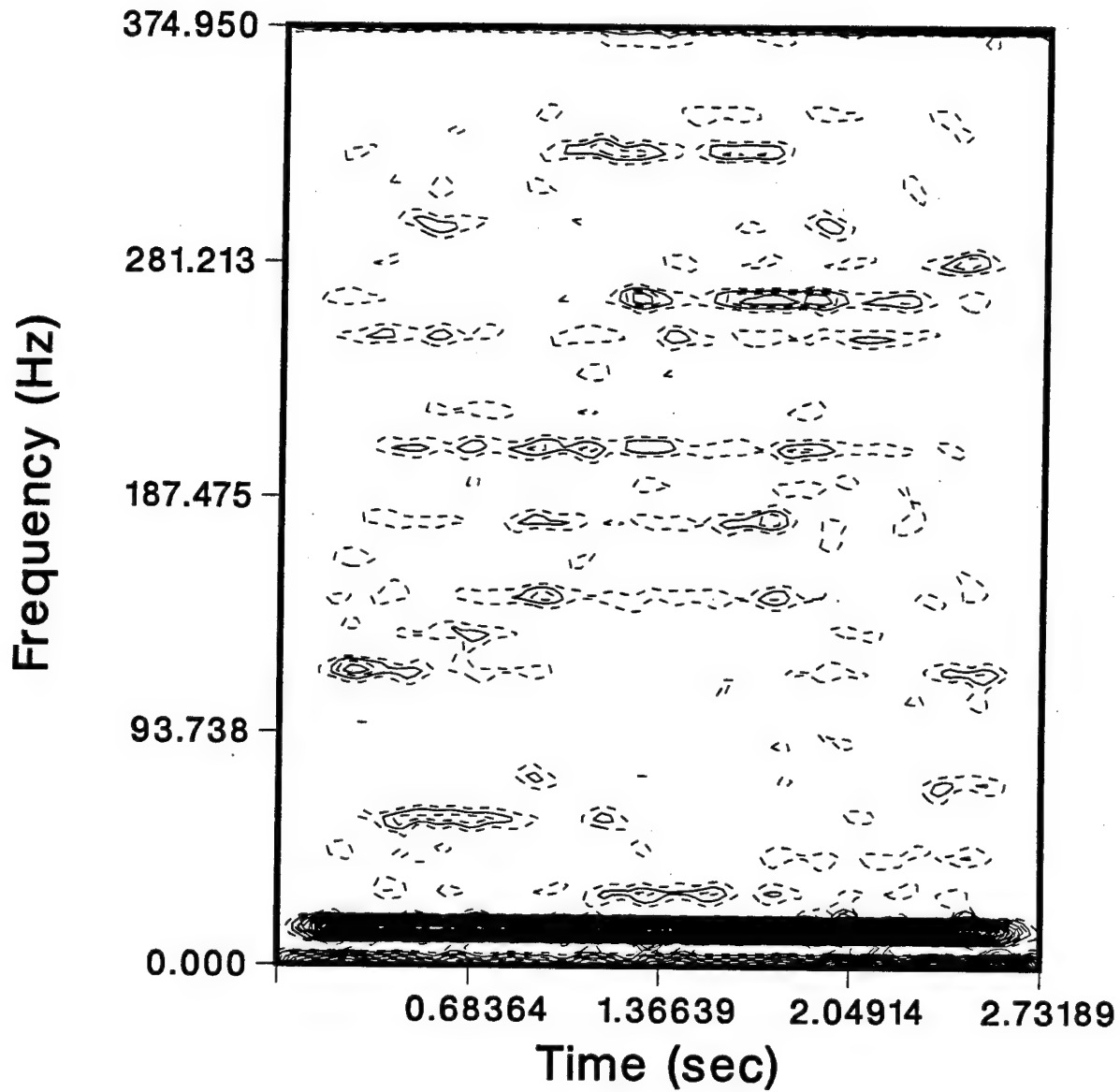


FIGURE 42: PWVD Results, MID 115 Compressor
Sampled at 750 HZ, Axial Direction

PWVD CONTOUR MAP



**FIGURE 43: PWVD Contour Map, MID 115 Compressor
Sampled at 750 HZ, Axial Direction**

PSEUDO WIGNER-VILLE DISTRIBUTION

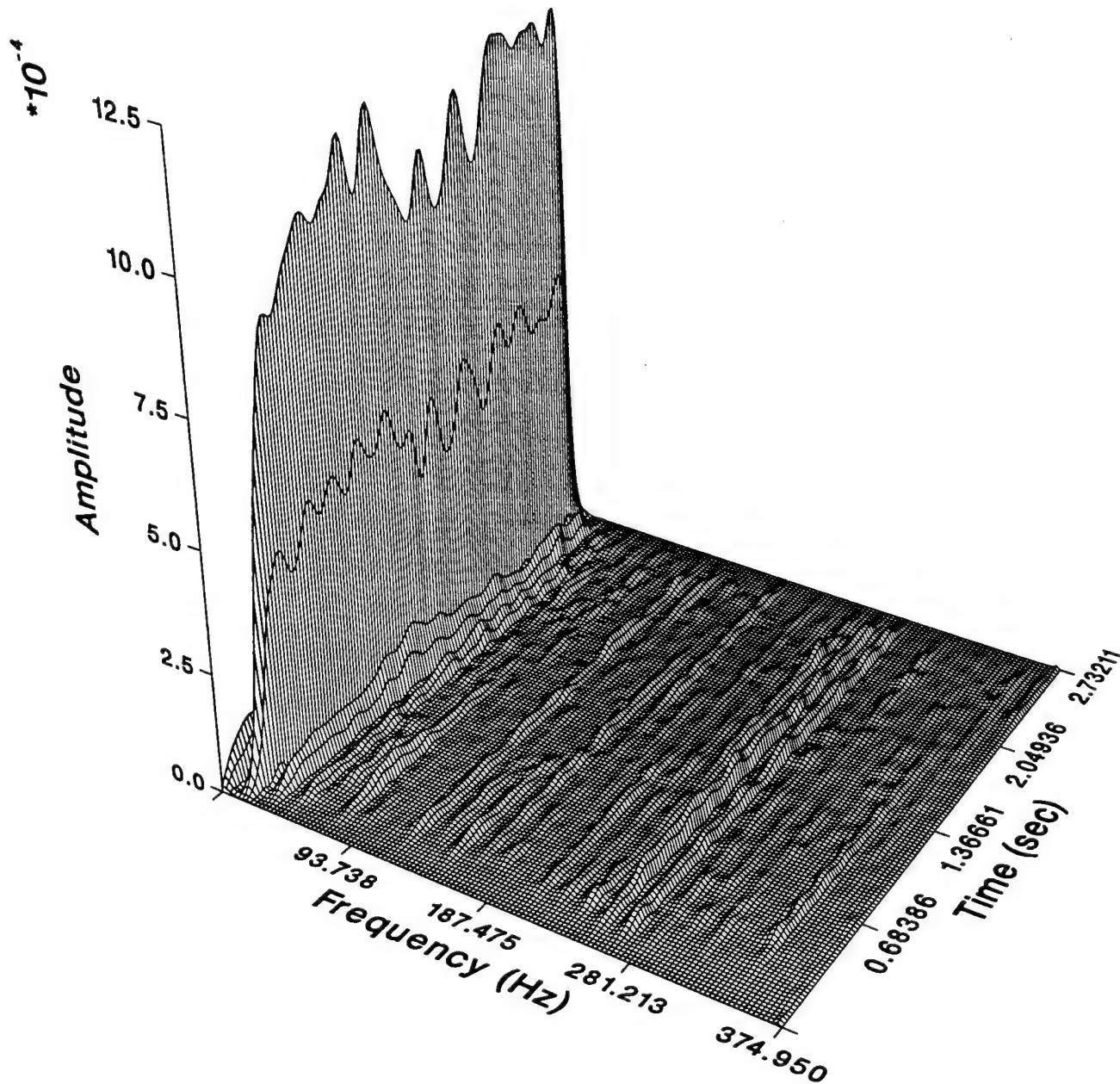
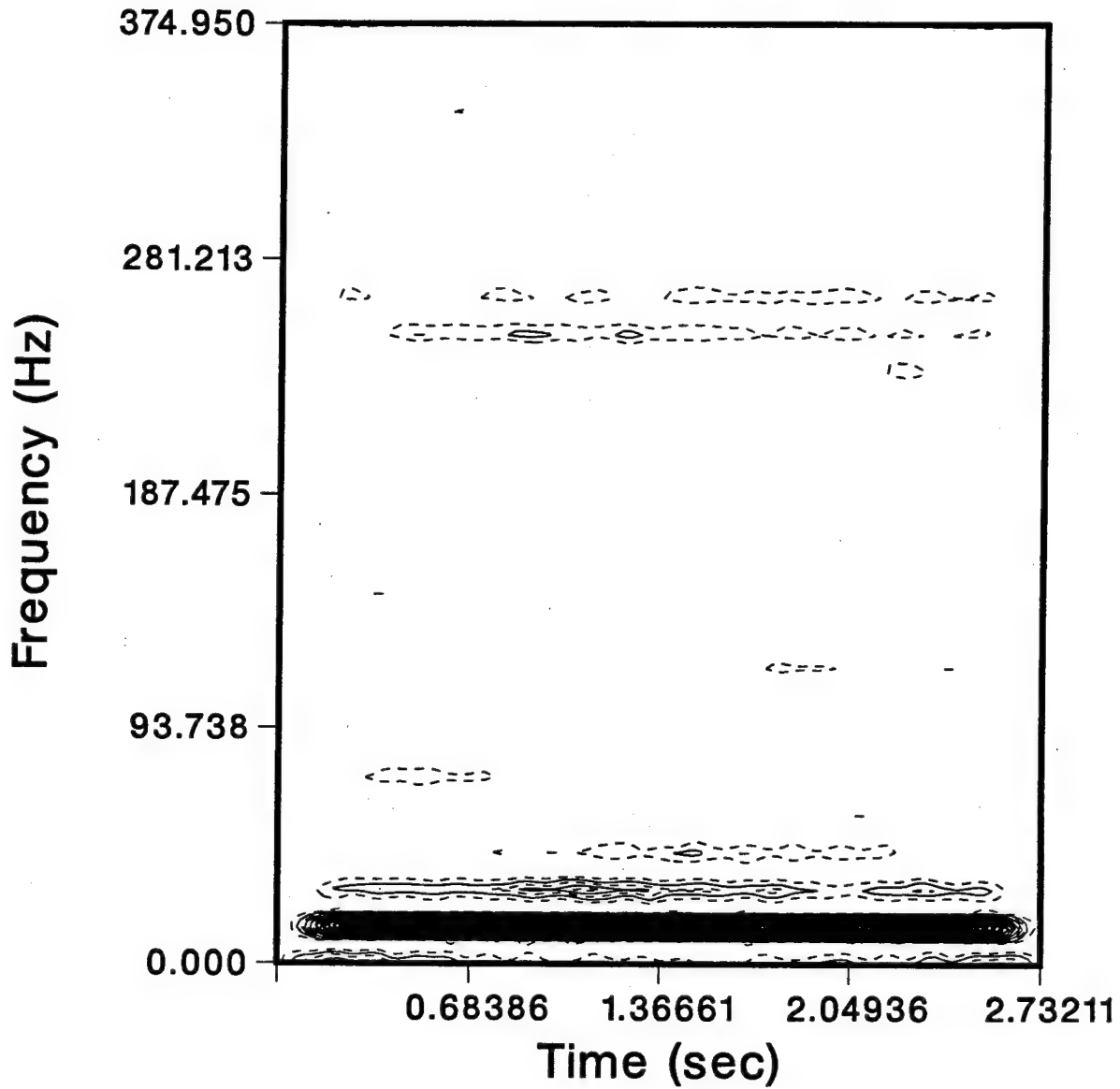


FIGURE 44: PWVD Results, MID 115 Compressor
Sampled at 750 HZ, Radial Direction

PWVD CONTOUR MAP



**FIGURE 45: PWVD Contour Map, MID 115 Compressor
Sampled at 750 HZ, Radial Direction**

PSEUDO WIGNER-VILLE DISTRIBUTION

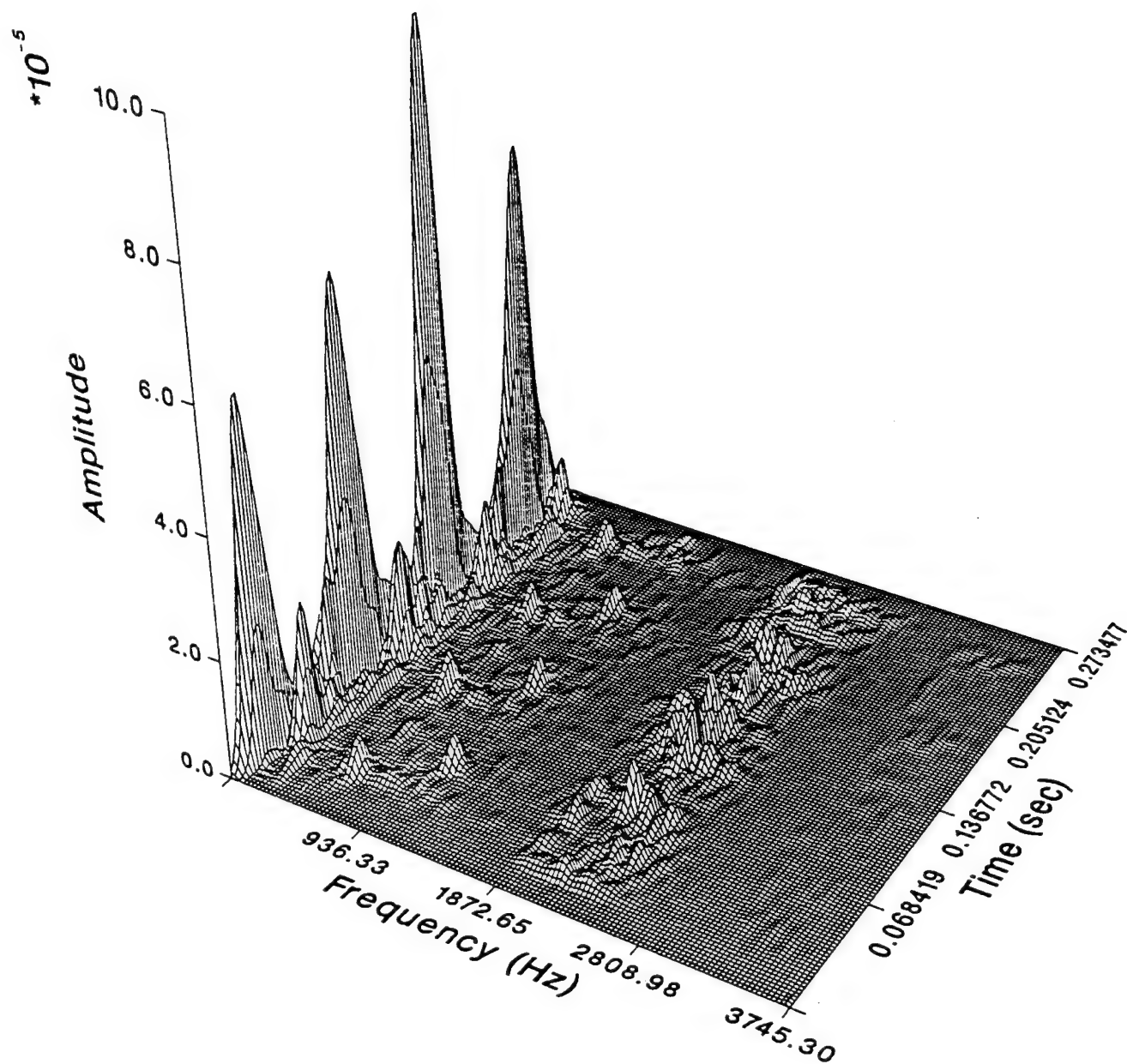


FIGURE 46: PWVD Results, MID 115 Compressor
Sampled at 7500 HZ, Tangential Direction

PWVD CONTOUR MAP

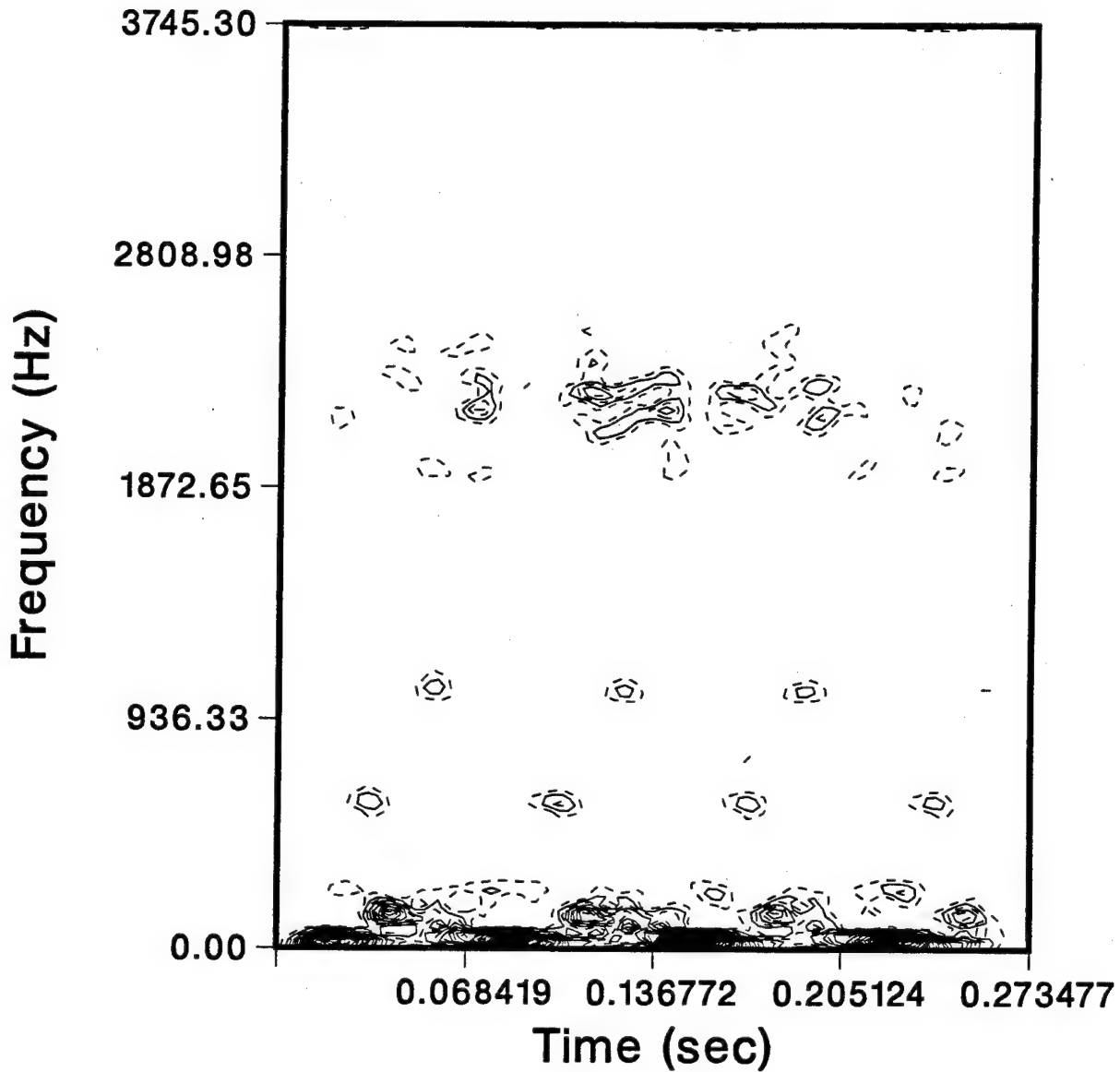


FIGURE 47: PWVD Contour Map, MID 115 Compressor
Sampled at 7500 HZ, Tangential Direction

PSEUDO WIGNER-VILLE DISTRIBUTION

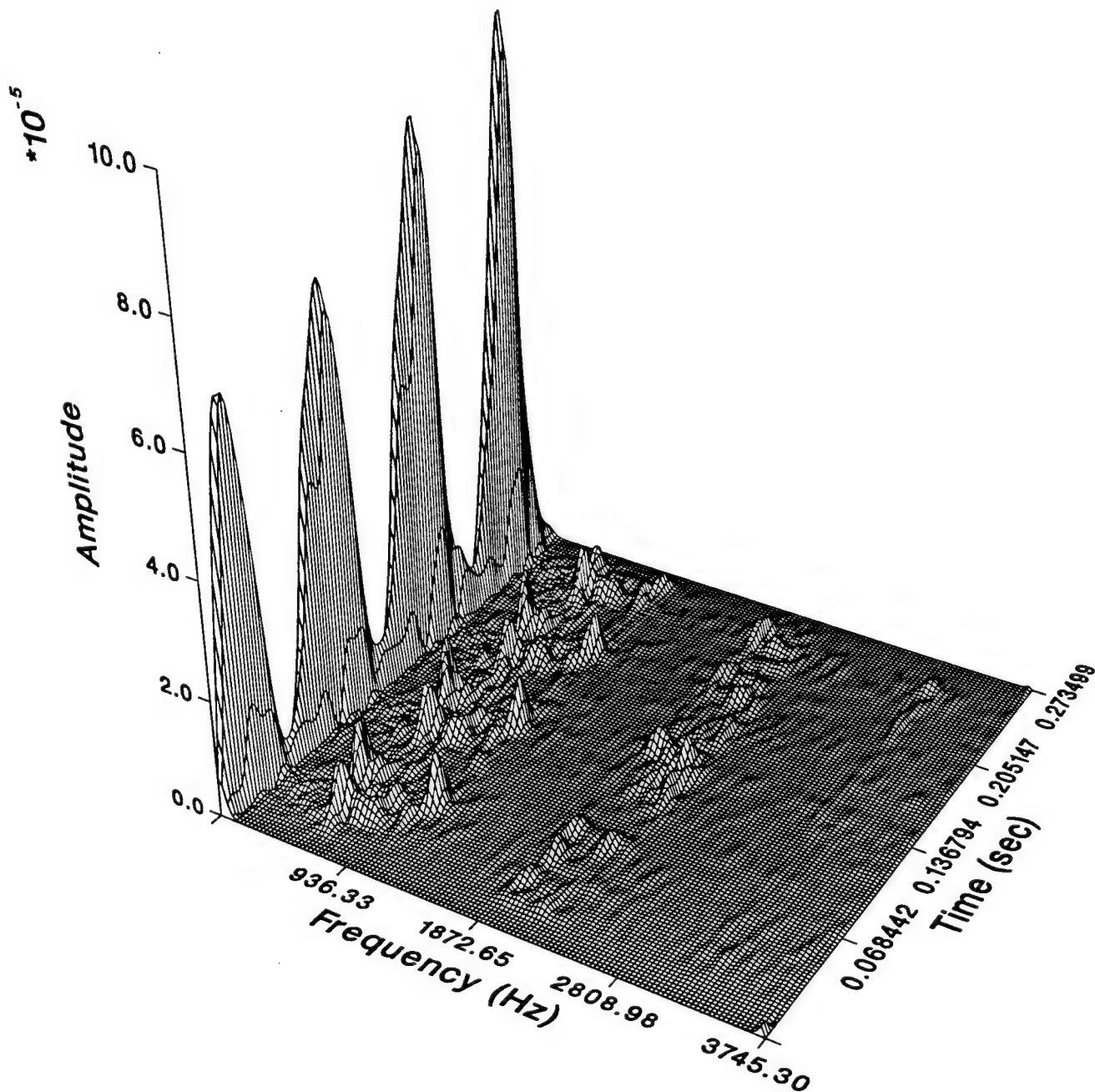
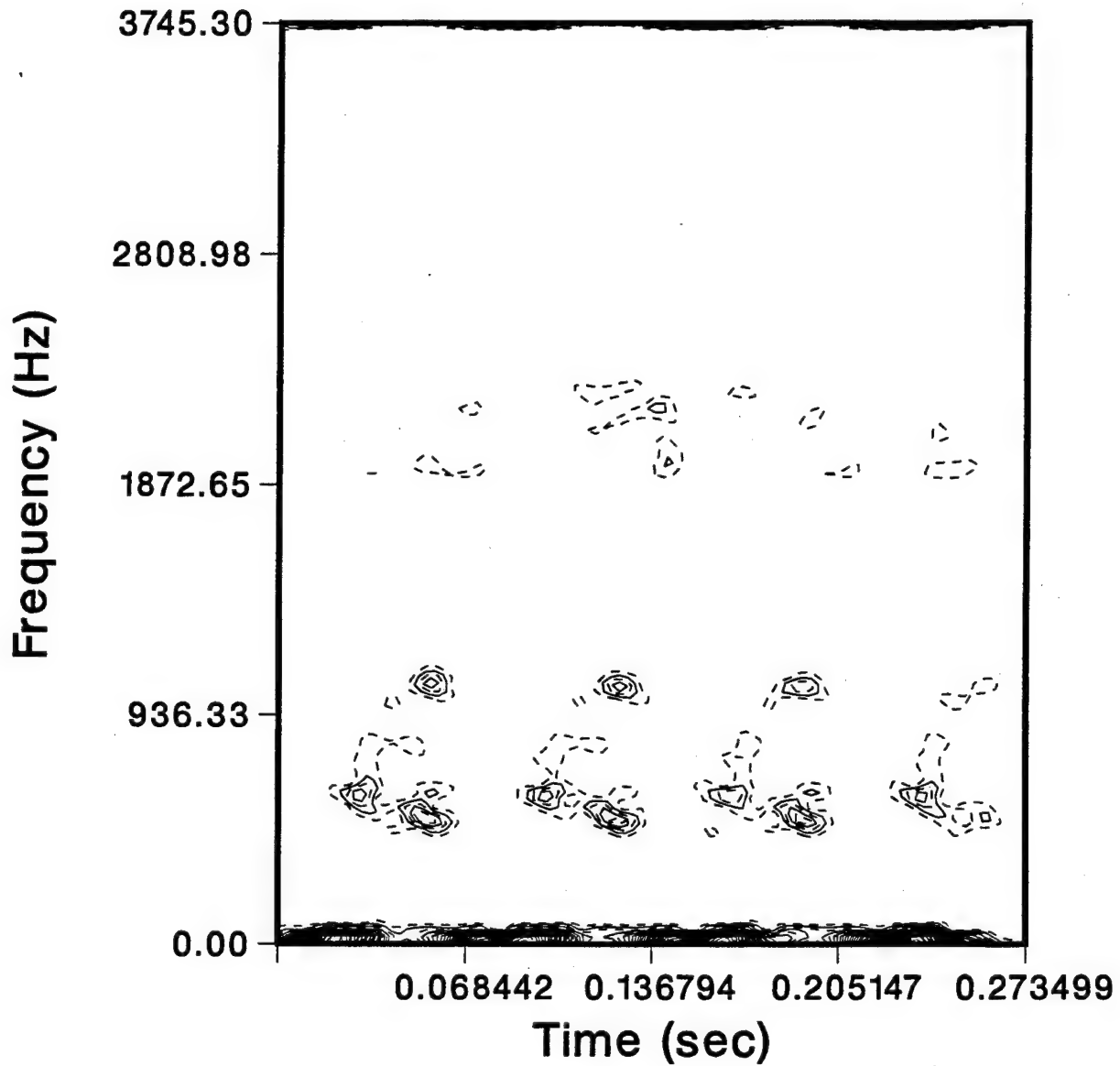


FIGURE 48: PWVD Results, MID 115 Compressor
Sampled at 7500 HZ, Axial Direction

PWVD CONTOUR MAP



**FIGURE 49: PWVD Contour Map, MID 115 Compressor
Sampled at 7500 HZ, Axial Direction**

PSEUDO WIGNER-VILLE DISTRIBUTION

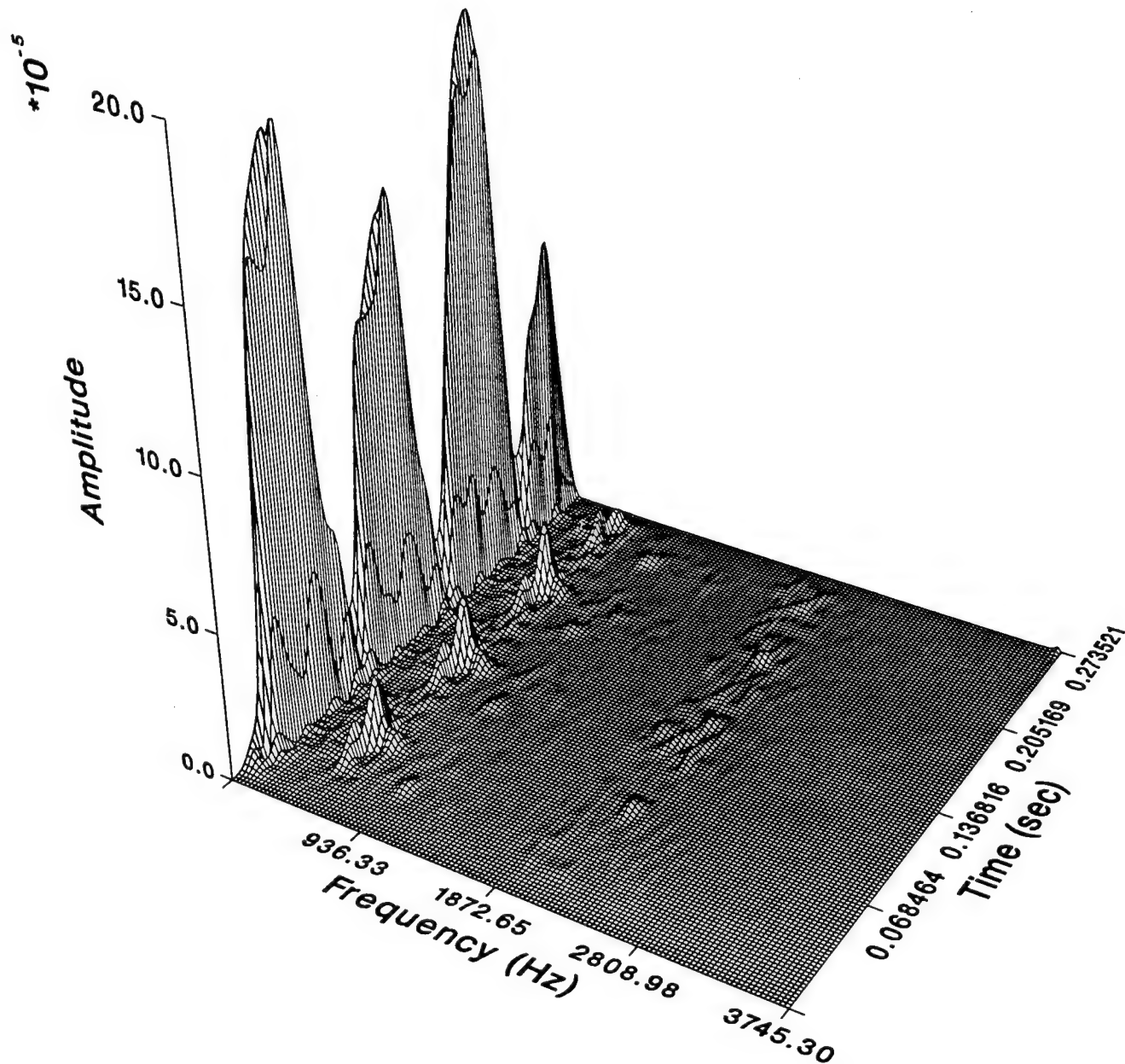
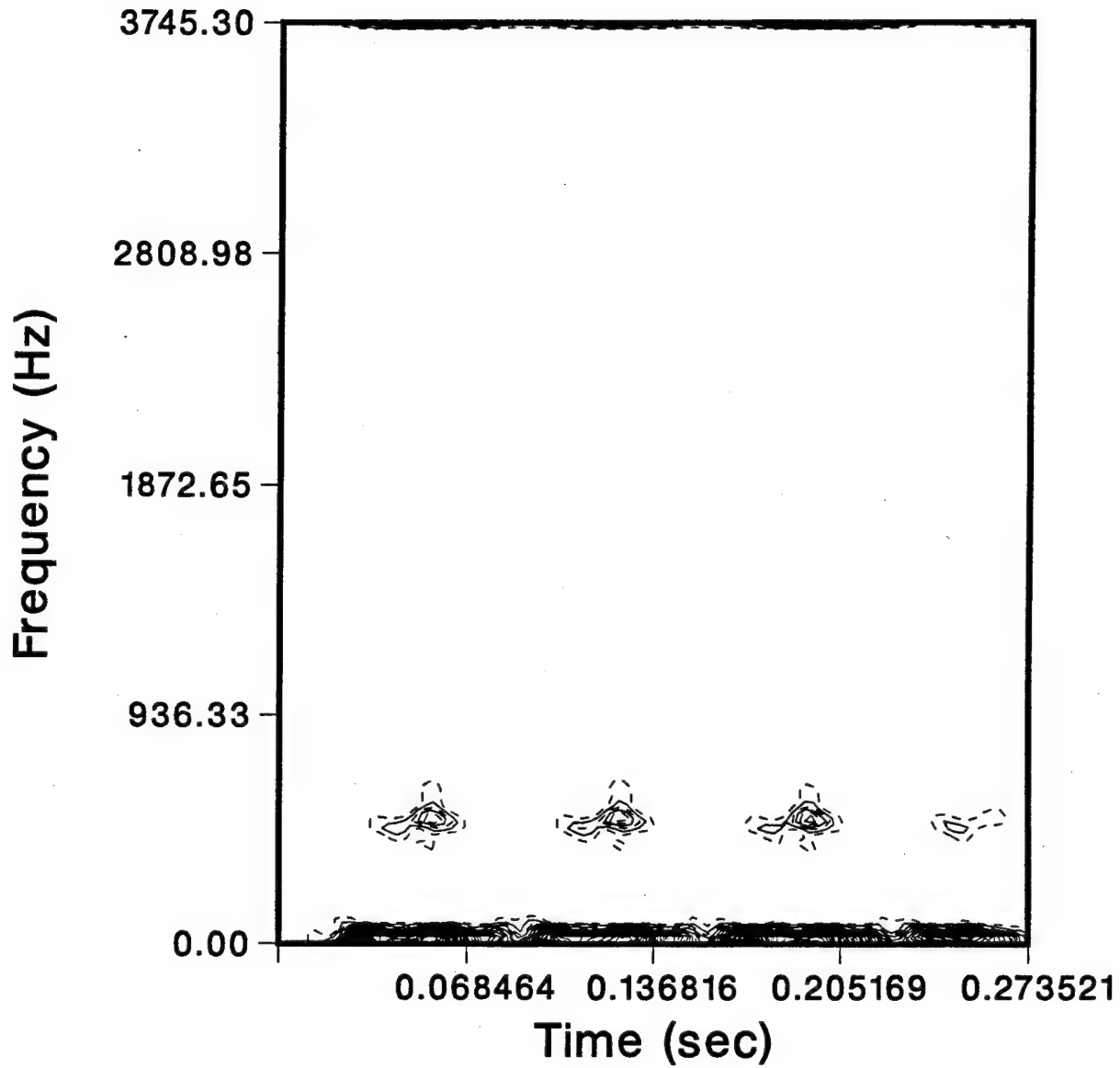


FIGURE 50: PWVD Results, MID 115 Compressor
Sampled at 7500 HZ, Radial Direction

PWVD CONTOUR MAP



**FIGURE 51: PWVD Contour Map, MID 115 Compressor
Sampled at 7500 HZ, Radial Direction**

PSEUDO WIGNER-VILLE DISTRIBUTION

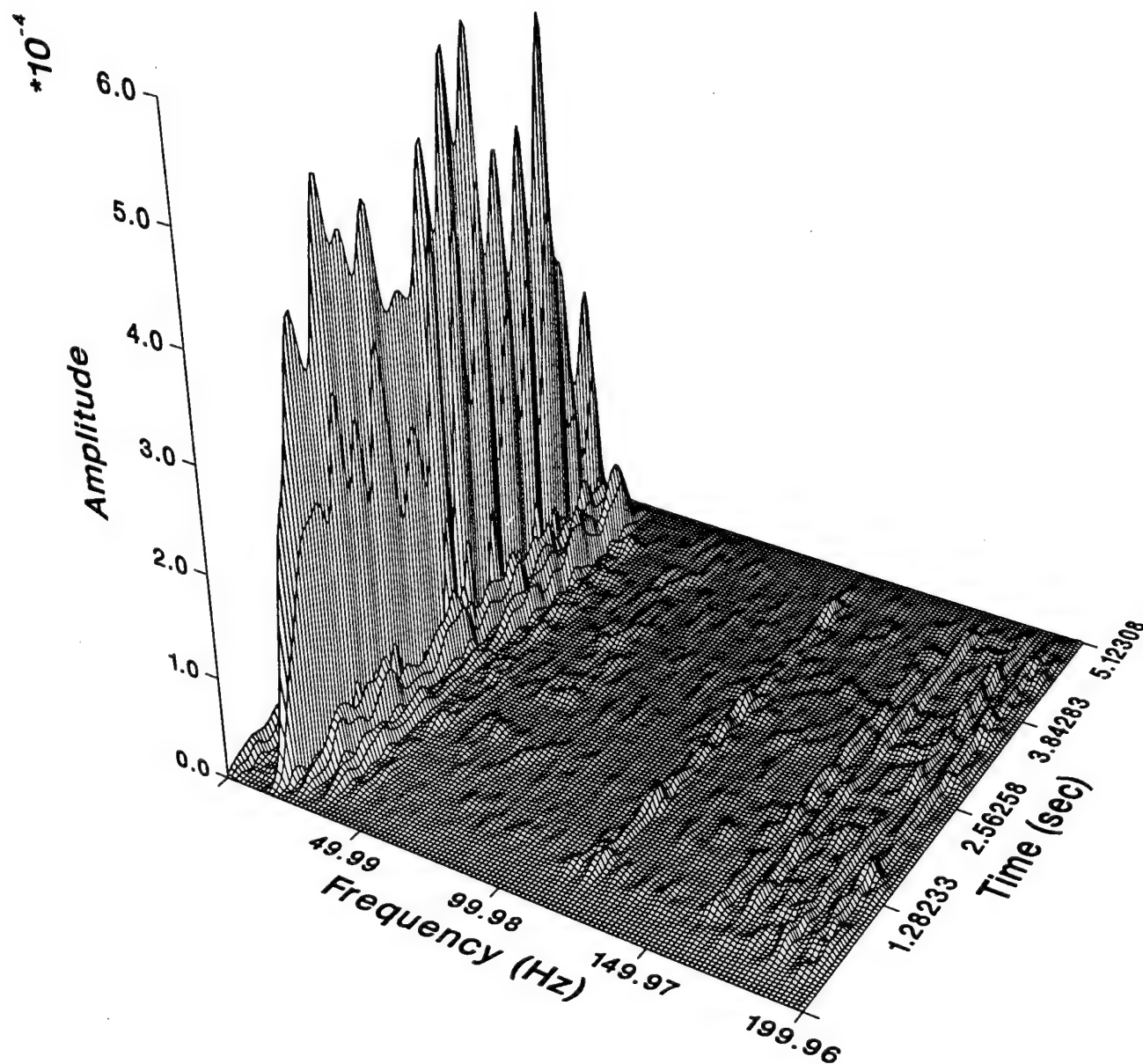
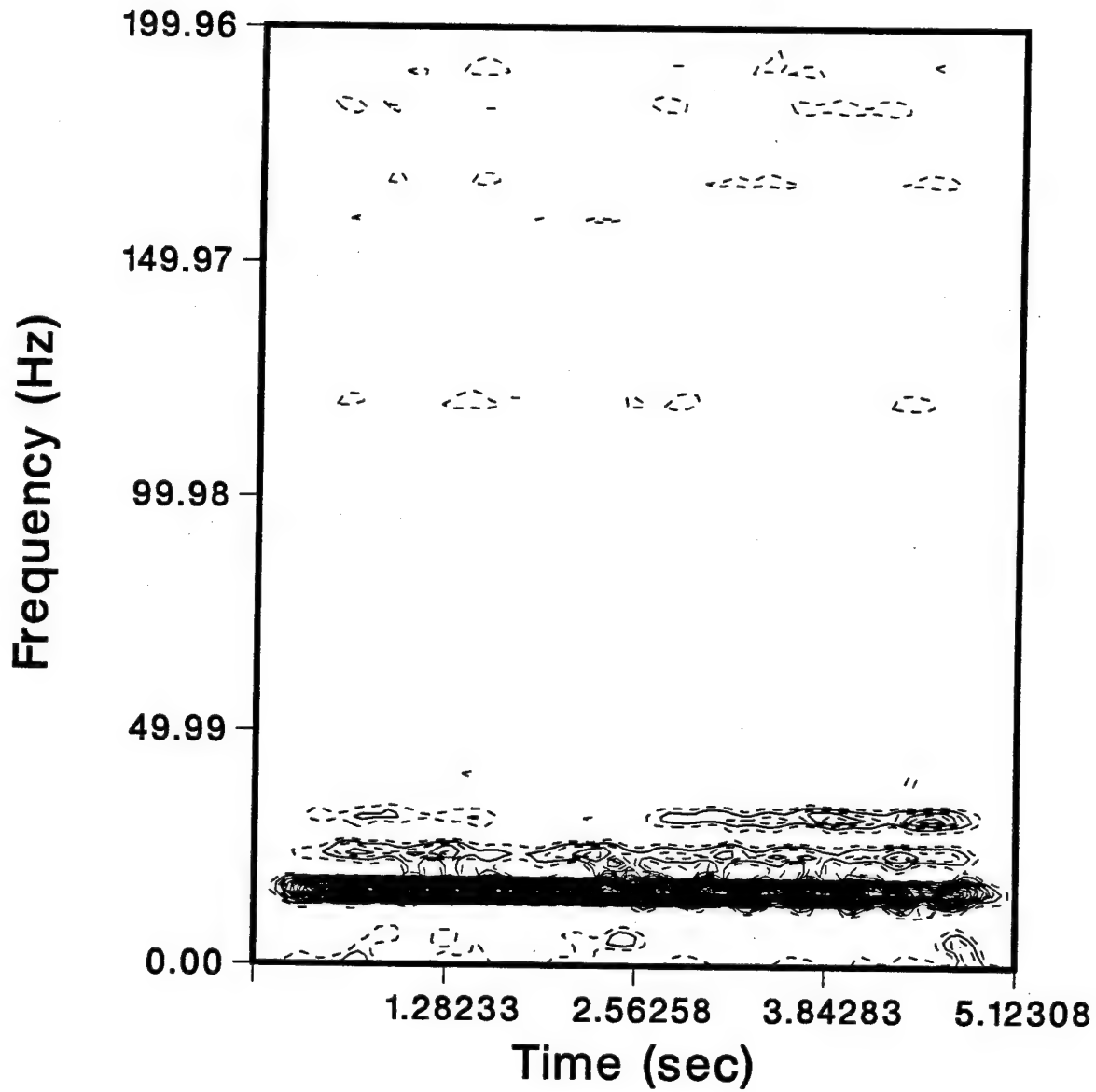


FIGURE 52: PWVD Results, MID 524 Compressor
Sampled at 400 HZ, Tangential Direction

PWVD CONTOUR MAP



**FIGURE 53: PWVD Contour Map, MID 524 Compressor
Sampled at 400 HZ, Tangential Direction**

PSEUDO WIGNER-VILLE DISTRIBUTION

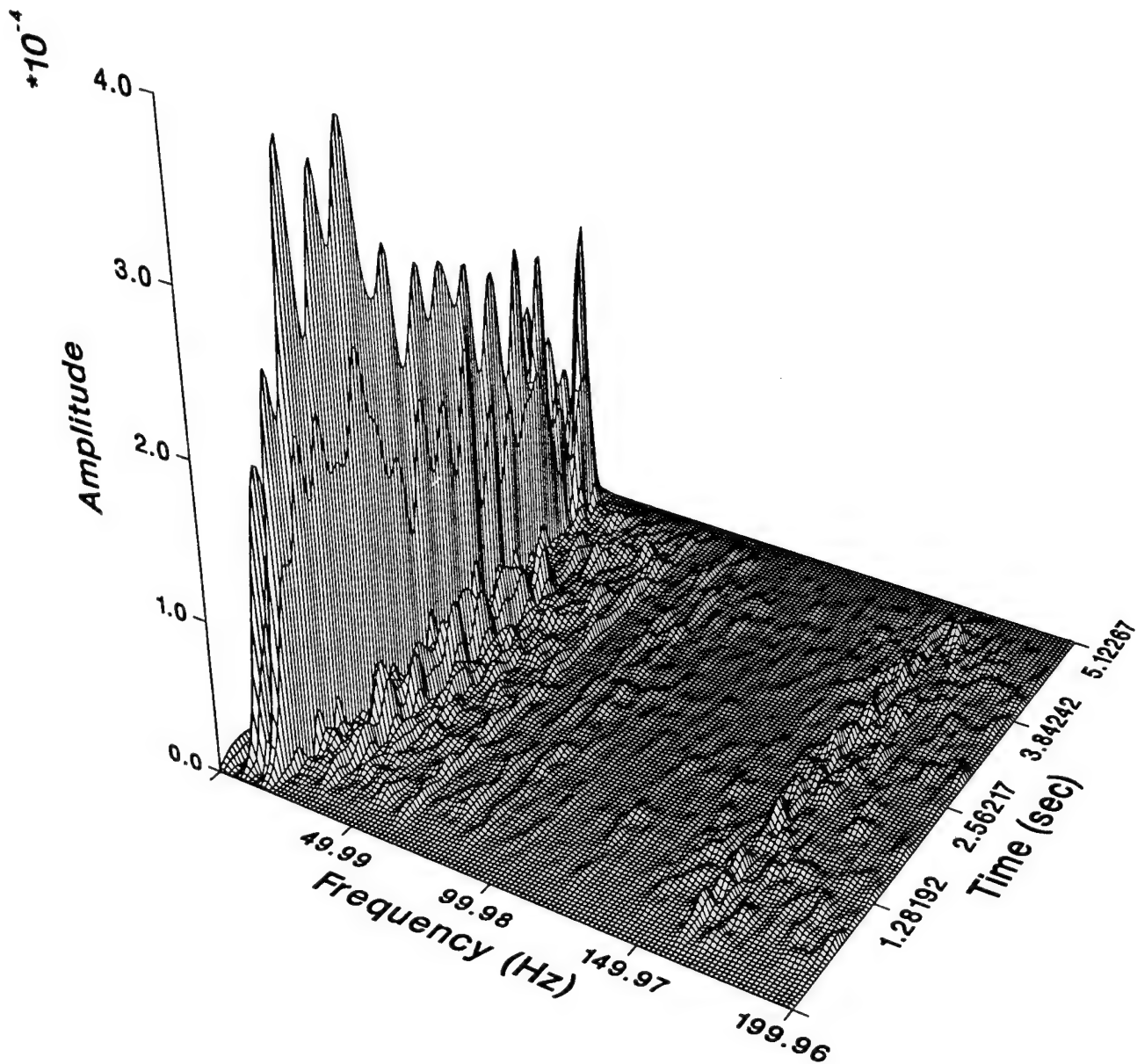
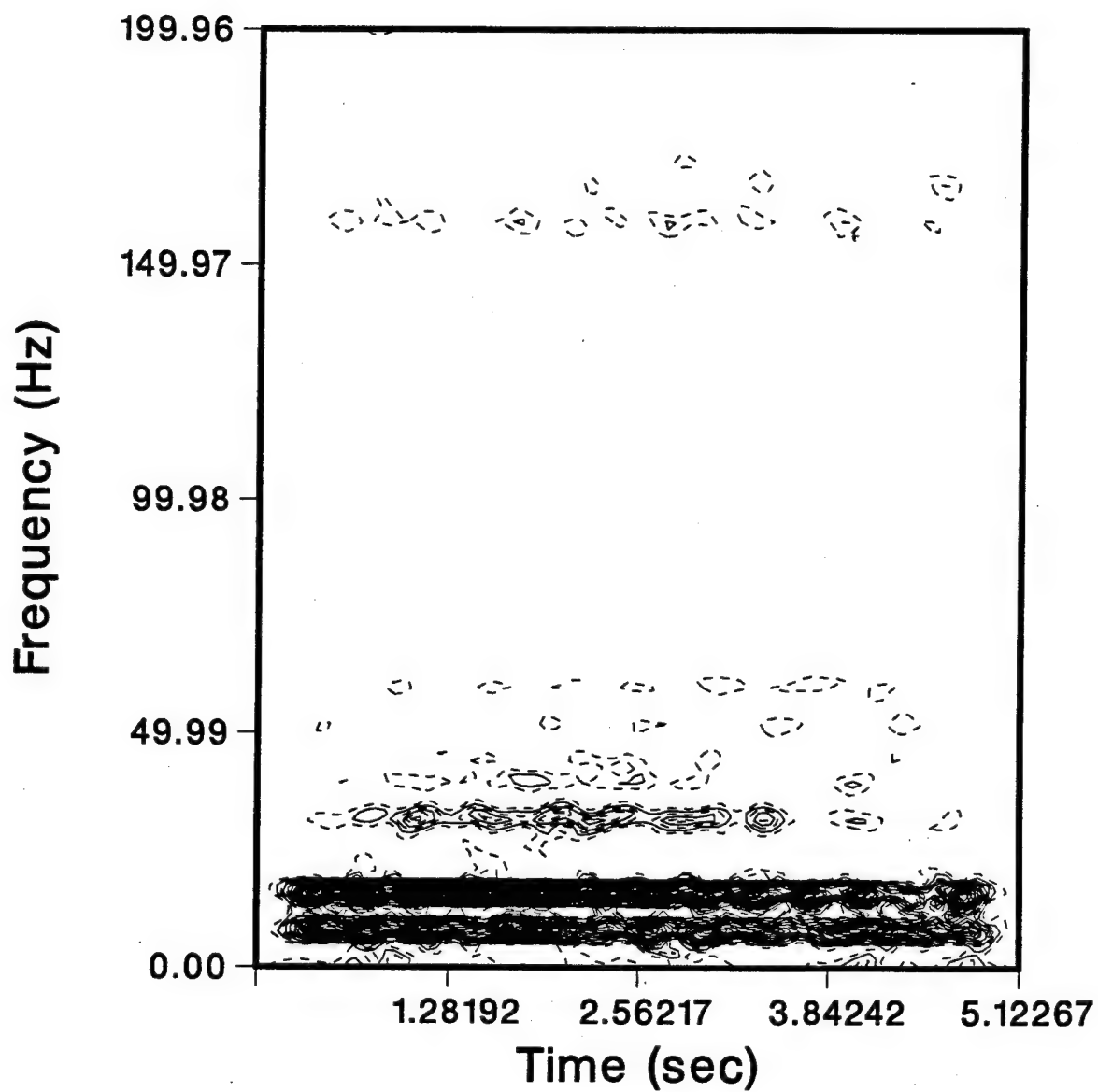


FIGURE 54: PWVD Results, MID 524 Compressor
Sampled at 400 HZ, Axial Direction

PWVD CONTOUR MAP



**FIGURE 55: PWVD Contour Map, MID 524 Compressor
Sampled at 400 HZ, Axial Direction**

PSEUDO WIGNER-VILLE DISTRIBUTION

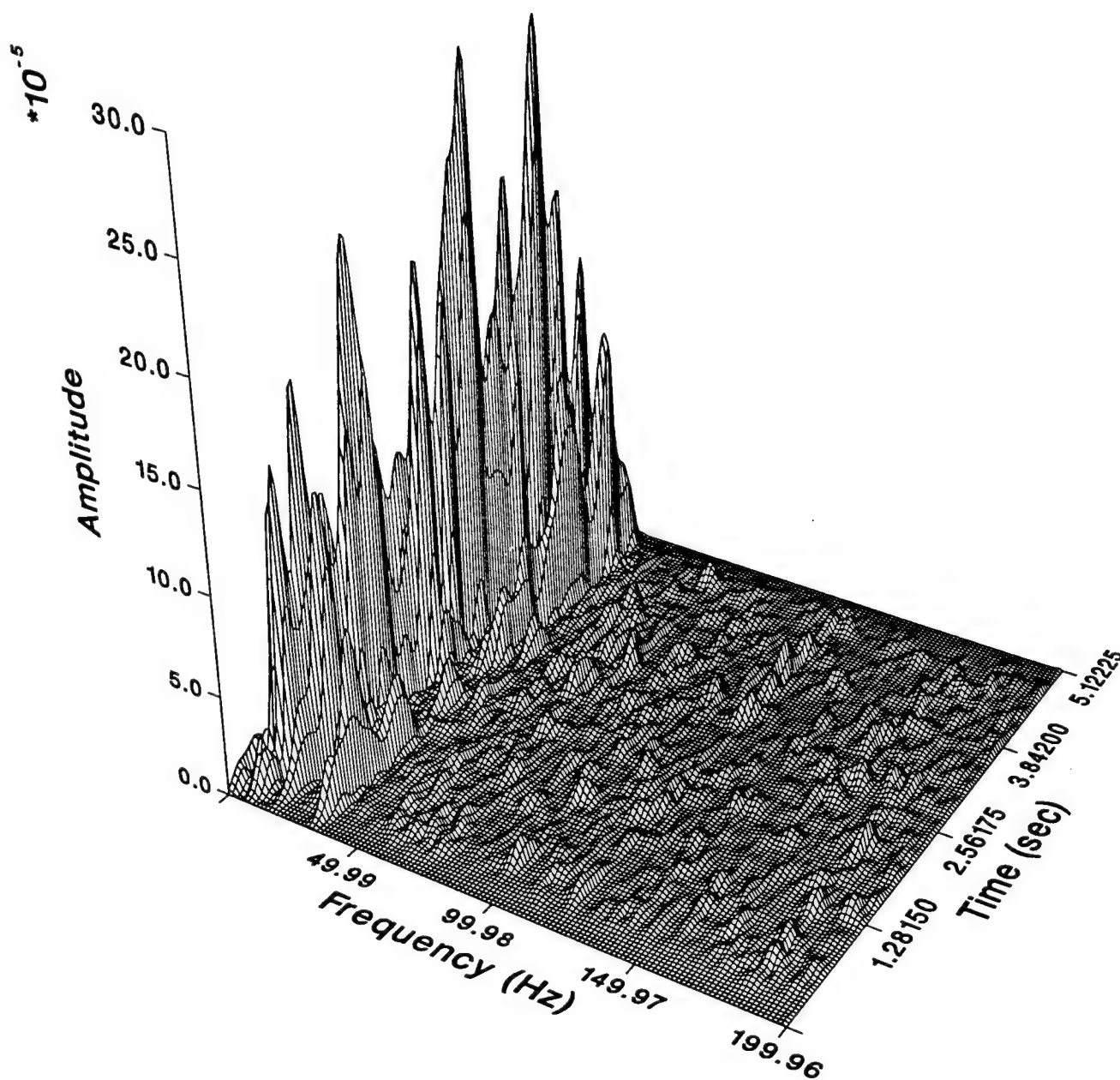
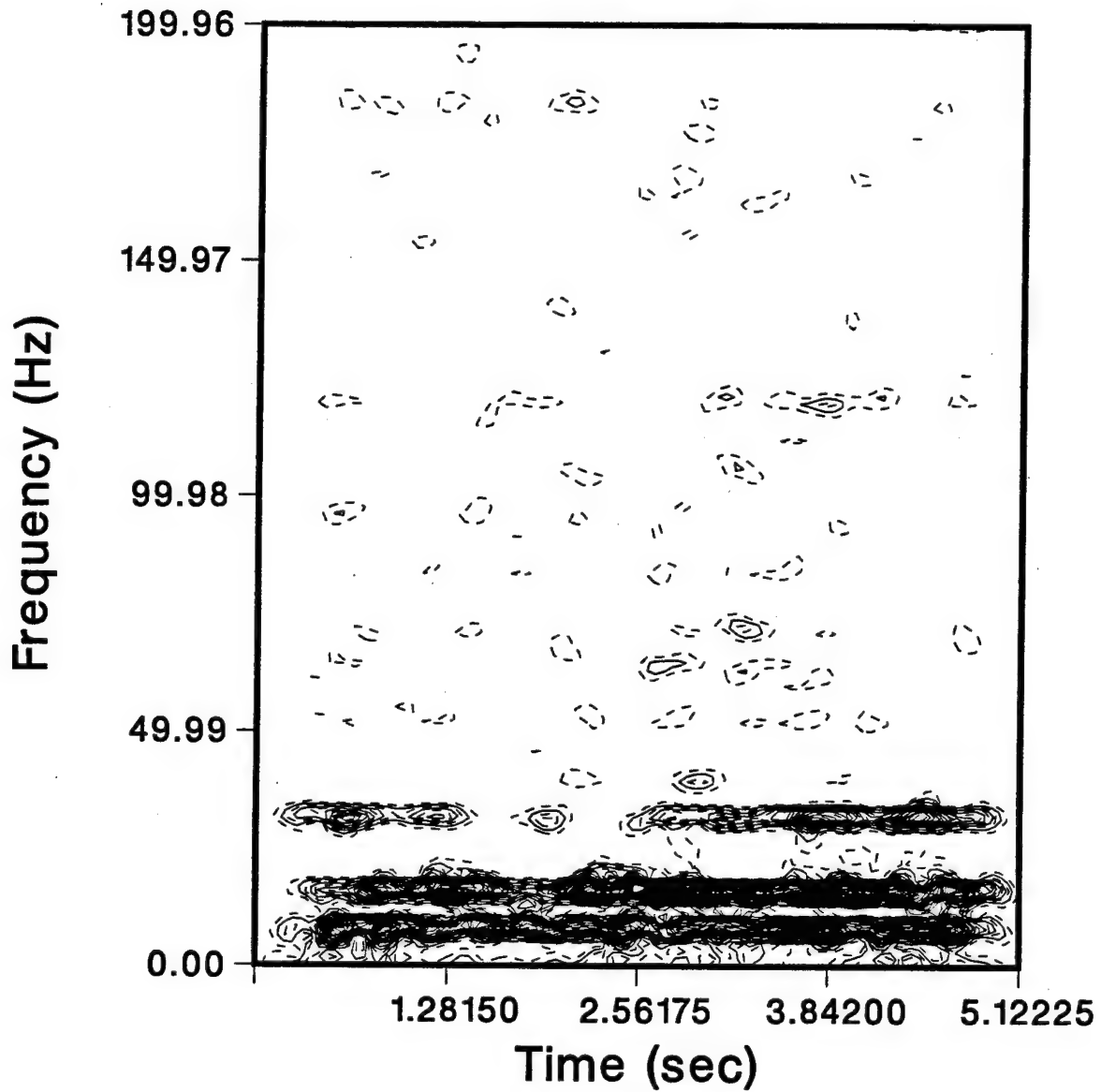


FIGURE 56: PWVD Results, MID 524 Compressor
Sampled at 400 HZ, Radial Direction

PWVD CONTOUR MAP



**FIGURE 57: PWVD Contour Map, MID 524 Compressor
Sampled at 400 HZ, Radial Direction**

PSEUDO WIGNER-VILLE DISTRIBUTION

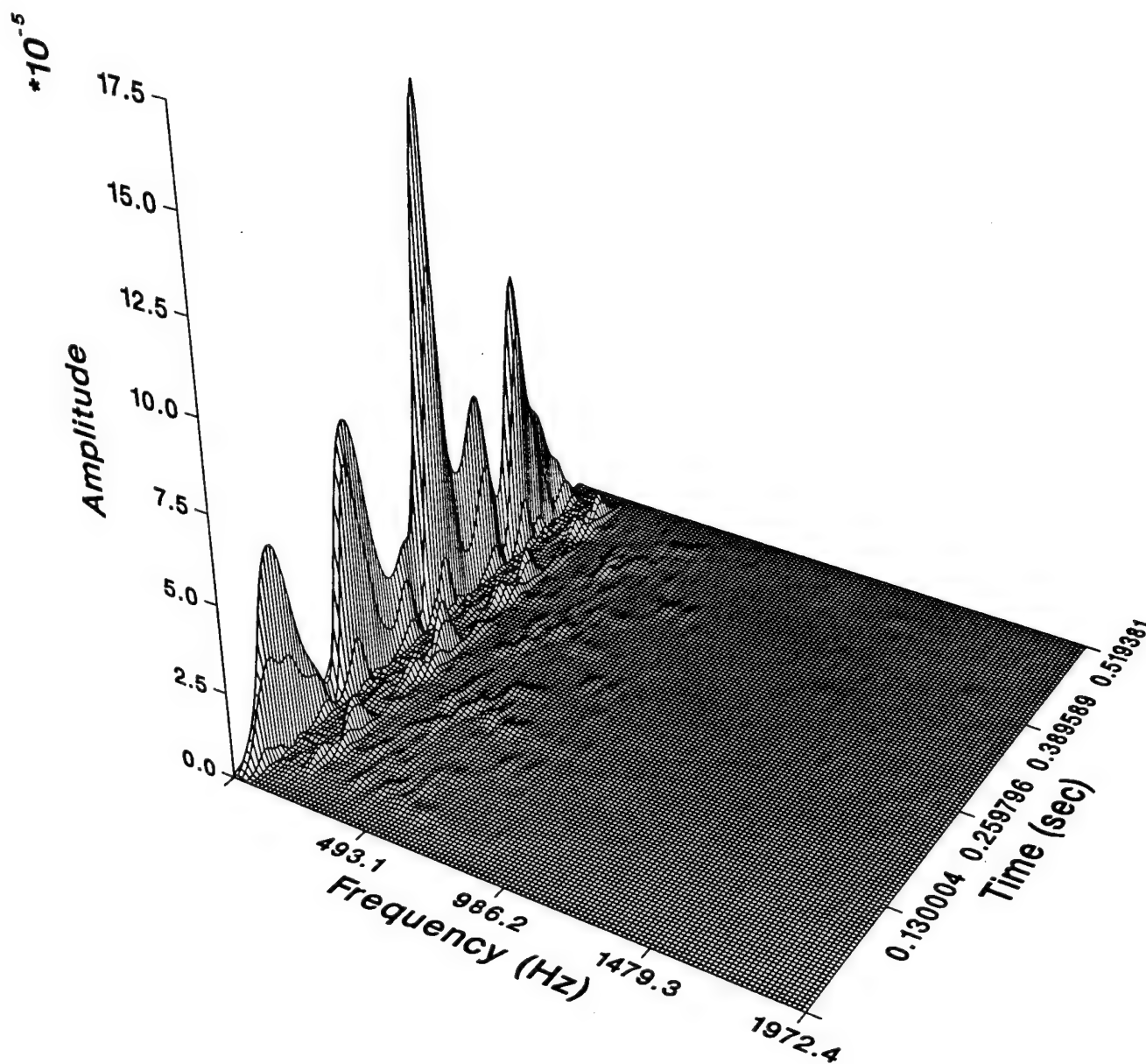
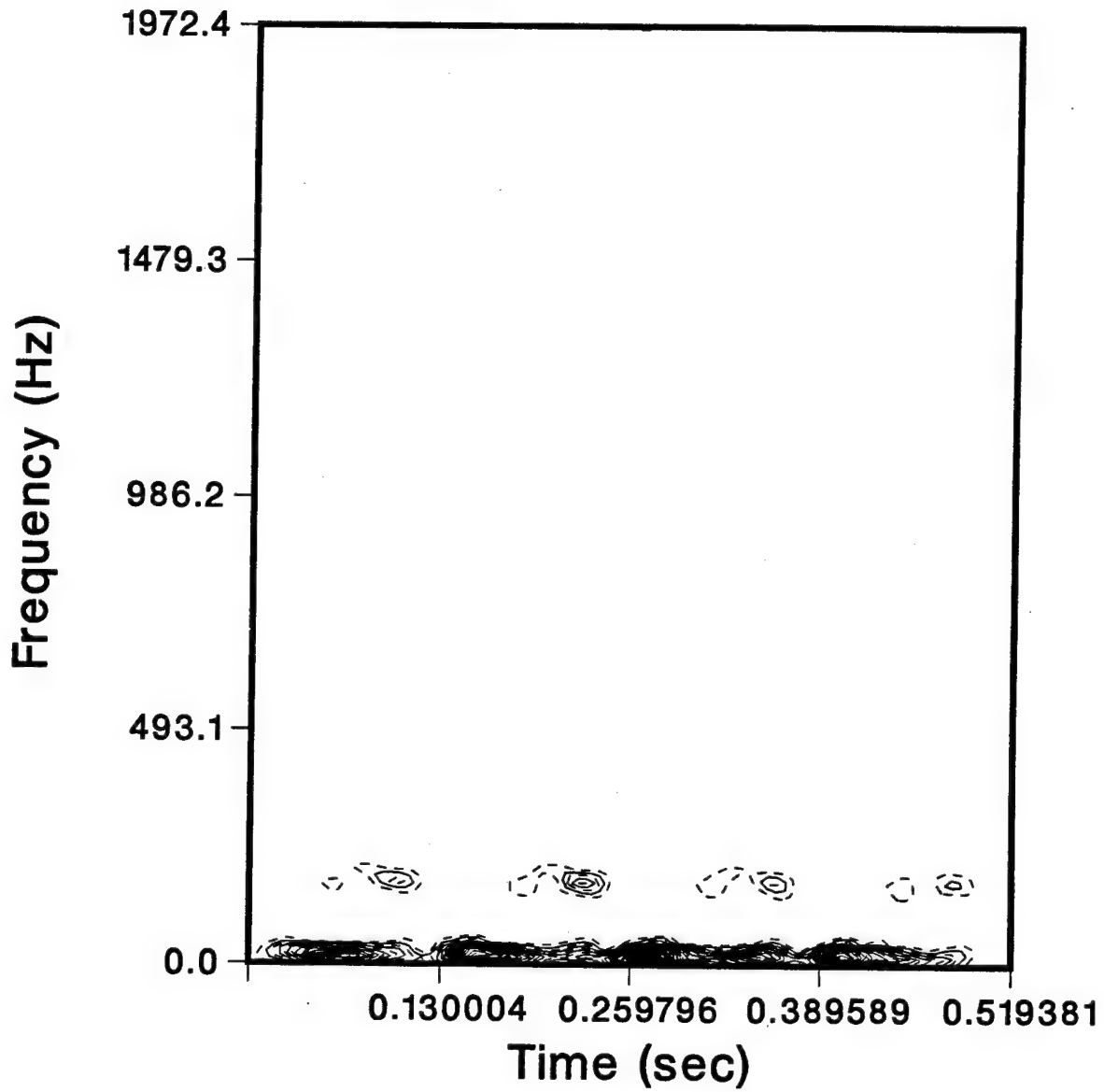


FIGURE 58: PWVD Results, MID 524 Compressor
Sampled at 3950 HZ, Tangential Direction

PWVD CONTOUR MAP



**FIGURE 59: PWVD Contour Map, MID 524 Compressor
Sampled at 3950 HZ, Tangential Direction**

PSEUDO WIGNER-VILLE DISTRIBUTION

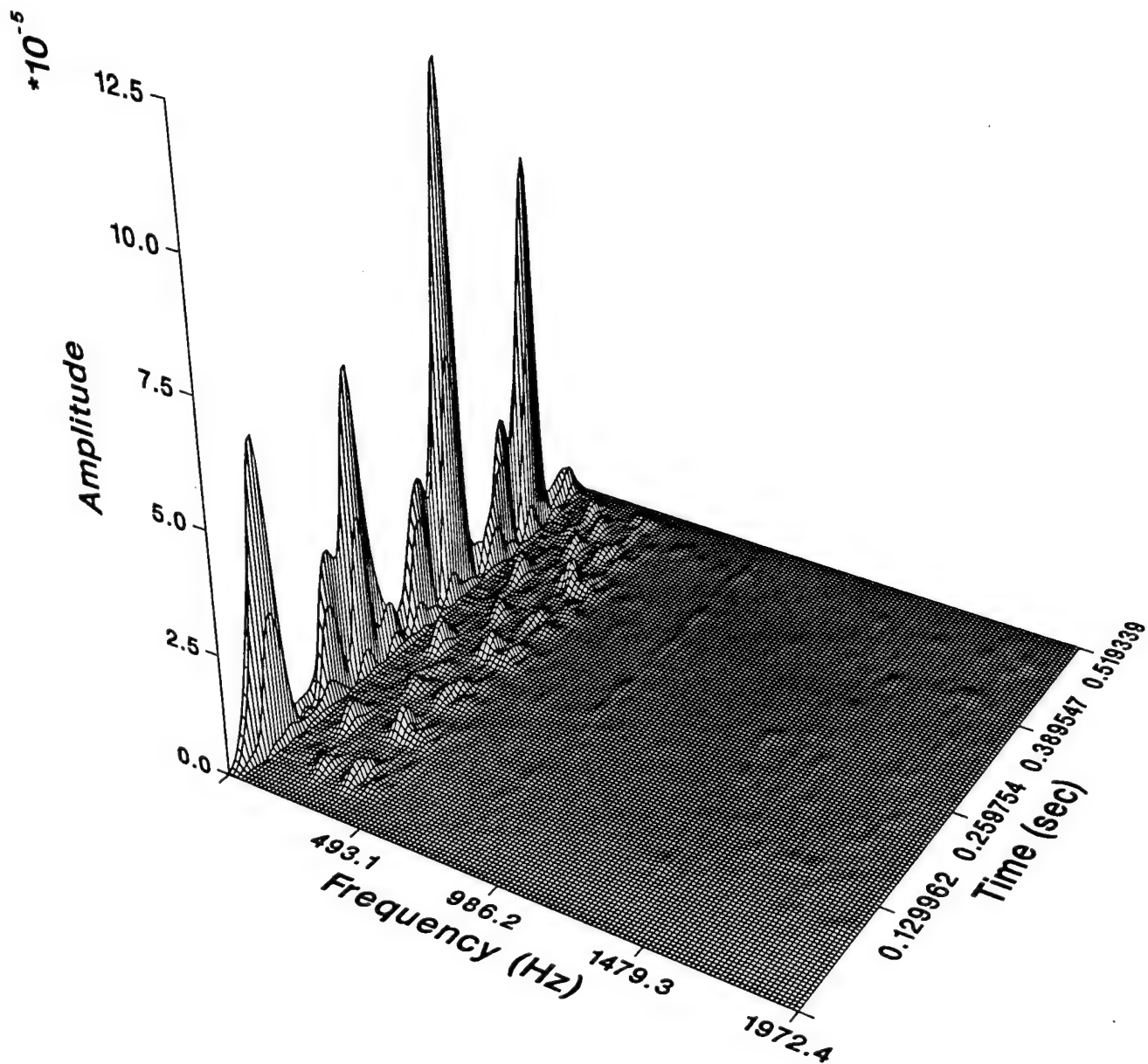


FIGURE 60: PWVD Results, MID 524 Compressor
Sampled at 3950 HZ, Axial Direction

PWVD CONTOUR MAP

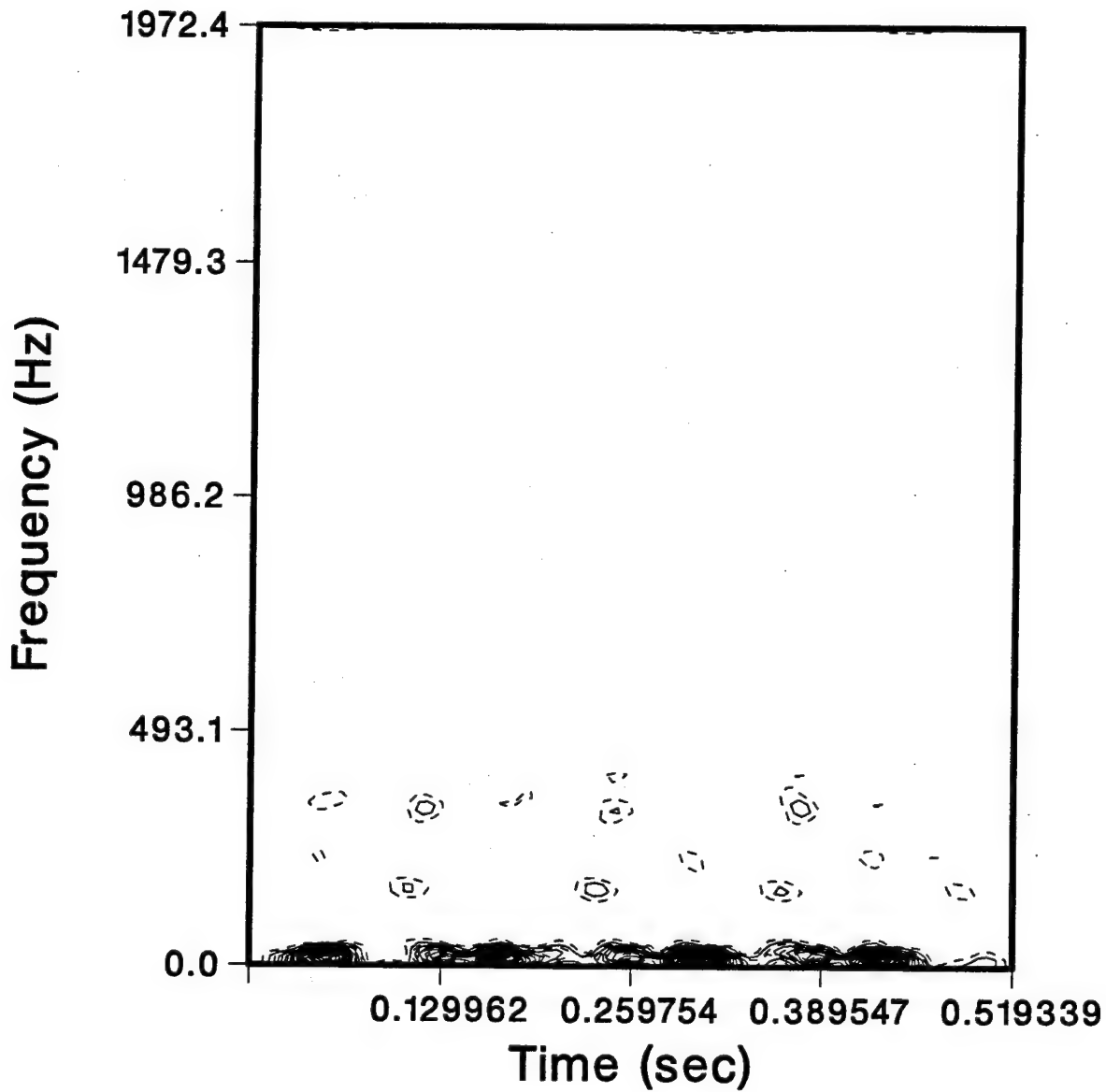


FIGURE 61: PWVD Contour Map, MID 524 Compressor
Sampled at 3950 HZ, Axial Direction

PSEUDO WIGNER-VILLE DISTRIBUTION

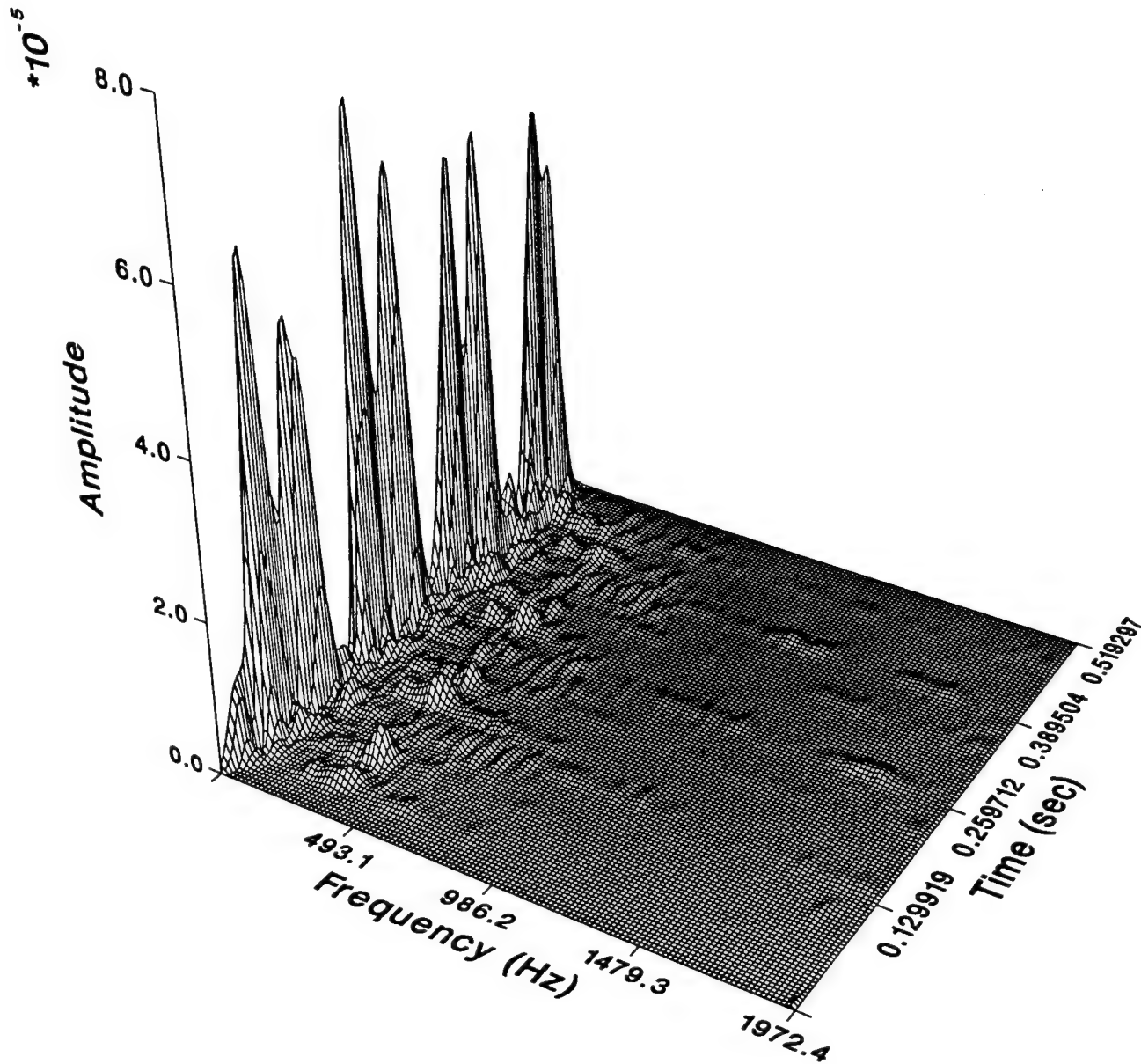
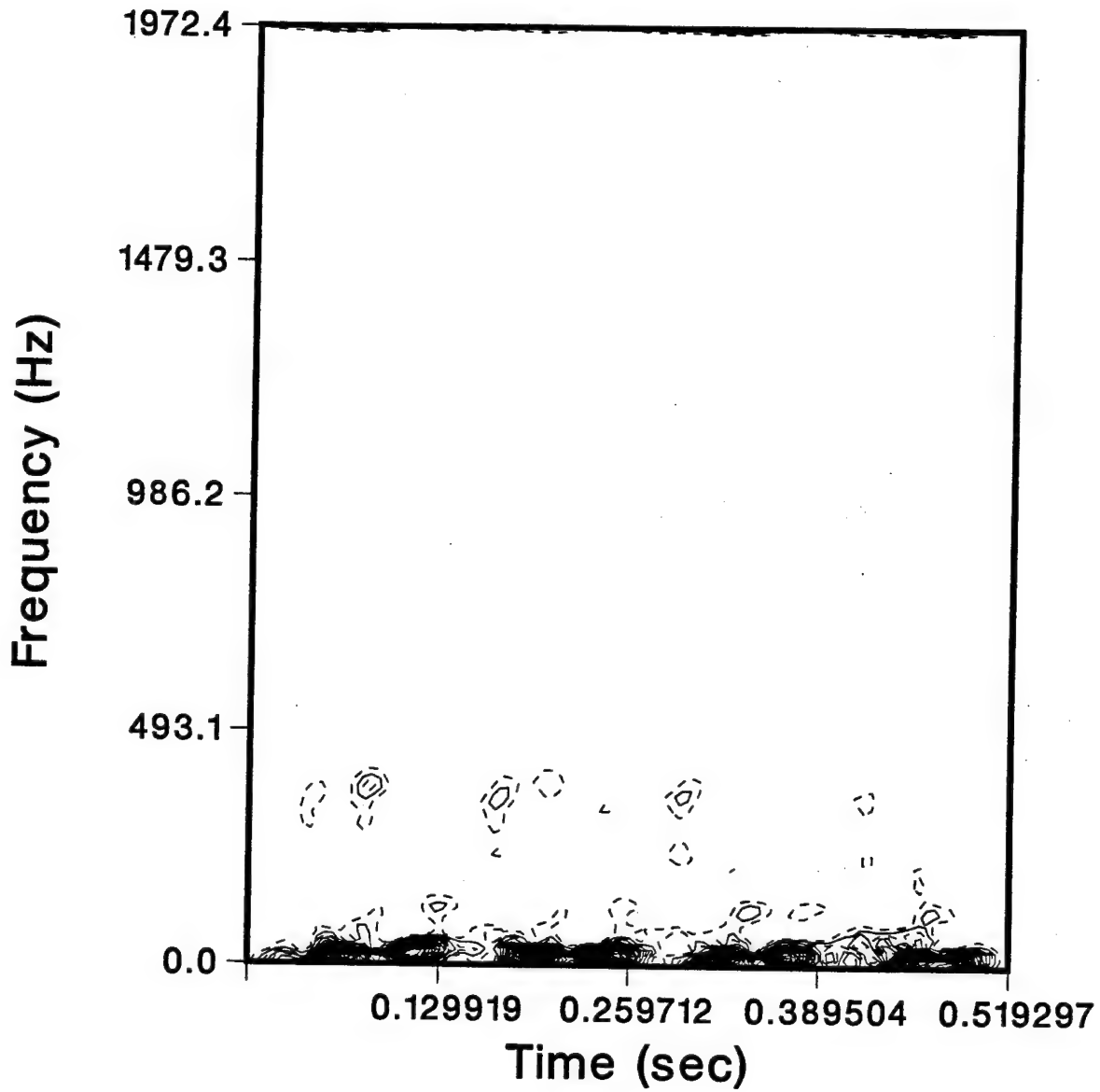


FIGURE 62: PWVD Results, MID 524 Compressor
Sampled at 3950 HZ, Radial Direction

PWVD CONTOUR MAP



**FIGURE 63: PWVD Contour Map, MID 524 Compressor
Sampled at 3950 HZ, Radial Direction**

Analyzing the graphical output from the PWVD results, the particularities of each compressor unit is readily apparent. The PWVD results of the measured vibration data clearly display the harmonic nature of the compressor assemblies. The harmonics of the compressor assemblies are denoted by the narrow-band frequency levels lasting the duration of the signal time span. Although harmonic information can be detected in spectral analysis, the PWVD results include the additional information of signal duration. The time aspect of the signal is what clearly denotes it as a harmonic of the compressor unit. The dominant harmonic response common to all of the figures results from the baseline running speed frequency of the compressor unit. The second and higher harmonic responses result from different mechanical events and components.

Statistical analysis can be used to examine any distributions and peak amplitude levels of the harmonic responses. Amplitude probability criterion method is a sophisticated analysis tool which uses either peak-to-peak, peak, or RMS readings of displacement, velocity, or acceleration. This method is currently employed in some vibration analysis programs to decipher the vibration data under spectral analysis. However, in spectral analysis such characterization for reciprocating machinery is not completely satisfactory for two reasons. First, there may exist an abnormal situation for which no time or frequency signature is

clearly apparent. Secondly, if the abnormal situation is apparent, there is generally not enough information to pinpoint the cause and thus achieve diagnosis [Ref.7]. Since time events and frequency are simultaneously relevant, the three-dimensional display from the PWVD results is a natural choice. The severity of the fault would directly effect the amplitude level of the PWVD results. Of course, in order to discriminate between a normal situation and a defective one, baseline vibration data would be required. Alarm levels could then be established based on the mean of the signal plus a set standard deviation.

3. PWVD of Artificial Fault Simulation

PWVD analysis was also conducted on the manipulated data from a MID 115 type compressor component to display the effects of glitches in otherwise harmonic vibration patterns. Recall from Chapter III, a fault signal in the form of impulse disturbances was added to the measured vibration data. The fault signal was comprised of a series of instantaneous impulses of constant amplitude at equidistant spacing along the time axis. To correspond to the sampling size of the machine data, a total of seven spikes were added to the measured data. Figures 64 through 69 display the PWVD results. These figures are arranged in the same fashion at the previous PWVD results.

PSEUDO WIGNER-VILLE DISTRIBUTION

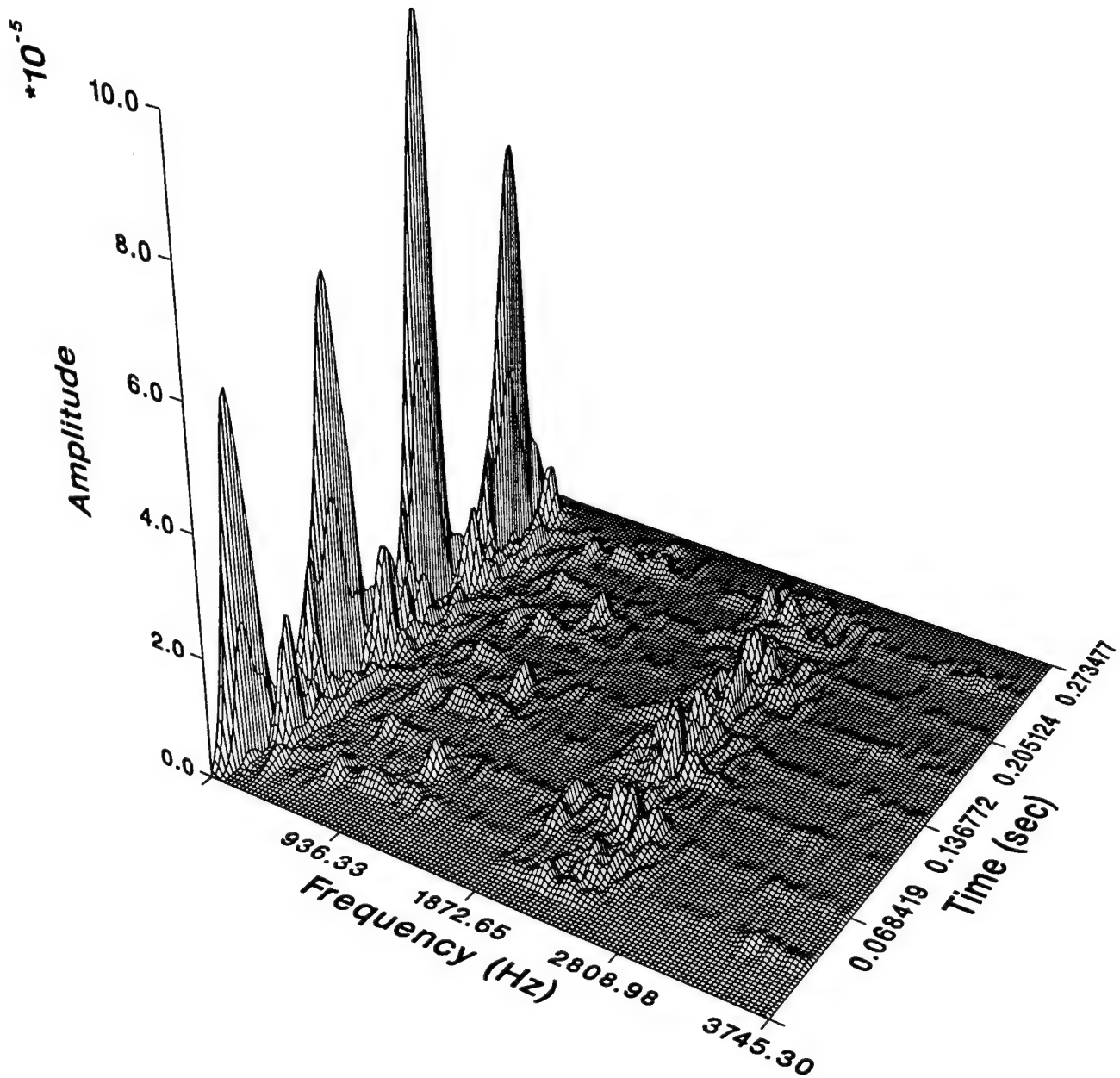
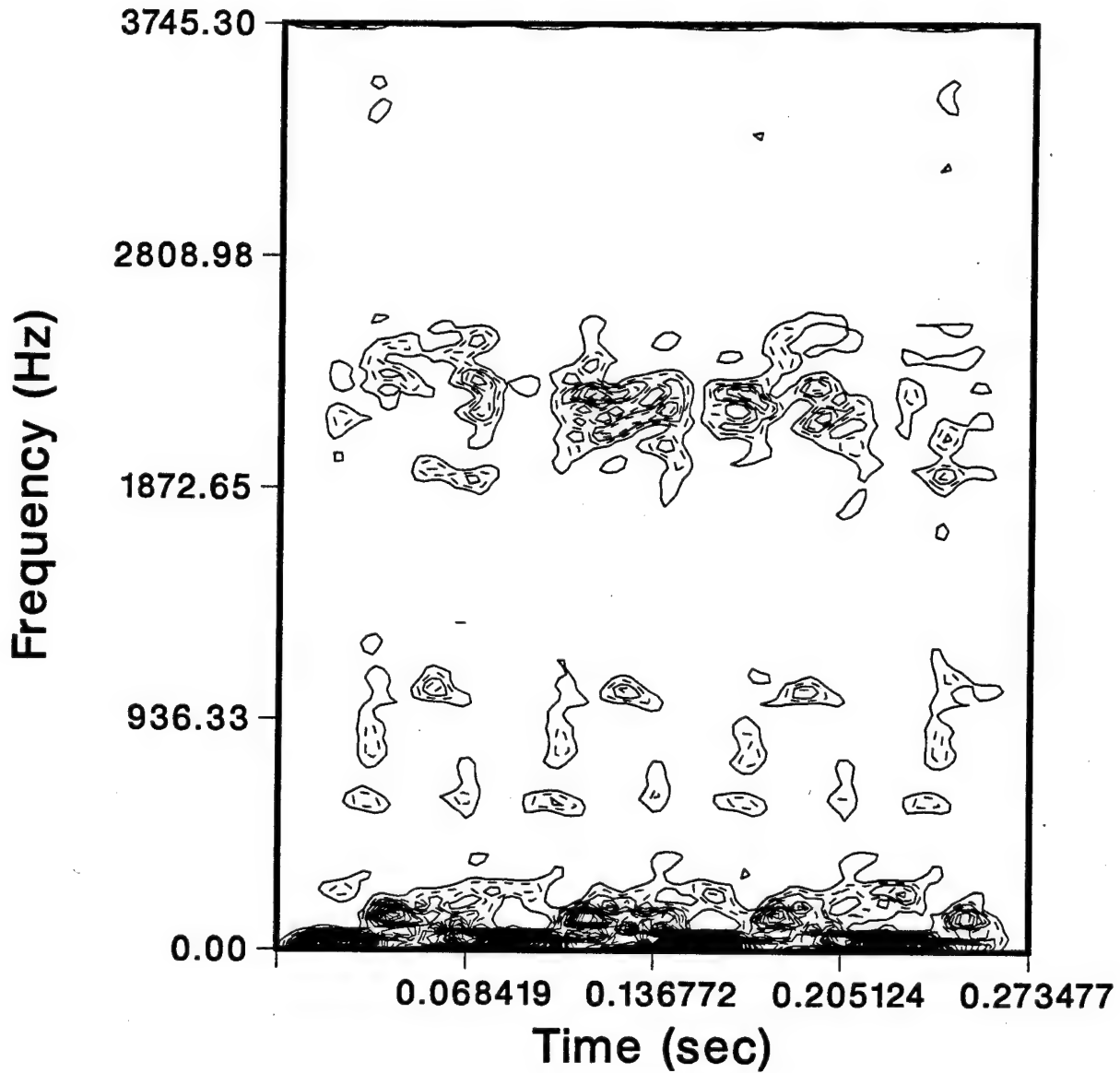


FIGURE 64: PWVD Results, Artificial Fault Simulation
Tangential Direction

PWVD CONTOUR MAP



**FIGURE 65: PWVD Contour Map, Artificial Fault Simulation
Tangential Direction**

PSEUDO WIGNER-VILLE DISTRIBUTION

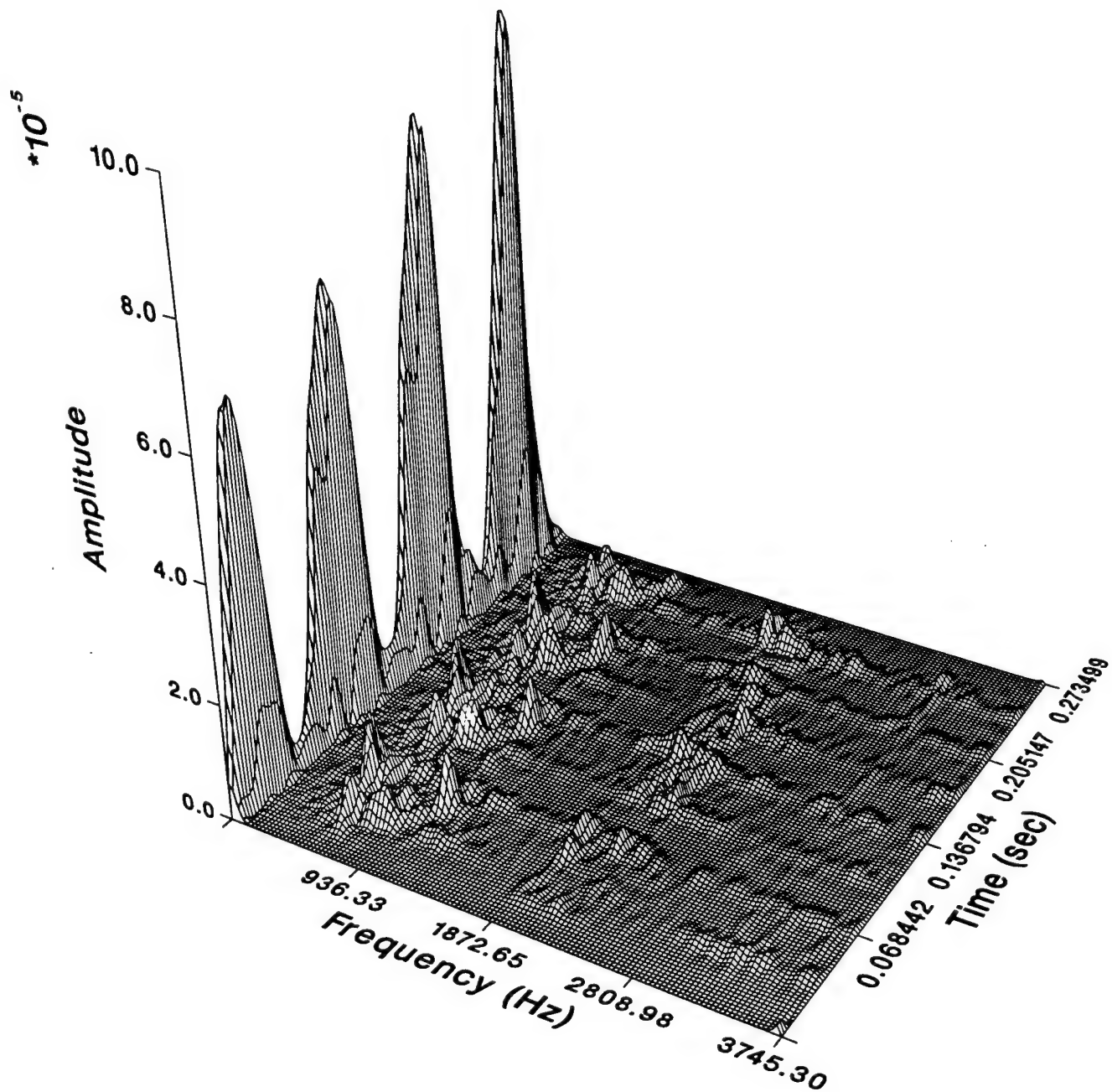
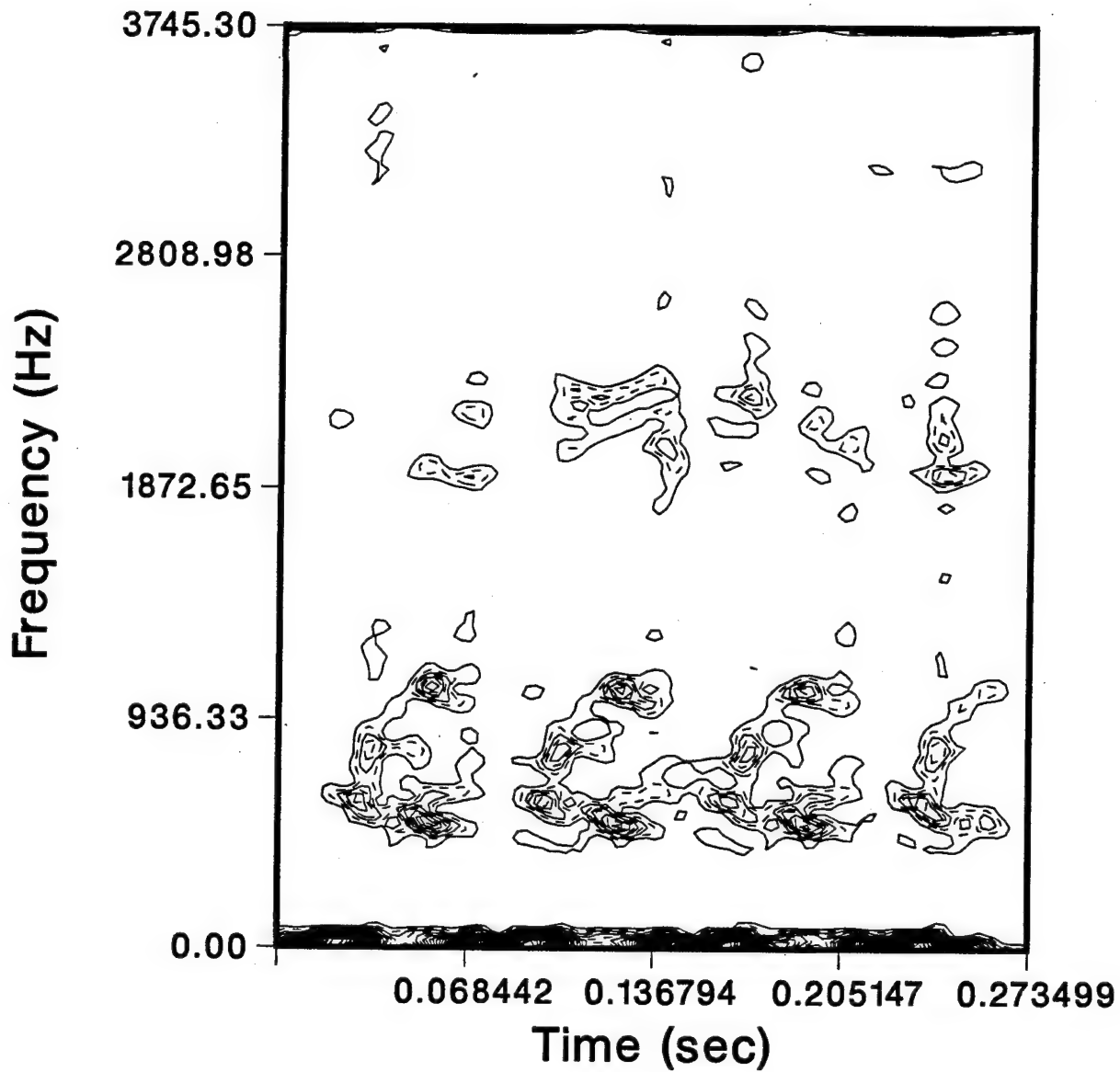


FIGURE 66: PWVD Results, Artificial Fault Simulation
Axial Direction

PWVD CONTOUR MAP



**FIGURE 67: PWVD Contour Map, Artificial Fault Simulation
Axial Direction**

PSEUDO WIGNER-VILLE DISTRIBUTION

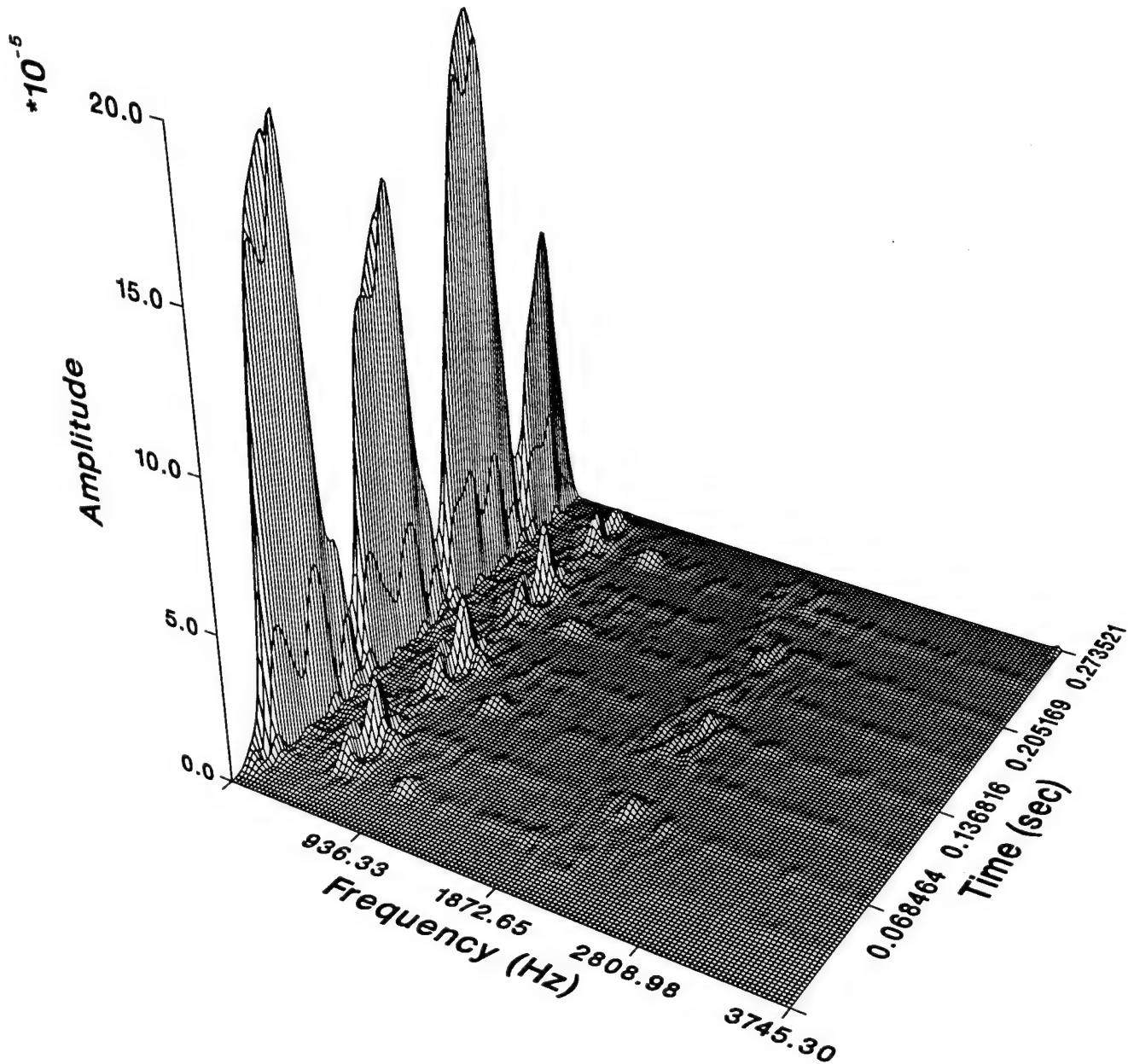


**FIGURE 68: PWVD Results, Artificial Fault Simulation
Radial Direction**

PWVD CONTOUR MAP

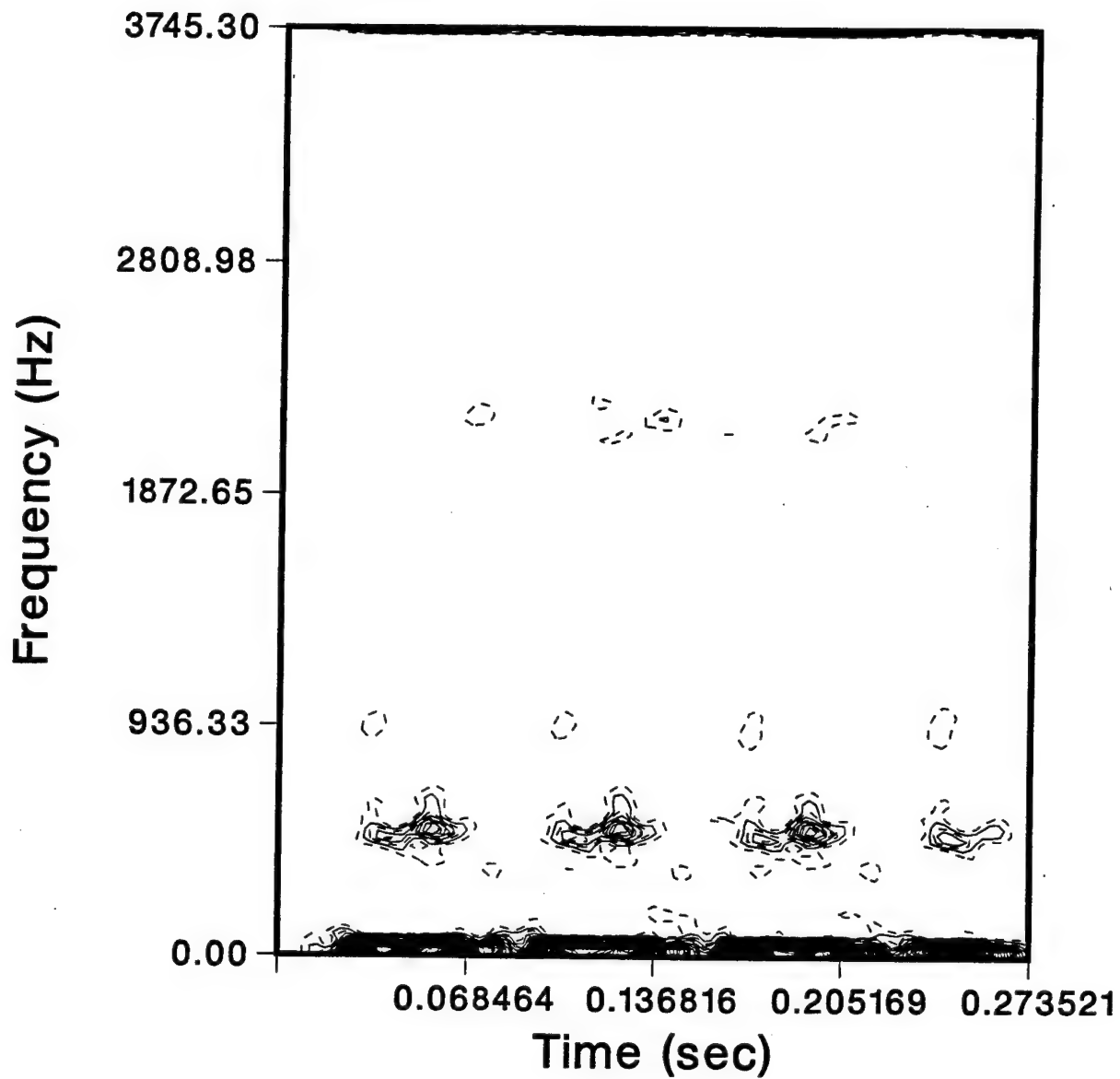


FIGURE 69: PWVD Contour Map, Artificial Fault Simulation
Radial Direction

These figures clearly depict the glitches appear as time-dependent disruptions, perpendicular to the harmonic vibration patterns of the measured data. The time component (location), and frequency range of each impulse is accurately established in the PWVD results. This trait is paramount in the assessment of machinery condition. By viewing time and frequency responses simultaneously provides diagnostic information not readily apparent in either the time-domain or frequency spectrum representations when viewed separately. In two-dimensional time-domain analysis the location of each impulse event may not be as easily detected. For example, the location of the impulse events were especially obscured when viewed in the tangential direction. In addition, actual machine faults may contain a wide range of frequencies. The glitches introduced into the machine data to simulate faulty conditions for this demonstration encompassed all frequency levels in the range of analysis. In the frequency spectrum representations the impulse events are almost elusive. As noted earlier, the disruptions to the normal patterns are only slightly visible in the higher frequency levels. From the PWVD results, the disruptions are clearly shown to span the entire frequency range considered in the analysis.

As mentioned in the previous chapter, the vibration data for the two compressor types was captured using traditional rotating analysis techniques. This limitation precluded the demonstration of transient vibration patterns in

actual reciprocating machine vibration data. To demonstrate the benefits of a time-frequency domain analysis, the transient vibration signals from the free vibration of the thin aluminum plate were inputted into the PWVD program. Figure 70 displays the PWVD results for the single impact event with Figure 71 being the corresponding contour map. Figures 72 and 73 display the PWVD results for the two almost simultaneous impacts. Comparing these figures to their respective time-domain and frequency spectrum representations, the benefits of the combined time-frequency analysis is evident. The PWVD results clearly display the time-dependency and major frequency components of the transient vibration signals.

PSEUDO WIGNER-VILLE DISTRIBUTION

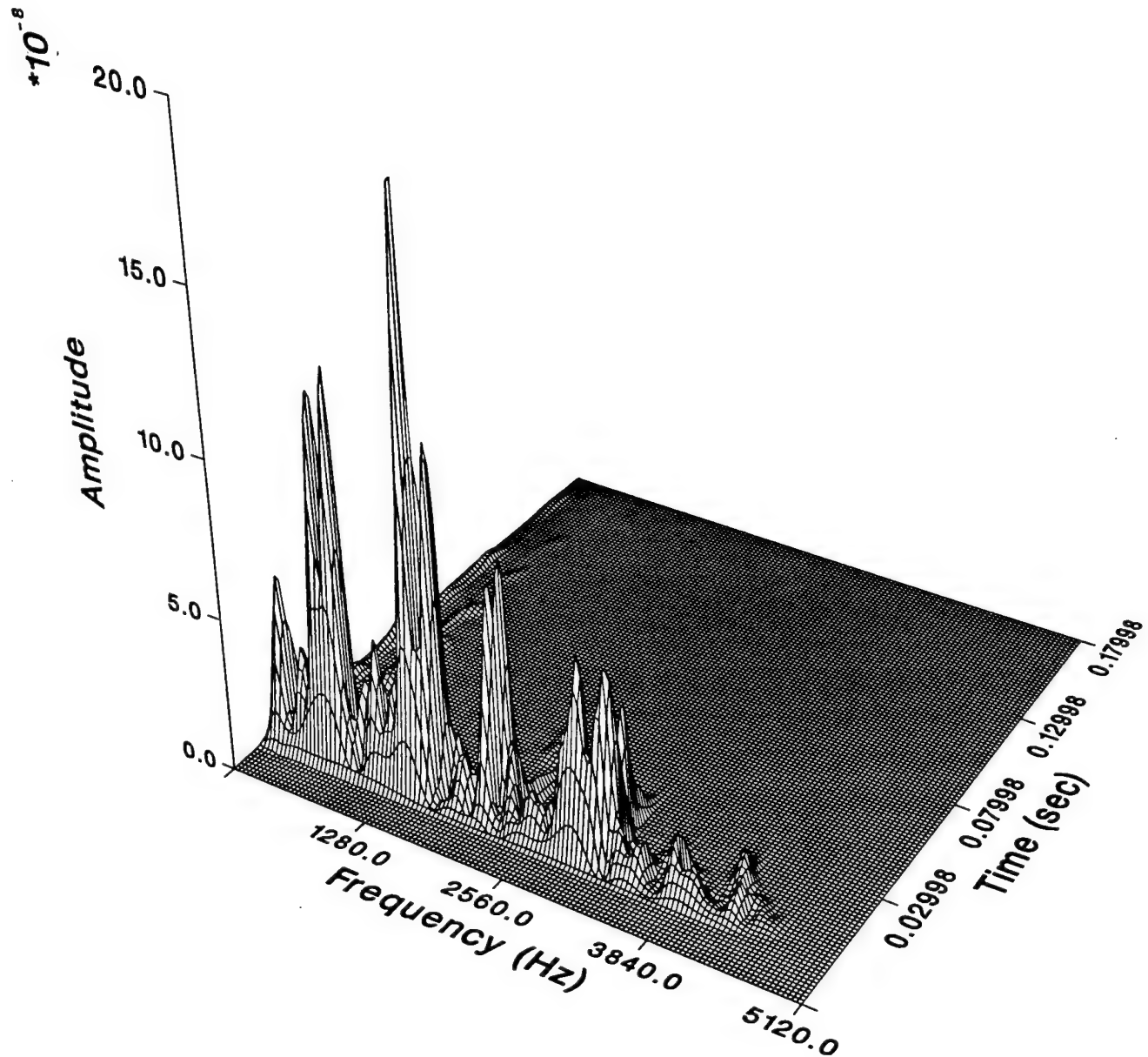


FIGURE 70: PWVD Results, Typical Transient Vibration
Single Impact

PWVD CONTOUR MAP

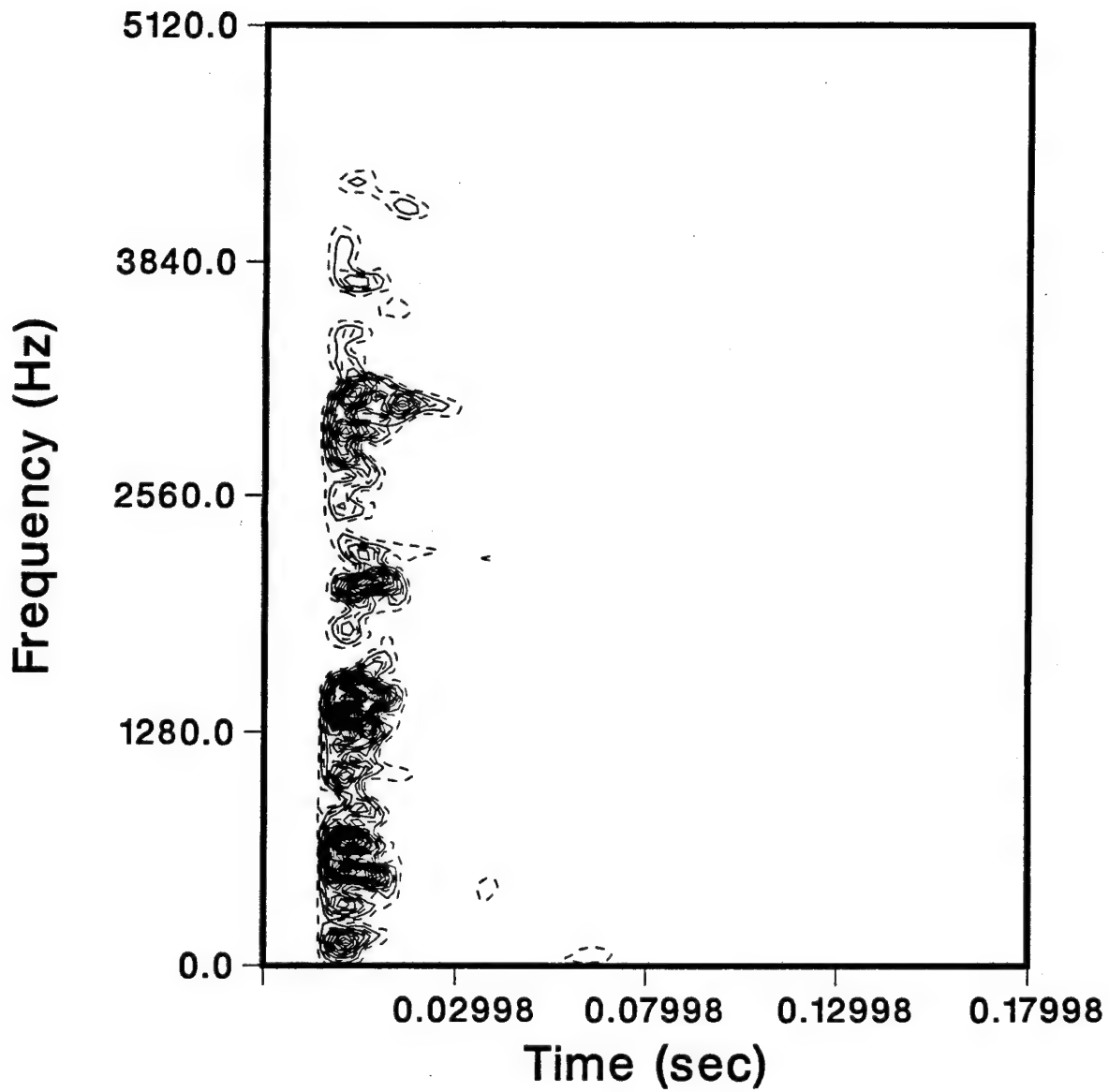


FIGURE 71: PWVD Contour Map, Typical Transient Vibration Single Impact

PSEUDO WIGNER-VILLE DISTRIBUTION

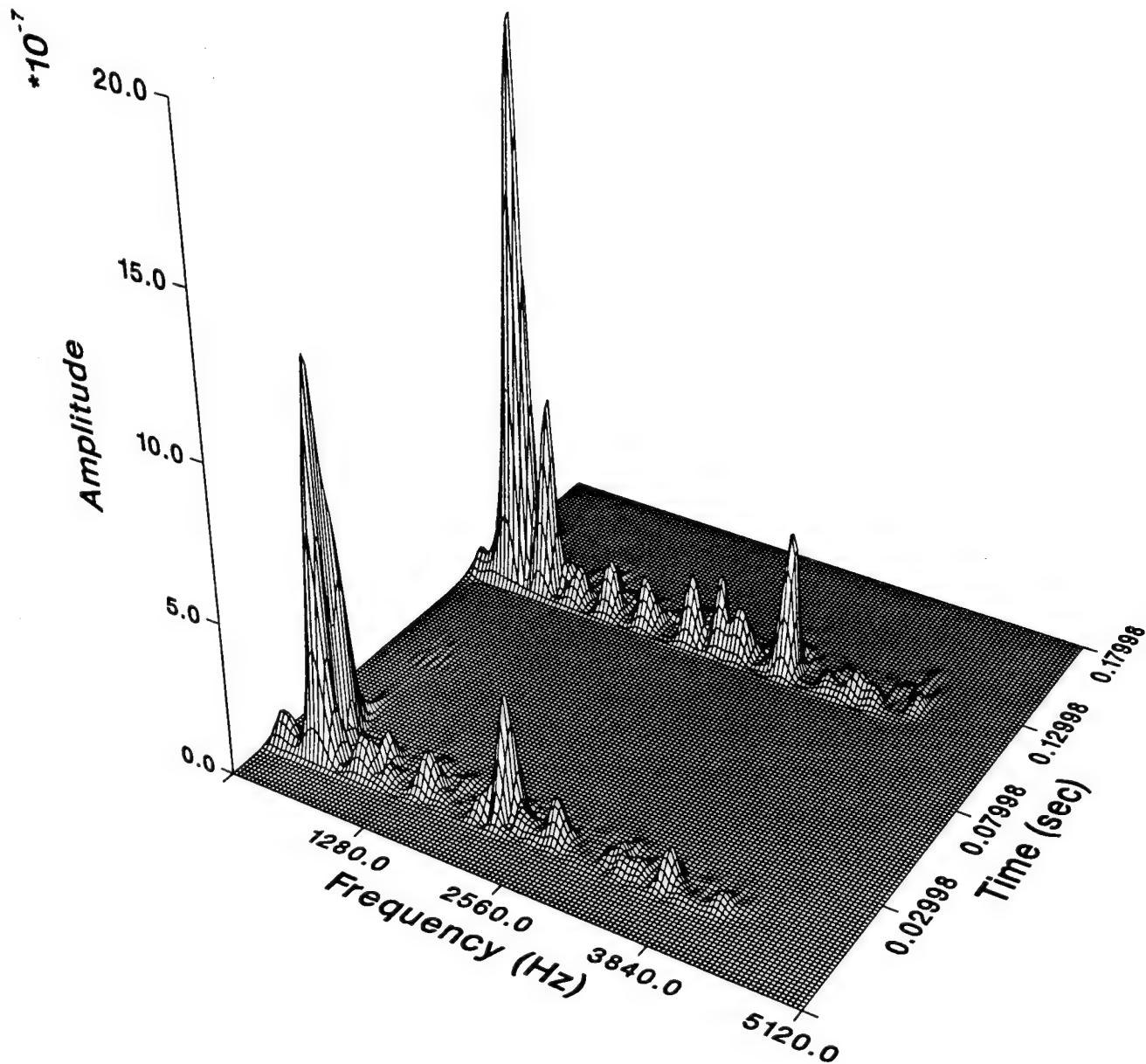


FIGURE 72: PWVD Results, Typical Transient Vibration
Dual Impact

PWVD CONTOUR MAP

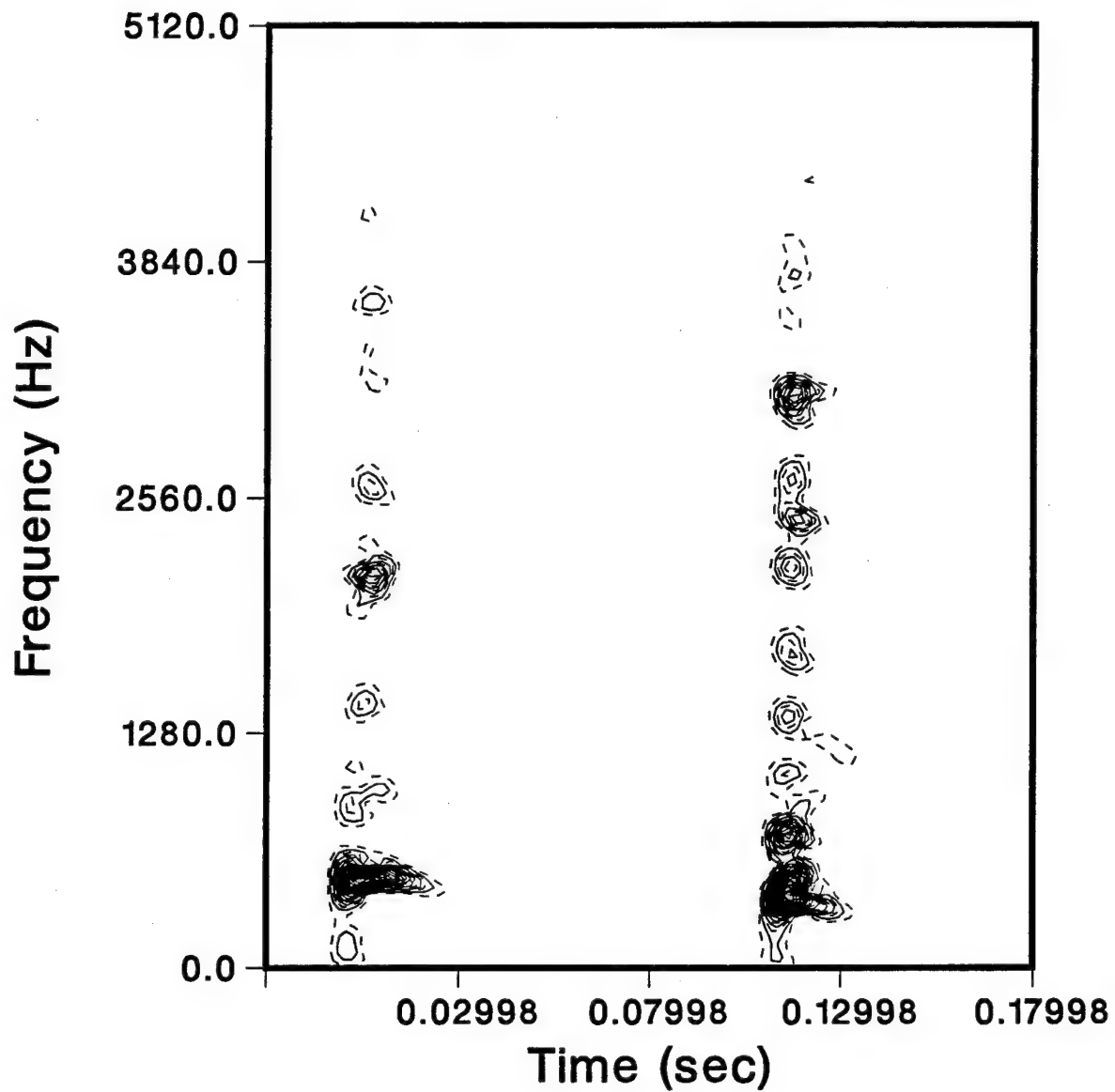


FIGURE 73: PWVD Contour Map, Typical Transient Vibration
Dual Impact

B. WAVELET ANALYSIS

1. History of Wavelet Analysis

Wavelet analysis was considered as a complimentary technique to the time-frequency domain analysis provide by PWVD. Wavelet transform is ideally suited for detecting small disturbances in wide-band transient or non-stationary vibration signals in the time-frequency domain. Although the disturbances in the harmonic waveforms created by the impulse events were visible in the PWVD results, it is proposed that further analysis of the disruptive events could be conducted with Wavelet analysis. It should be noted that a full explanation of wavelet transforms will not be presented here. The purpose of introducing Wavelet analysis in this study is to further develop the foundation for the application of time-frequency domain analysis for reciprocating machines. Wavelet analysis provides the possible expansion from analysis and condition monitoring to diagnostics.

When compared with PWVD analysis, the use of wavelet transform in vibration analysis is relatively new. Newland [Ref.15] investigated the properties and application of wavelet transform to vibration analysis. Wang and McFadden [Ref.16] demonstrated how wavelet transform may be applied to the analysis of the vibration signals produced by the meshing of a gear. The premise of this previous research was based on the ability of the wavelet transform to easily characterize the local regularity of a function. Simply by a change of the

scale parameter (dilation) in the wavelet transform, many scales of local structure can be described by a distribution in the time-scale plane [Ref.17]. The simultaneous display of both large and small scale features enables the detection of both distributed and local faults.

2. Wavelet Analysis of Artificial Fault Simulation

To provide a brief demonstration on the effectiveness of Wavelet analysis, wavelet transform was conducted on the vibration data taken from a MID 115 type compressor component in the tangential direction with the added effects of the impulse disturbances. Figures 74 and 75 display the wavelet transform results in the three dimensional; time, frequency, amplitude orientation, and in the two dimensional; time and frequency contour map respectively. These figures demonstrate the effectiveness of wavelet transforms to characterize the local regularity of the vibration data as well as amplify the influence of the constructed fault signal. The impulse disturbances have a dramatic effect in the upper frequency range of the input data where the harmonic responses are not as dominant. This feature of wavelet transform provides a great advantage for analysis of vibration data containing small disturbances. Also, wavelet transform sweeps along the frequency line in octaves which makes it more effective for the analysis of an input signal with a lengthy time record [Ref.17]. A 1/1 octave sweep step was selected for the displayed wavelet transform results.

WAVELET TRANSFORM

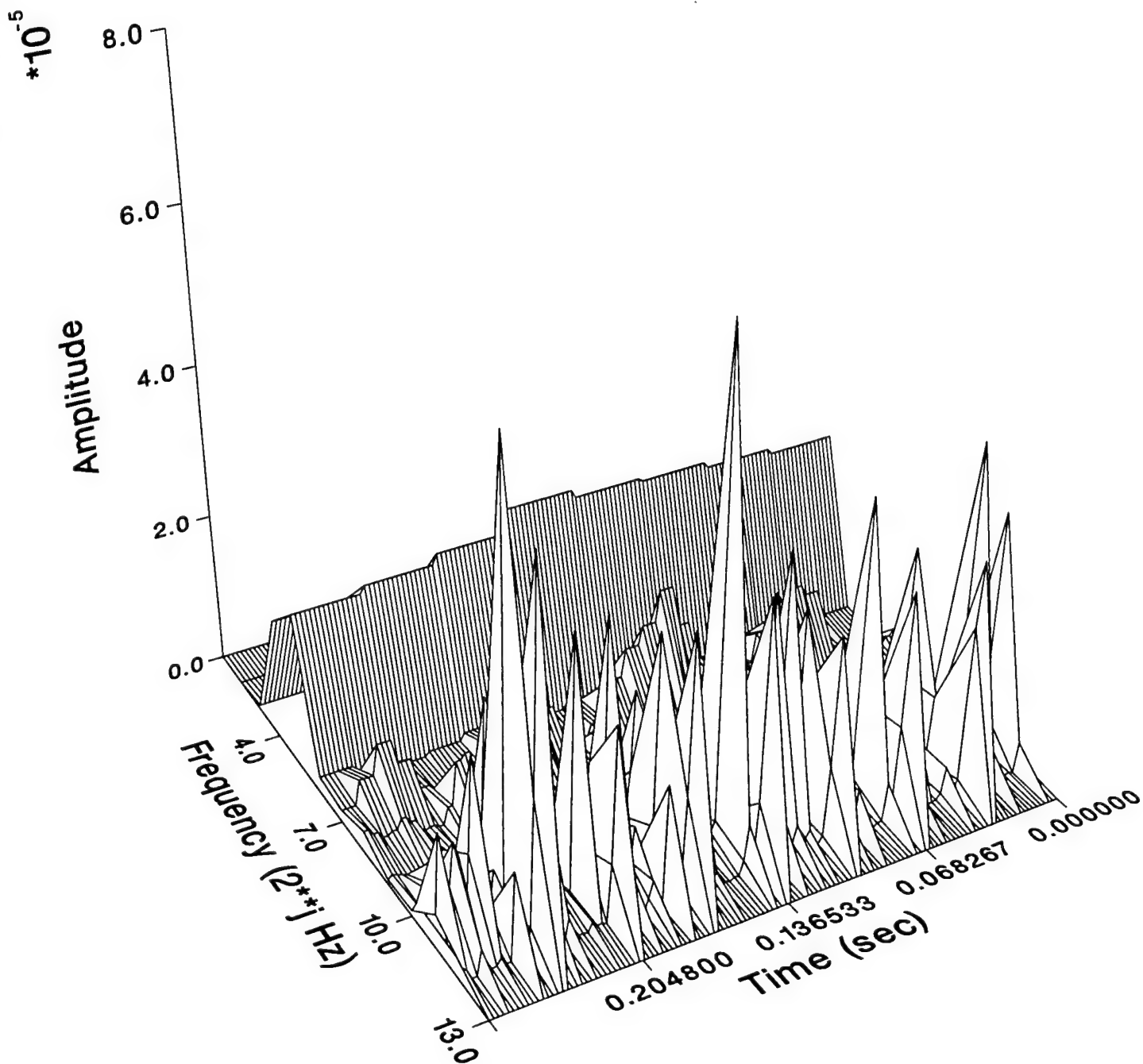


FIGURE 74: Wavelet Transform Results, Artificial Fault Simulation, Tangential Direction

WAVELET TRANSFORMATION CONTOUR

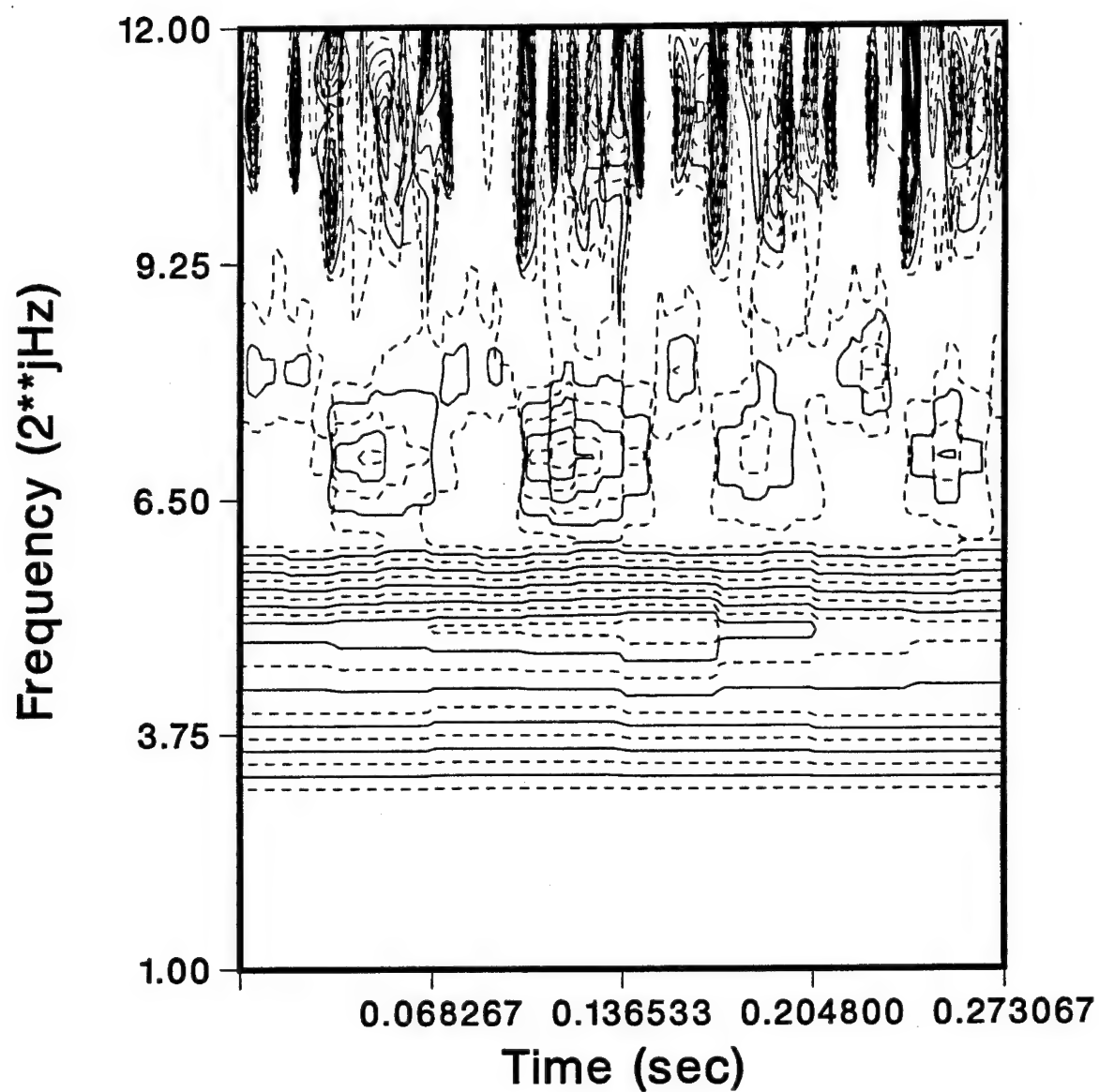


FIGURE 75: Wavelet Transform Contour Map, Artificial Fault Simulation, Tangential Direction

V. CONCLUSIONS AND RECOMMENDATIONS

Pseudo Wigner-Ville Distribution and wavelet transform provide two advanced analysis techniques for condition monitoring of non-stationary and transient machines. The inadequacy of pure time domain analysis or spectral analysis to provide a total assessment of reciprocating type machinery demands that new analysis techniques be employed. The logical progression would be to view time and frequency responses simultaneously. Time-frequency domain distribution allows for the detection of fault location as well as severity level. The three dimensional results from PWVD and wavelet transforms are two opportunities to fill the gap resulting from rotating machinery programs, and provide for better condition monitoring and diagnostics of reciprocating type machines.

The use of a personal computer for the data reduction demonstrates the versatility of the PWVD technique. Although the time demands for a complete analysis using PWVD technique may be consuming, the PWVD results provide a complete representation of the harmonic nature of the compressor component. In addition, the simulated fault signal was clearly depicted in the graphical output. Alarm levels to indicate a change in the mechanical condition of the machine could be established by conducting PWVD analysis on a routine schedule.

The brief introduction of Wavelet analysis was present to demonstrate that even the smallest disturbances in the vibration patterns could be characterized in the time-frequency domain. Wavelet transform requires very short computation time, but it does not describe the magnitude of the main frequency components well. This was the primary reason why Wavelet analysis was presented as a complementary analysis method to the PWVD technique.

Based on the information presented in this study, the following recommendations are made:

a. Obtain vibration measurement data from reciprocating compressors around the cylinder frame to capture the non-stationary and transient vibration patterns of the reciprocating components. For other types of reciprocating machinery, the transducer should be moved around the reciprocating components of the machine to observe the highest response area(s).

b. Record crank-angle position along with vibration data to establish machine timing. Obtain crankshaft RPM and timing of mechanical events to establish a relationship between mechanical events and vibration patterns.

c. Obtain manufacturer data to conduct a thorough analysis of the operating condition of the machine. Establish optimal pressures, loading, horse-power, etc.

d. Based on time-frequency domain analysis, develop diagnostic methods and establish alarm levels.

APPENDIX: MATLAB PROGRAM CODE FOR FFT CALCULATION

```
function [Ya,fx] = fftcalc(y,t,nblock,itext)
%
% This function returns the averaged fft results and
% plots the frequency spectrum
%
% INPUTS:
%       y       : Acceleration vector (calibrated)
%       t       : time vector
%       nblock  : number of data block
%
% OUTPUTS:
%       Ya      : average fft vector of y
%       fx      : frequency vector
%
% Developed by: Liu, Chao-Shih  10/15/93
% Revised by:  John Harding    08/94
%
%       dt = t(2) - t(1); % establish time step
%       fs = 1/dt;        % establish sampling frequency
%       gref = 1e-6;      % establish scaling factor
%
% Standardized The Size of "y"
%       y = y(:); t = t(:);
%       ny = length(y);
%       my = mean(y);
%       stdy = std(y);
%
% Compute The Averaged FFT Data
%       n = ny/nblock; % number of data points/block
%       n2 = n/2;
%       n1 = 1;
%
%       Y = zeros(n,nblock); % establish matrix dimensions
%       for nb = 1:nblock
%           nh = nb*n;
%           Y(1:n,nb) = abs(fft(w.*y(n1:nh)));
%           n1 = nh + 1;
%       end
%
%       if nblock~=1
%           Y = sqrt(sum((Y').^2));
%       end
%
%       Ya = Y*dt;
%       Ya(1) = 0; % remove DC component
```

```

%
f = fs/2*(0:n2)/n2;
Ya(n2+2:n) = [];
fx = f(1:n2+1);
df = fx(2)-fx(1);
%
Ya = 20*log10(Ya/gref); % Gdb transformation:
%
% Plot Frequency Domain:
figure(1); clf;
plot(fx,Ya,'r');
upper = (ceil(max(Ya)/10)+1)*10;
if upper < 60
    lower = 0;
else
    lower = 20;
end
%
axis([0 max(fx) lower 120]);
title(itext);
xlabel('Frequency (Hz)')
ylabel('Acceleration in Gdb')
%
% Print FFT Results
set(1, 'PaperPosition',[0.25 1 8 9.25]);
print

```

LIST OF REFERENCES

1. Marshall, B. R., "A Surface Navy Vibration Program Overview: Standardization and State-of-the-Art", Naval Engineers Journal, Vol. 100, May 1988, pp. 90-100.
2. Chapman, C. L., and Jolley, R., "Systems and Equipment Maintenance Monitoring for Surface Ships (SEMMSS) Program", Naval Engineers Journal, Vol. 99, November 1987, pp. 63-69.
3. Update International, Inc., "A Practical Approach to Reciprocating Machinery Analysis".
4. Taylor, C. F., "The Internal-Combustion Engine in Theory and Practice, Volume II: Combustion, Fuels, Materials, Design, Revised Edition", The M.I.T. Press, 1985, Chapter 8.
5. Compressed Air and Gas Institute, "Compressed Air and Gas Handbook, Fourth Edition", 1973, Chapter 2.
6. Reciprocating Machinery Vibration Data, NAVSEA DET PERA(CV), January, 1994.

7. Flandrin, P., Garreau, D., and Puyal, C., "Improving Monitoring of PWR Electrical Power Plants 'In Core' Instrumentation with Time-Frequency Signal Analysis", IEEE International Conference on Acoustics, Speech, and Signal Processing, vol. 4, pp. 2246-2249, May 1989.
8. Forrester, B., "Analysis of Gear Vibration in the Time-Frequency Domain", Proceedings of the 44th Meeting of the Mechanical Failures Prevention Group, pp. 225-234, Apr 1990.
9. Wigner, E., "On the Quantum Correction for Thermodynamic Equilibrium", Physics Review, vol. 40, pp. 749-759, June 1932.
10. Ville, J., "Theorie et Applications de la Notion de Signal Analytique", Cables et Transmission, Vol 2a, No. 1, pp. 61-74, 1948.
11. Classen, T. and Mecklenbrauker, W., "The Wigner Distribution - A Tool for Time-Frequency Signal Analysis Part I: Continuous-Time Signals", Philips Journal of Research, vol. 35, nos. 3, pp. 217-250, 1980.

12. Classen, T. and Mecklenbrauker, W., "The Wigner Distribution - A Tool for Time-Frequency Signal Analysis Part II: Discrete-Time Signals, "Philips Journal of Research, vol. 35, nos 4/5, pp. 276-300, 1980.
13. Classen, T. and Mecklenbrauker, W., "The Wigner Distribution - A Tool for Time-Frequency Signal Analysis Part III: Relations with other Time-Frequency Signal Transformations", Philips Journal of Research, vol. 35. nos. 6, pp. 372-389, 1980.
14. Shin, Y. and Jeon, J., "Pseudo Wigner-Ville Time-Frequency Distribution and Its Application to Machinery Condition Monitoring", Shock and Vibration, vol. 1, no. 1, pp. 65-76, 1993.
15. Newland, D., "Wavelet Analysis of Vibration", ASME PD-Vol. 52, Structural Dynamics and Vibration - 1993, pp. 1-12, The 16th Annual Energy-Source Technology Conference, Houston, TX., 31 Jan. - 4 Feb., 1993.
16. Wang, W. and McFadden, P., "Application of the Wavelet Transform to Gearbox Vibration Analysis", ASME PD-Vol. 52, Structural Dynamics and Vibration - 1993, pp. 13-20, The 16th Annual Energy-Source Technology Conference, Houston, TX., 31 Jan. - 4 Feb., 1993.

17. Shin, Y. and Jeon, J., "Wavelet Analysis of Nonstationary Acoustic and Vibration Signatures", Proceeding of inter-noise 94 Conference, Vol. III, pp. 1903-1906, Yokohama, Japan, 29-31 August, 1994.

INITIAL DISTRIBUTION LIST

	No. of Copies
1. Defense Technical Information Center Cameron Station Alexandria, VA 22304-6145	2
2. Dudley Knox Library, Code 52 Naval Postgraduate School Monterey, CA 93943-5002	2
3. Department Chairman, Code ME Department of Mechanical Engineering Naval Postgraduate School Monterey, CA 93940	1
4. Naval/Mechanical Engineering Curricular Office Code 34 Naval Postgraduate School Monterey, CA. 93940	1
5. Prof. Y. S. Shin, Code ME/Sg Department of Mechanical Engineering Naval Postgraduate School Monterey, CA 93940	2
6. Mr. Lynn Hampton, Program Manager Machinery Condition Analysis NAVSEADDET PERA(CV) Code 1822 1305 Ironsides Bremerton, WA 98310-4924	3

7. Mr. Ken Jacobs, Deputy Director 1
Surface Ship Maintenance Division
Naval Sea Systems Command
Code 915B
Washington, D.C. 20362-5101
8. COMMANDANT (G-ENE-3C) 2
United States Coast Guard
2100 Second Street, S.W.
Washington, DC 20593-0001
9. LT J. E. Harding, USCG 1
USCGC MIDGETT (WHEC 726)
FPO AP, 96698-3915